CHARACTERIZATION AND FUNCTIONAL SIGNIFICANCE OF Msc2p & Zrg17p, WHICH FORM A ZINC TRANSPORT COMPLEX IN THE ENDOPLASMIC RETICULUM OF *SACCHAROMYCES CEREVISIAE*

A Dissertation
presented to
the Faculty of the Graduate School
University of Missouri-Columbia

In Partial Fulfillment
of the Requirements for the Degree
Doctor of Philosophy

---

by

CHARISSA D. ELLIS

Dr. David J. Eide, Dissertation Supervisor

DECEMBER 2004

The undersigned, appointed by the Dean of the Graduate School, have examined the dissertation entitled

CHARACTERIZATION AND FUNCTIONAL SIGNIFICANCE OF Msc2p & Zrg17p, WHICH FORM A ZINC TRANSPORT COMPLEX IN THE ENDOPLASMIC RETICULUM OF *SACCHAROMYCES CEREVISIAE*

presented by Charissa D. Ellis

a candidate for the degree of Doctor of Philosophy

and hereby certify that in their opinion it is worthy of acceptance.

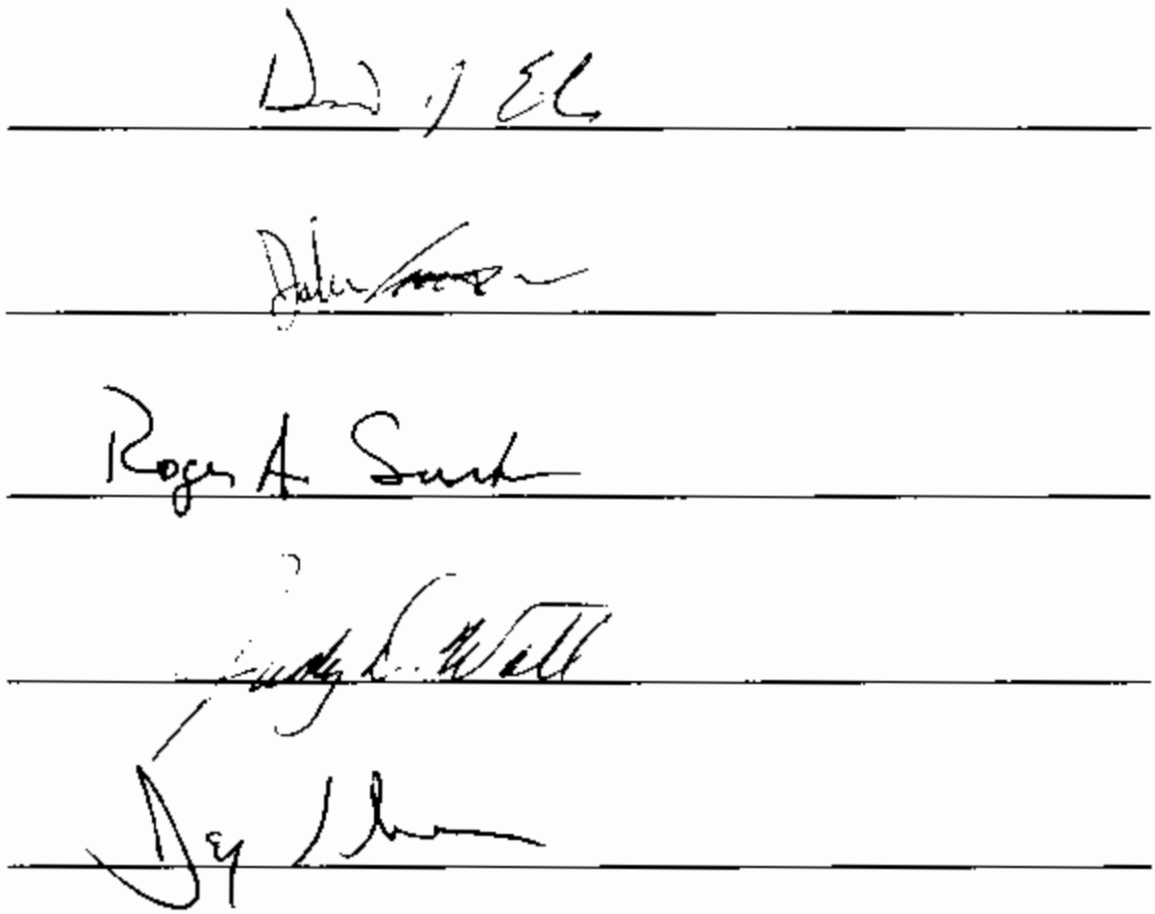

To my Family

ACKNOWLEDGMENTS

First and foremost, I acknowledge my parents, who instilled in me a love for God's earth and a love of learning. Thank you for everything.

I could not have made it through graduate school without the love and emotional support of my husband. Bill, thank you for putting up with all my long hours and late nights at the lab, especially when I was always waiting for cultures to grow!

I also acknowledge my college advisor, Dr. John Bohmfalk, who inspired me to pursue a graduate degree and has remained a good friend.

My numerous activities at the Evangelical Free Church of Columbia gave me an outlet for my creativity and my spirituality throughout my graduate career. I wish to acknowledge the pastoral staff and all the many friends I have made there. You will always have a special place in my heart.

My research could not have happened without the former labs on the second floor of Gwynn Hall. I acknowledge both past and present members of the Sunde, Petris, and Rogers labs for their helpful insights and their meaningful conversations—both about science and about life!

In particular, I have to acknowledge the current and former members of the Eide lab, who have all shown me how I can become a better scientist, including Dr. Amanda Bird, Ms. Suzanne Clark, Dr. L. Alex Gaither, Dr. Raad Gitan, Dr. Andrew Herbig, Dr. Thomas Lyons, Dr. Colin MacDiarmid, Mrs. Michelle Mooney, Mrs. Wei Qiao, Dr. Monir Shababi, Dr. Claudia Simm, Dr. Fudi Wang, Dr. Brian Waters, and Mr. Chang-Yi (Charlie) Wu.

My committee has been instrumental in my progress, and I wish to thank Dr. John Cannon, Dr. Joseph Polacco, Dr. Roger Sunde, and Dr. Judy Wall for their commitment to me in my graduate career.

Last, but definitely not least, I would not be where I am today without my advisor, Dr. David Eide. Dave has taught me so many things, including how to think like a scientist, the integrity and character of being a scientist, and determining if there is another possible model to explain results. Dave has been immensely patient with me and stuck with me even through my difficult periods with depression. Thank you, Dave, for your compassion and your ability to see potential in me when I could not.

TABLE OF CONTENTS

LIST OF TABLES

LIST OF FIGURES

LIST OF ABBREVIATIONS

AE—acrodermatitis enteropathica

ATP—adenosine triphosphate

BLAST—basic local alignment search tool

CDF—cation diffusion facilitator

Co-IP—co-immunoprecipitation

CPY—carboxypeptidase Y

DNA—deoxyribonucleic acid

ECL—enhanced chemiluminescence, chemiluminescent Western blotting substrate

EDTA—ethylenediamine tetraacetic acid

ER—endoplasmic reticulum

ERAD—ER-associated degradation

EST—expressed sequence tag

GEV—GAL4.ER.VP16, β-estradiol inducible activator consisting of the Gal4p DNA binding domain, the hormone binding domain of the human β-estradiol α-receptor, and the VP16 activation domain

GFP—green fluorescent protein

GPI—glycosylphosphatidylinositol

HA—hemagglutinin

HRP—horseradish peroxidase

IgG—immunoglobulin G

lacZ—*E. coli* β-galactosidase gene

LZM—limited zinc medium

ORF—open reading frame

PCR—polymerase chain reaction

PMSF—phenylmethylsulfonylfluoride

POD—peroxidase, chemiluminescent Western blotting substrate

PSI-BLAST—position specific interated-BLAST

RNA—ribonucleic acid

SD—synthetic defined

TAP—tandem affinity purification

TMs—transmembrane domains

TPEN—N,N,N´,N´-tetrakis-(2-pyridylmethyl)ethylenediamine

UPR—unfolded protein response

UPRE—unfolded protein response element

WT—wild type

YPD—yeast peptone dextrose

YPGE—yeast peptone glycerol ethanol

ZIP—Zrt-, Irt-like protein

ZRE—zinc responsive element

LIST OF PROTEINS

Cot1p	Vacuolar influx transporter of cobalt and zinc
CPY	Vacuolar carboxypeptidase Y
CPY*	Point mutant in CPY that is retained in the ER for degradation
Dpm1p	Dolichol phosphate mannose synthase, ER marker protein
Fet4p	Low affinity plasma membrane transporter of iron, copper, and zinc
Hac1p	UPR transcription factor, part of UPR signaling pathway
Hsp150p	Cell wall protein of unknown function
Ire1p	ER/nuclear transmembrane endoribonuclease that initiates the UPR, part of UPR signaling pathway
Jem1p	DnaJ-like ER protein chaperone involved in ERAD
Kex2p	Calcium-dependent serine endopeptidase of the trans-Golgi network, Golgi marker protein
Pma1p	Plasma membrane proton ATPase, plasma membrane marker protein
Scj1p	DnaJ homologue, ER zinc-binding protein chaperone involved in ERAD
Zap1p	Zinc-responsive transcriptional activator protein
Zrc1p	Vacuolar zinc influx transporter
Zrt1p	High affinity plasma membrane zinc transporter
Zrt2p	Low affinity plasma membrane zinc transporter
Zrt3p	Vacuolar zinc efflux transporter

CHARACTERIZATION AND FUNCTIONAL SIGNIFICANCE OF Msc2p & Zrg17p, WHICH FORM A ZINC TRANSPORT COMPLEX IN THE ENDOPLASMIC RETICULUM OF *SACCHAROMYCES CEREVISIAE*

Charissa D. Ellis

Dr. David J. Eide, Dissertation Supervisor

ABSTRACT

Zinc is an essential nutrient for all organisms because of the many important roles zinc plays in cells. In particular are the structural and catalytic roles zinc plays in proteins. To obtain zinc from their environment, cells use zinc transport proteins in their plasma membranes. Eukaryotic cells must also use zinc transporters to supply zinc to their intracellular organelles, including those of the secretory pathway. Members of the cation diffusion facilitator (CDF) family have been shown to transport heavy metals out of the cytoplasm of cells, and many eukaryotic CDF members transport zinc into intracellular compartments. All six currently known CDF members in the budding yeast *Saccharomyces cerevisiae* transport metals into intracellular organelles. This study focuses on the characterization and function of two CDF members in yeast.

In chapter two, we show that zinc is required for endoplasmic reticulum (ER) function in *S. cerevisiae*. Zinc deficiency in this yeast induces the unfolded protein response (UPR), a system normally activated by unfolded ER proteins. Msc2p, a member of the CDF family, was previously implicated in zinc homeostasis. Our results indicate that Msc2p is one route of zinc entry into the ER. Msc2p localizes to the ER when expressed at normal levels. UPR induction in low zinc is exacerbated in an *msc2* mutant. Genetic and biochemical evidence

indicate that this UPR induction is due to genuine ER dysfunction. Notably, we found that ER-associated protein degradation (ERAD) is defective in zinc-limited *msc2* mutants. We also show that the vacuolar CDF proteins Zrc1p and Cot1p are other pathways of ER zinc acquisition. Finally, zinc deficiency up-regulates the mammalian ER stress response, indicating a conserved requirement for zinc in ER function among eukaryotes.

In chapter three, we demonstrate a novel interaction between two CDF family members: Msc2p and a newly recognized CDF family member in yeast, Zrg17p. *ZRG17* was previously identified as a zinc-regulated gene controlled by the zinc-responsive Zap1p transcription factor. A *zrg17* mutant exhibits the same zinc-suppressible phenotypes as an *msc2* mutant, including an induction of the UPR in low zinc. Zrg17p localizes to the ER and is regulated by zinc at the protein level. Msc2p and Zrg17p physically interact, as determined by co-immunoprecipitation. Therefore, we propose that Msc2p and Zrg17p form a zinc transport complex in the ER membrane, supplying zinc to the ER to maintain the function of this compartment. We also demonstrate that ZnT5 and ZnT6, the closest mammalian homologues of Msc2p and Zrg17p, functionally interact. These results indicate that interactions between CDF members may be a common phenomenon.

In summary, we demonstrate a novel interaction between two CDF proteins in yeast. Msc2p and Zrg17p interact to form a complex in the ER. The purpose of this complex is to transport zinc into the ER to maintain the proper function of this compartment. These results in yeast are reflected in mammalian

cells, suggesting that all eukaryotes require zinc for ER function, and that the interaction between CDF members is a universal phenomenon.

CHAPTER 1

INTRODUCTION

Charissa D. Ellis

Department of Biochemistry, University of Missouri, Columbia, MO 65211

Overview

This dissertation details the characterization and functional importance of the zinc transport proteins Msc2p and Zrg17p in the endoplasmic reticulum (ER) of the budding yeast *Saccharomyces cerevisiae*. To have a better understanding of the research presented on these transport proteins, this chapter introduces important concepts about zinc and zinc transporters. First, we outline the essentiality of zinc and the many roles zinc plays in cells. This leads to the examination of proteins that require zinc transporters, specifically those in the secretory pathway. The current model of zinc transport and regulation in yeast is discussed, followed by an overview of the different families of zinc transporters. Lastly, we focus on one specific family of zinc transporters, the cation diffusion facilitator (CDF) family, of which Msc2p and Zrg17p are members.

Essentiality and roles of zinc

All life on earth requires zinc. In fact, zinc is the second most abundant trace metal found in eukaryotic organisms, second only to iron (1). Additionally, Coleman claims that if one were to subtract the iron in hemoglobin, zinc would become the most abundant trace metal in the human body (1)! The reason for this widespread use of zinc may be due to the unique properties of zinc itself. First, unlike iron or copper which undergo Fenton chemistry, zinc is not a redox active metal, so there is no potential damage to DNA or proteins due to free radical cascades (2, 3). Second, zinc is a borderline Lewis acid, which allows it to interact strongly with several different ligands. In particular, zinc favors binding

to the following ligands in proteins: the sulfur from cysteine, the nitrogen from histidine, and the oxygen from aspartate, glutamate, and water (2). Third, zinc can undergo ligand exchange reactions rather quickly, making it kinetically labile (2). Finally, while zinc is most often bound to four ligands in a tetrahedral coordination geometry, it exhibits flexibility in the types of ligand coordination geometries it accepts (3, 4).

These properties of zinc allow it to play many important roles in cells. In particular are the structural and catalytic roles zinc plays in proteins. More than ten different classes of structural zinc-binding domains have been identified (2). Perhaps the best known of these is the zinc finger. In the classical C_2H_2 type zinc finger, a span of ~30 amino acids folds around a single zinc ion, which is coordinately bound by two cysteine residues on a beta sheet and two histidine residues on an alpha helix (5). This type of zinc finger was originally discovered in the TFIIIA transcription factor in *Xenopus laevis* (6). Now, with the sequencing of the human genome, Venter et al. found 4500 C_2H_2 type zinc finger domains in 564 human proteins: approximately 1-2% of the human genome (7)! In fact, zinc finger domains are the most abundant DNA binding motif in eukaryotic transcription factors (2). The alpha helical portion of the zinc finger is able to fit into the major groove of a DNA double helix, allowing the amino acid residues there to make site-specific interactions with DNA bases (5).

Other zinc structural domains bind two or more atoms of zinc. RING finger domains consist of eight amino acid residues (mostly cysteines) that form two overlapping zinc binding sites (8). The zinc cluster in the Gal4p DNA-binding

domain of *S. cerevisiae* has two zinc ions bound by six cysteine residues (9). A last example is the zinc cluster domains found in mammalian metallothioneins. These metallothioneins are small 62 amino acid proteins which bind zinc in two separate metal clusters: Zn_4Cys_{11} and Zn_3Cys_9 (3).

In terms of a catalytic role, zinc is found in the active site of more than 300 different enzymes in all six enzyme classes (4). Zinc is the only metal found in all enzyme classes (4). The different types of catalysis performed by zinc metalloenzymes is determined by the ligands coordinating the zinc in the active site, as well as the spacing between these ligands (4). Unlike structural zinc sites, catalytic zinc is bound to three amino acid ligands in all active sites, the most common ligand being histidine. The fourth ligand is always water (3, 4). This being the case, often zinc acts as an electrophilic catalyst to activate the water molecule (3, 8). For example, in carbonic anhydrase, the zinc atom promotes the deprotonation of water to a hydroxide ion, which then attacks the carbon on carbon dioxide, generating bicarbonate (10). Alternatively, zinc plays a different role in the active site of alcohol dehydrogenase. Here, zinc functions to coordinate the alcohol substrate and keep it in the appropriate conformation so that a hydride (H^-) can be transferred from the alcohol to the cofactor NAD^+, thereby converting the alcohol to acetaldehyde (10).

Besides these roles in proteins, zinc may potentially play a role as a neuromodulator in the brains of mammals. Zinc is stored in synaptic vesicles in the mossy fiber projections of neurons in the hippocampus and in neurons of the cerebral cortex (11, 12). Upon high-frequency stimulation, these vesicles

exocytose, releasing their zinc into the synaptic cleft between neurons (13, 14). Here, zinc is proposed to modulate the activity of various receptors. The activities of ionotropic glutamate receptors, such as the N-methyl-D-aspartate (NMDA) receptors, and gamma-aminobutyric acid (GABA) receptors have been shown to be inhibited by zinc *in vitro* (15, 16).

To further demonstrate the essentiality of zinc in humans is the hereditary zinc deficiency disease acrodermatitis enteropathica (AE). People suffering from AE show typical characteristics of nutritional zinc deficiency, including alopecia (hair loss), dermatitis, low serum zinc and alkaline phosphatase levels, and mental disorders (17, 18). Patients can be successfully treated with zinc supplementation (18). The cause of AE has recently been attributed to mutations in a gene encoding a zinc transport protein, hZip4 (17, 19). The hZip4 protein was localized to the apical membrane of intestinal enterocytes, and has been postulated to take up zinc from the diet (17). Therefore, it can be seen that mutations rendering the hZip4 transporter ineffective would result in zinc deficiency, and hence the AE disease.

The need for zinc transport proteins

The many roles of zinc demonstrate the need for zinc in cells. However, since zinc is an ion, it cannot merely pass through a lipid bilayer membrane. Therefore, cells require zinc transporters in their plasma membranes to obtain zinc from their extracellular environment. Eukaryotic cells also require zinc

transporters in the membranes of their intracellular organelles to supply zinc to those compartments.

There are many zinc metalloproteins that reside in or move through the secretory pathway that require zinc. In pancreatic beta cells, the maturation of proinsulin to insulin granules requires zinc. Early in the secretory pathway in the ER and/or Golgi, proinsulin binds zinc to form homohexamers (20, 21). Later in the secretory pathway, insulin granule core formation is also facilitated by zinc (20). Matrix metalloproteases are secreted zinc-containing enzymes that dissolve extracellular matrix for cell migration, invasion, tissue resorption and remodeling, and development (22, 23). These proteins would need to acquire zinc in the secretory pathway in order to be functional. Killer T cells display a large variety of antigen peptides on their cell surface through major histocompatibility complex (MHC) class I molecules. A lumenal ER zinc metalloenzyme known as the ER-associated aminopeptidase (ERAAP) is responsible for processing some of these peptides by cleaving the N-terminal amino acid residues (24, 25). Resident ER transferase enzymes responsible for attaching phosphoethanolamine groups to glycosylphosphatidylinositol- (GPI-) anchors are zinc-requiring enzymes (26, 27). Lastly, the Scj1p chaperone protein found in the ER of *S. cerevisiae* is a type I homologue of the *Escherichia coli* DnaJ (Hsp40) protein (28, 29). All DnaJ type I homologues contain two zinc binding centers, which are necessary for the chaperone activity of these proteins (30). Since all of these (and many other) proteins described above need to

acquire zinc, they illustrate the need for zinc transporters in the ER and other organelles of the secretory pathway.

Zinc transport and regulation in *Saccharomyces cerevisiae*

The budding yeast, *S. cerevisiae*, has been an excellent model to elucidate and understand the zinc transport proteins that supply zinc to the cell and its intracellular organelles, as well as how these proteins are regulated. Initially, zinc enters the yeast cell through one of several transporters on the plasma membrane (**Figure 1.1**). Zrt1p is a high affinity zinc transporter responsible for most of the zinc coming into the yeast cell in times of zinc deficiency (31). Zrt2p and Fet4p are low affinity transporters that supply zinc under more moderate conditions of zinc deficiency (32, 33). The genes for all three of these proteins are up-regulated in zinc-limiting conditions by the zinc-regulated transcription factor, Zap1p (34). Zap1p recognizes an eleven base pair consensus sequence, a zinc-responsive element or ZRE, found in one or more copies in the promoters of each of its target genes (35, 36). Lyons et al. determined there to be at least 46 Zap1p targets in the yeast genome (36).

Two other Zap1p targets of note are *ZRT3* and *ZRC1*, which encode zinc transporters that localize to the membrane of the vacuole. The vacuole is the major site of zinc storage in yeast. In zinc deficiency, Zrt3p mobilizes vacuolar zinc stores so that they may used by the rest of the cell (37). However, when cytosolic zinc levels rise, Zrc1p, aided by Cot1p, pumps zinc into the vacuole for storage or detoxification (38). The purpose of the up-regulation of *ZRC1* in zinc

Figure 1.1. *Current model of zinc transport and regulation in Saccharomyces cerevisiae.* Plasma membrane transporters Zrt1p, Zrt2p, and Fet4p transport zinc into the cytoplasm. Zrc1p and Cot1p pump zinc into the vacuole for storage, while Zrt3p pumps zinc out of the vacuole to mobilize zinc stores. Msc2p and Zrg17p transport zinc into the ER and are discussed in Chapters 2 and 3, respectively. Zap1p is a zinc-regulated transcriptional activator that up-regulates genes in zinc deficiency, including the genes that encode all of the above transporters except Cot1p and Msc2p.

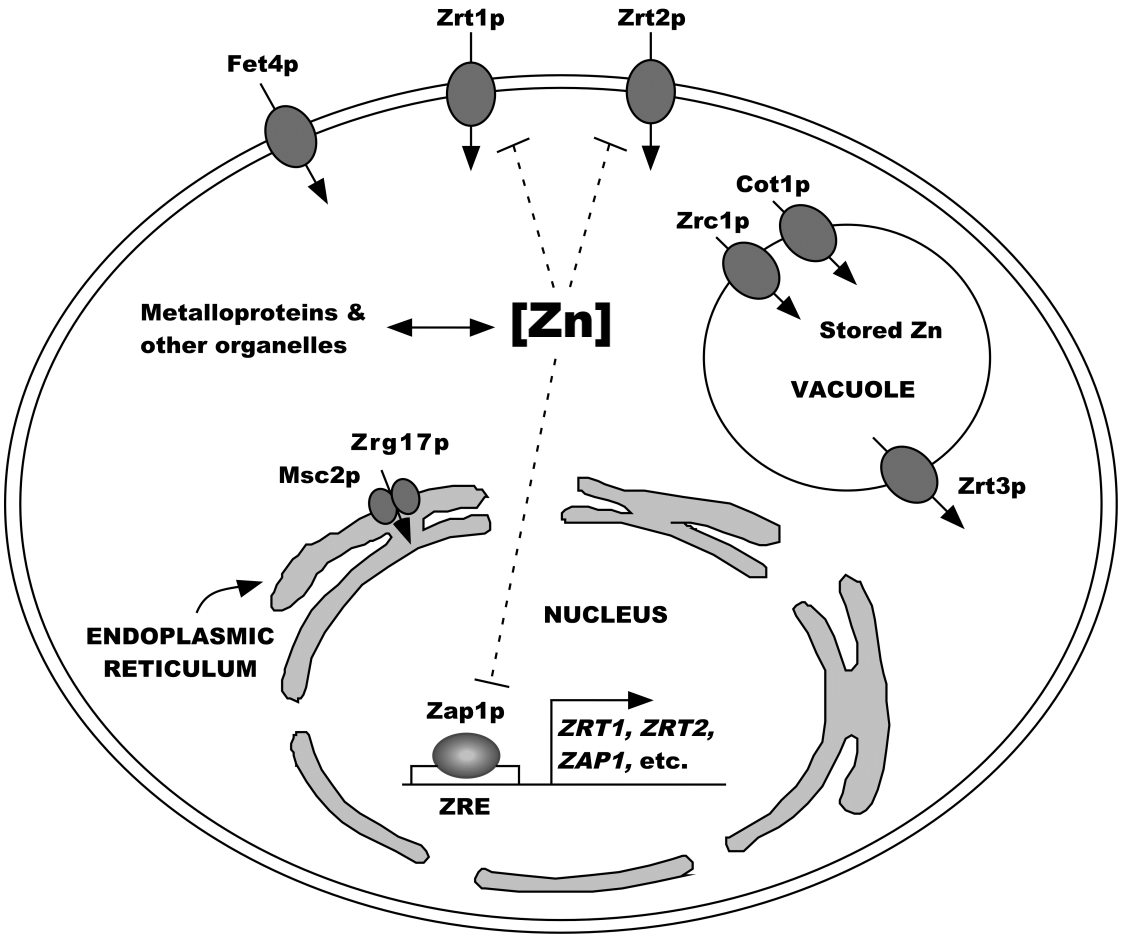
Zrt1p
Zrt2p
Fet4p
Cot1p
Zrc1p
Metalloproteins &
other organelles
[Zn]
Stored Zn
VACUOLE
Zrg17p
Msc2p
Zrt3p
ENDOPLASMIC
RETICULUM
NUCLEUS
Zap1p
ZRT1, ZRT2,
ZAP1, etc.
ZRE

deficiency may be a pro-active response, so that when the cell shifts from a zinc-deficient to a zinc-replete environment, the sudden influx of zinc into the cytosol may be quickly pumped into the vacuole for detoxification (39).

Classes of zinc transport proteins

Zinc transport proteins are found in five classes. Bacteria express proteins in all five classes, while yeast and mammalian cells express only two of these families. The resistance nodulation cell division (RND) family is only found in a few gram-negative bacteria. Members of this family, such as the CzcCBA system in *Ralstonia metallidurans* CH34 (40), export zinc across both the cytoplasmic and outer membranes of the bacterial cell (41). Members of the ATP-binding cassette (ABC) family that have been shown to transport zinc are also only found in bacteria. ABC transporters are primary transporters that bind and hydrolyze ATP to transport substrate across the membrane (42). In *E. coli*, the ZnuABC system consists of three proteins that function as an ABC transporting complex responsible for high-affinity zinc uptake (43). Zinc-transporting P-type ATPases have been found in both prokaryotes and plants. P-type ATPases, like ABC transporters, are also primary transporters that utilize the energy from ATP hydrolysis to transport substrate. However, P-type ATPases also undergo cycles of binding and phosphorylation events, including substrate binding, ATP binding, phosphorylation, ion release, and dephosphorylation (44). The *E. coli* ZntA P-type ATPase transports zinc out of the cell (45, 46), and the *Arabidopsis thaliana* Hma2 and Hma4 proteins appear

to be involved with the export of zinc from root cells into the inner vascular (xylem and phloem) tissue (47).

Zinc transport in yeast and mammalian cells is carried out exclusively by members of the Zrt-, Irt-like protein (ZIP) and cation diffusion facilitator (CDF) families. The ZIP family is named after the first identified members of this family: the Zrt1p and Zrt2p zinc uptake transporters in *S. cerevisiae* (31, 32) and the Irt1p iron uptake transporter in *A. thaliana* (48). This family now has over 90 members in both prokaryotes and eukaryotes (49), including ZupT in *E. coli* (50), Zip1-4 in *A. thaliana* (51), ZnT1 in the metal hyperaccumulator plant *Thlaspi caerulescens* (52), GmZip1 in soybean (53), and hZip1-14 in humans (54), including the previously mentioned hZip4 protein implicated in AE disease. Most members of this family have eight transmembrane domains (TMs) and a histidine-rich cytoplasmic loop between TMs three and four (54, 55). The extracellular loop between TMs two and three may affect the metal specificity of the transporter (56). The common function seen in all ZIP family members is transporting metals, usually zinc, into the cytoplasm, either from the extracellular environment or from intracellular compartments (54). The mechanism of this transport is not clearly understood, but is probably some kind of secondary transport, such as a symport or antiport mechanism with another ion (54).

The cation diffusion facilitator (CDF) family

While ZIP family members increase cytoplasmic zinc levels, CDF family members have the opposite function. The overall conserved function seen in this

family is in transporting zinc (or other heavy metals) out of the cytoplasm, either into intracellular organelles or to the extracellular environment (49, 57-59). Like the ZIP family, the CDF family is a very large family of heavy metal ion transporters, with over 100 putative members in prokaryotes and eukaryotes (**Figure 1.2**) (49). The first characterized members of this family were the CzcD protein found in *R. metallidurans* CH34 (60), and the Zrc1p protein of *S. cerevisiae* (61). The CzcD protein and other bacterial members have been shown to transport cadmium, zinc, and cobalt (60, 62). The MTP1 protein in the heavy metal hyperaccumulator plant *Thlaspi goesingense* has been shown to transport nickel (63). Most, if not all, members of the CDF family are involved with zinc transport. Most CDF proteins have six transmembrane domains, and the eukaryotic members have a histidine-rich cytoplasmic loop between TMs four and five (59). This loop may play a role in the metal-specificity of the transporter (59, 63).

The mechanism of transport for CDF members has been determined for a few family members. Both the CzcD protein in *Bacillus subtilis* and the ZitB protein in *E. coli* were shown to exhibit antiport mechanisms of transport. They both exchanged the efflux of zinc for the influx of potassium ions or protons (62, 64). Similarly, the Zrc1p protein in yeast was shown to require the proton gradient derived from the vacuolar H^+-ATPase and utilize a H^+/Zn^{2+} antiport mechanism to transport zinc into the vacuole (38). Despite only these three examples, since both prokaryotic and eukaryotic proteins utilize an antiport mechanism, this is probably the overall method of transport for the CDF family.

Figure 1.2. *Dendrogram of the CDF family.* This dendrogram is taken from reference (49); however, it has been modified to account for up-dated information in the literature and in the NCBI nonredundant protein database. Subfamily I contains mostly prokaryotic proteins, while subfamilies II and III contain mostly eukaryotic proteins. Interestingly, the yeast members fall into all three subfamilies: Mmt1p and Mmt2p in subfamily I, Msc2p in subfamily II, and Zrc1p and Cot1p in subfamily III. (Zrg17p was not known to be a CDF member when this dendrogram was generated, but would probably fall into subfamily III with ZnT6.)

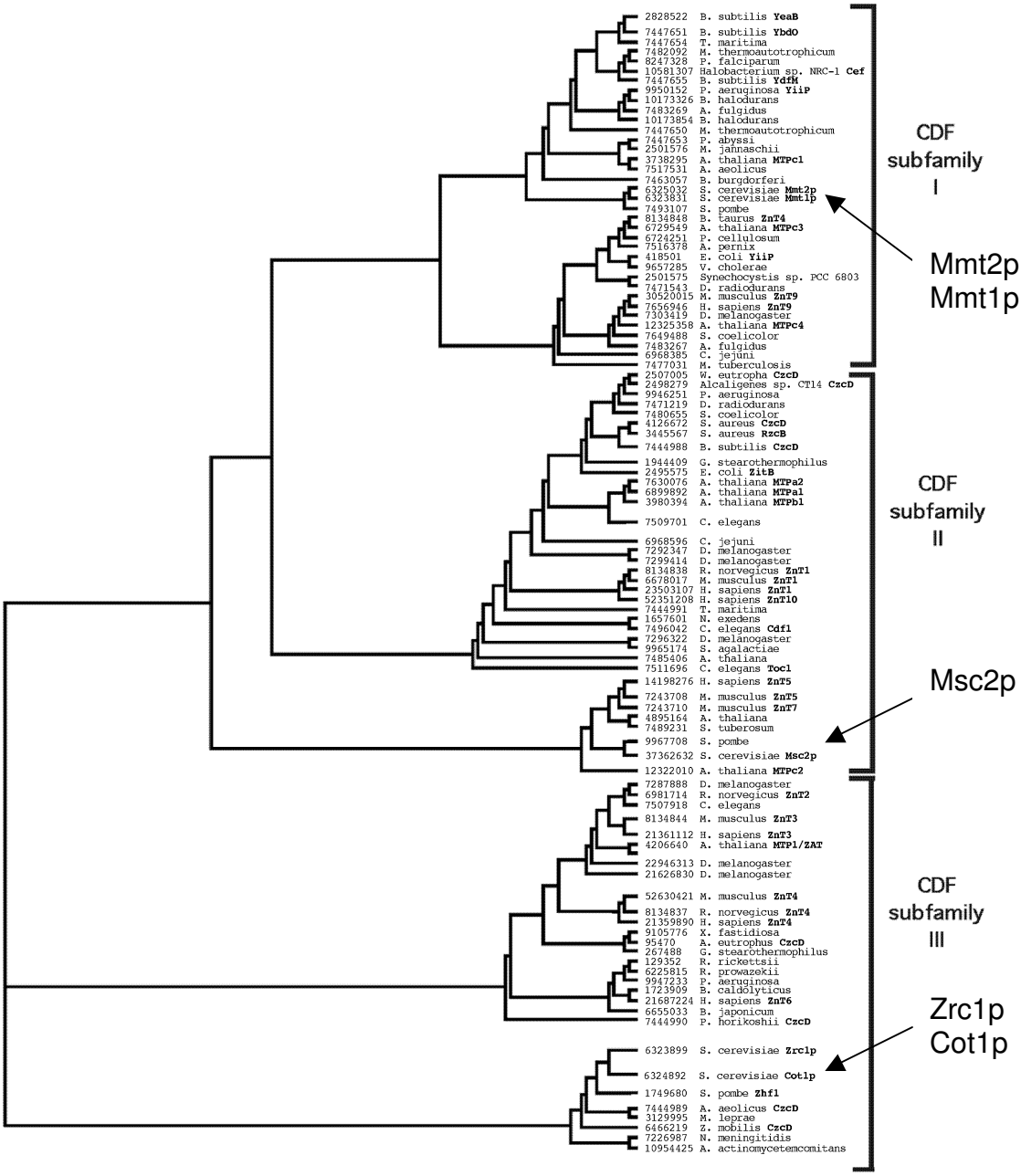
2828522 B. subtilis YeaB
7447651 B. subtilis YbdO
7447654 T. maritima
7482092 M. thermoautotrophicum
8247328 P. falciparum
10581307 Halobacterium sp. NRC-1 Cef
7447655 B. subtilis YdfM
9950152 P. aeruginosa YiiP
10173326 B. halodurans
7483269 A. fulgidus
10173854 B. halodurans
7447650 M. thermoautotrophicum
7447653 P. abyssi
2501576 M. jannaschii
3738295 A. thaliana MTPc1
7517531 A. aeolicus
7463057 B. burgdorferi
6325032 S. cerevisiae Mmt2p
6323831 S. cerevisiae Mmt1p
7493107 S. pombe
8134848 B. taurus ZnT4
6729549 A. thaliana MTPc3
6724251 P. cellulosum
7516378 A. pernix
418501 E. coli YiiP
9657285 V. cholerae
2501575 Synechocystis sp. PCC 6803
7471543 D. radiodurans
30520015 M. musculus ZnT9
7656946 H. sapiens ZnT9
7303419 D. melanogaster
12325358 A. thaliana MTPc4
7649488 S. coelicolor
7483267 A. fulgidus
6968385 C. jejuni
7477031 M. tuberculosis
2507005 W. eutropha CzcD
2498279 Alcaligenes sp. CT14 CzcD
9946251 P. aeruginosa
7471219 D. radiodurans
7480655 S. coelicolor
4126672 S. aureus CzcD
3445567 S. aureus RzcB
7444988 B. subtilis CzcD
1944409 G. stearothermophilus
2495575 E. coli ZitB
7630076 A. thaliana MTPa2
6899892 A. thaliana MTPa1
3980394 A. thaliana MTPb1
7509701 C. elegans
6968596 C. jejuni
7292347 D. melanogaster
7299414 D. melanogaster
8134838 R. norvegicus ZnT1
6678017 M. musculus ZnT1
23503107 H. sapiens ZnT1
52351208 H. sapiens ZnT10
7444991 T. maritima
1657601 N. exedens
7496042 C. elegans Cdf1
7296322 D. melanogaster
9965174 S. agalactiae
7485406 A. thaliana
7511696 C. elegans Tocl
14198276 H. sapiens ZnT5
7243708 M. musculus ZnT5
7243710 M. musculus ZnT7
4895164 A. thaliana
7489231 S. tuberosum
9967708 S. pombe
37362632 S. cerevisiae Msc2p
12322010 A. thaliana MTPc2
7287888 D. melanogaster
6981714 R. norvegicus ZnT2
7507918 C. elegans
8134844 M. musculus ZnT3
21361112 H. sapiens ZnT3
4206640 A. thaliana MTP1/ZAT
22946313 D. melanogaster
21626830 D. melanogaster
52630421 M. musculus ZnT4
8134837 R. norvegicus ZnT4
21359890 H. sapiens ZnT4
9105776 X. fastidiosa
95470 A. eutrophus CzcD
267488 G. stearothermophilus
129352 R. rickettsii
6225815 R. prowazekii
9947233 P. aeruginosa
1723909 B. caldolyticus
21687224 H. sapiens ZnT6
6655033 B. japonicum
7444990 P. horikoshii CzcD
6323899 S. cerevisiae Zrc1p
6324892 S. cerevisiae Cot1p
1749680 S. pombe Zhf1
7444989 A. aeolicus CzcD
3129995 M. leprae
6466219 Z. mobilis CzcD
7226987 N. meningitidis
10954425 A. actinomycetemcomitans
CDF subfamily I
Mmt2p
Mmt1p
CDF subfamily II
Msc2p
CDF subfamily III
Zrc1p
Cot1p

Perhaps the best-characterized members of this family are the mammalian ZnT proteins. These proteins demonstrate the wide variety of subcellular localizations and functional roles of CDF proteins. Ten ZnT proteins have been identified (65), and of these, ZnT1-8 have been characterized, all demonstrating involvement with zinc homeostasis (57). ZnT1 is the only ZnT protein that has been localized to the plasma membrane. It is responsible for pumping zinc into the extracellular environment to prevent a toxic build up of zinc in the cytosol (66, 67). Consistent with this is the finding that the *Znt1* gene is a target of MTF1, the transcription factor that up-regulates metallothionein genes in times of zinc sufficiency (68). However, ZnT1 is also found on the basolateral membrane of intestinal enterocytes and could be involved in the transfer of zinc from the diet to the bloodstream (69, 70). Interestingly, *Znt1* knock-out mice are embryonically lethal; however, the reason for this essentiality is unclear (71).

ZnT2 has a similar function to ZnT1 in detoxifying the cytosol, but by putting zinc into an endosomal compartment (72). ZnT2 may have a similar role as Zrc1p in yeast by putting zinc into a compartment for storage. ZnT3 has been localized to synaptic vesicles in neurons of the hippocampus, and is responsible for transporting zinc into these vesicles so zinc can act as a neuromodulator in the brain (73, 74). *ZNT4* was identified as the gene that when mutated resulted in the lethal milk mouse phenotype. Pups born to mice with these mutations died due to a lack of zinc in the milk (75). Consistent with this, ZnT4 has been localized to intracellular/secretory vesicles in mammary tissue (76, 77).

ZnT5-7 have all been localized to the Golgi apparatus, but have different tissue distributions, and ZnT8 has been localized to intracellular secretory vesicles. The exact roles of these four proteins in the secretory pathway are still to be determined. Both *ZnT5* and *ZnT8* have high expression in pancreatic beta cells and have been suggested to be involved with zinc transport into insulin secretory granules (78, 79). Besides the pancreas, analysis of expressed sequence tags (ESTs) suggest that *ZnT5* is ubiquitously expressed in human tissues (65). ZnT5 belongs to a small subset of the CDF family in which these proteins contain between 12 and 15 transmembrane domains instead of six. The last six TMs are the most homologous to other members of the family (78). ZnT6 and ZnT7 have both been implicated in supplying zinc to proteins of the trans-Golgi network. The tissue distribution of ZnT6 and ZnT7 vary widely, as determined by different groups. *ZnT6* mRNA and protein are consistently seen in lung, small intestine, kidney, and brain (65, 80). *ZnT7* mRNA, while seen only in low levels, is expressed mostly in liver, prostate, small intestine, spleen, eye, and colon (65, 81).

Prior to the work presented here, six CDF family members had been identified in yeast: one in *Schizosaccharomyces pombe* and five in *Saccharomyces cerevisiae*. The Zhf1 protein in *S. pombe* was localized to the endoplasmic reticulum, and pumps zinc into this compartment for storage (82, 83). Mmt1p and Mmt2p of *S. cerevisiae* were localized to the inner mitochondrial membrane and have been implicated with mitochondrial iron uptake (84), though their exact role is not clearly understood (85). Zrc1p and Cot1p were originally

discovered by their ability to give tolerance to zinc and cobalt, respectively (61, 86). Both localize to the membrane of vacuole and transport zinc into this compartment (38). The last member in yeast is Msc2p. This protein is described in detail in chapter two.

Characterization and functional importance of ER zinc transporters in yeast

Zinc transporters in the secretory pathway, including those in the membrane of the ER, are largely unknown. For those that have been identified, such as the mammalian ZnT5-8 proteins, the exact role of these transporters and their downstream effects in the secretory pathway are also unknown. Given the different classes of zinc transporters, those that would pump zinc into the secretory pathway are most likely CDF family members. The focus of this dissertation is on the characterization and functional importance of two CDF members that transport zinc into the ER of yeast. The next chapter characterizes Msc2p. Msc2p was found to be important for zinc transport into the ER to maintain proper function of this compartment. The third chapter characterizes Zrg17p. Zrg17p is a newly identified CDF member that was found to physically interact with Msc2p, and together, they may form a complex to transport zinc into the ER. The last chapter discusses the implications of an Msc2p-Zrg17p zinc transport complex and the future studies of this project.

REFERENCES

1. Coleman JE. 1992. Zinc proteins: Enzymes, storage proteins, transcription factors, and replication proteins. *Annu Rev Biochem* **61**: 897-946.
2. Berg JM and Shi Y. 1996. The galvanization of biology: a growing appreciation for the roles of zinc. *Science* **271**: 1081-1085.
3. Vallee BL and Auld DS. 1990. Zinc coordination, function, and structure of zinc enzymes and other proteins. *Biochemistry* **29**: 5647-5659.
4. Vallee BL and Falchuk KH. 1993. The biochemical basis of zinc physiology. *Physiol Rev* **37**: 79-118.
5. Klug A and Schwabe JW. 1995. Protein motifs 5. Zinc fingers. *FASEB J* **9**: 597-604.
6. Hanas JS, Hazuda DJ, Bogenhagen DF, Wu F, and Wu C. 1983. *Xenopus* transcription factor A requires zinc for binding to the 5S RNA gene. *J Biol Chem* **258**: 14120-14125.
7. Venter JC, Adams MD, Myers EW, Li PW, Mural RJ, Sutton GG, Smith HO, Yandell M, Evans CA, Holt RA, et al. 2001. The sequence of the human genome. *Science* **291**: 1304-1351.
8. Schwabe JW and Klug A. 1994. Zinc mining for protein domains. *Nat Struct Biol* **1**: 345-349.
9. Schjerling P and Holmberg S. 1996. Comparative amino acid sequence analysis of the C_6 zinc cluster family of transcriptional regulators. *Nucleic Acids Res* **24**: 4599-4607.

10. Lipscomb WN. 1983. Structure and catalysis of enzymes. *Annu Rev Biochem* **52**: 17-34.

11. Perez-Clausell J and Danscher G. 1985. Intravesicular localization of zinc in rat telencephalic boutons. A histochemical study. *Brain Res* **337**: 91-98.

12. Huang EP. 1997. Metal ions and synaptic transmission: think zinc. *Proc Natl Acad Sci U S A* **94**: 13386-13387.

13. Assaf SY and Chung SH. 1984. Release of endogenous Zn^{2+} from brain tissue during activity. *Nature* **308**: 734-736.

14. Howell GA, Welch MG, and Frederickson CJ. 1984. Stimulation-induced uptake and release of zinc in hippocampal slices. *Nature* **308**: 736-738.

15. Westbrook GL and Mayer ML. 1987. Micromolar concentrations of Zn^{2+} antagonize NMDA and GABA responses of hippocampal neurons. *Nature* **328**: 640-643.

16. Xie XM and Smart TG. 1991. A physiological role for endogenous zinc in rat hippocampal synaptic neurotransmission. *Nature* **349**: 521-524.

17. Wang K, Zhou B, Kuo YM, Zemansky J, and Gitschier J. 2002. A novel member of a zinc transporter family is defective in acrodermatitis enteropathica. *Am J Hum Genet* **71**: 66-73.

18. Neldner KH and Hambidge KM. 1975. Zinc therapy of acrodermatitis enteropathica. *New Eng J Med* **292**: 879-882.

19. Küry S, Dreno B, Bezieau S, Giraudet S, Kharfi M, Kamoun R, and Moisan JP. 2002. Identification of *SLC39A4*, a gene involved in acrodermatitis enteropathica. *Nature Genet* **31**: 239-240.

20. Huang XF and Arvan P. 1995. Intracellular transport of proinsulin in pancreatic β-cells. *J Biol Chem* **270**: 20417-20423.

21. Dodson G and Steiner D. 1998. The role of assembly in insulin's biosynthesis. *Curr Opin Struct Biol* **8**: 189-194.

22. Vu TH and Werb Z. 2000. Matrix metalloproteinases: effectors of development and normal physiology. *Genes Dev* **14**: 2123-2133.

23. Nagase H and Woessner JF, Jr. 1999. Matrix metalloproteinases. *J Biol Chem* **274**: 21491-21494.

24. Rock KL, York IA, and Goldberg AL. 2004. Post-proteasomal antigen processing for major histocompatibility complex class I presentation. *Nat Immunol* **5**: 670-677.

25. Serwold T, Gonzalez F, Kim J, Jacob R, and Shastri N. 2002. ERAAP customizes peptides for MHC class I molecules in the endoplasmic reticulum. *Nature* **419**: 480-483.

26. Galperin MY and Jedrzejas MJ. 2001. Conserved core structure and active site residues in alkaline phosphatase superfamily enzymes. *Proteins* **45**: 318-324.

27. Mann KJ and Sevlever D. 2001. 1,10-Phenanthroline inhibits glycosylphosphatidylinositol anchoring by preventing phosphoethanolamine addition to glycosylphosphatidylinositol anchor precursors. *Biochemistry* **40**: 1205-1213.

28. Shen Y, Meunier L, and Hendershot LM. 2002. Identification and characterization of a novel endoplasmic reticulum (ER) DnaJ homologue,

which stimulates ATPase activity of BiP in vitro and is induced by ER stress. *J Biol Chem* **277**: 15947-15956.

29. Silberstein S, Schlenstedt G, Silver PA, and Gilmore R. 1998. A role for the DnaJ homologue Scj1p in protein folding in the yeast endoplasmic reticulum. *J Cell Biol* **143**: 921-933.

30. Linke K, Wolfram T, Bussemer J, and Jakob U. 2003. The roles of the two zinc binding sites in DnaJ. *J Biol Chem* **278**: 44457-44466.

31. Zhao H and Eide D. 1996. The yeast *ZRT1* gene encodes the zinc transporter of a high affinity uptake system induced by zinc limitation. *Proc Natl Acad Sci U S A* **93**: 2454-2458.

32. Zhao H and Eide D. 1996. The *ZRT2* gene encodes the low affinity zinc transporter in *Saccharomyces cerevisiae*. *J Biol Chem* **271**: 23203-23210.

33. Waters BM and Eide DJ. 2002. Combinatorial control of yeast *FET4* gene expression in response to iron, zinc, and oxygen. *J Biol Chem* **277**: 33749-33757.

34. Zhao H and Eide DJ. 1997. Zap1p, a metalloregulatory protein involved in zinc-responsive transcriptional regulation in *Saccharomyces cerevisiae*. *Mol Cell Biol* **17**: 5044-5052.

35. Zhao H, Butler E, Rodgers J, Spizzo T, and Duesterhoeft S. 1998. Regulation of zinc homeostasis in yeast by binding of the ZAP1 transcriptional activator to zinc-responsive promoter elements. *J Biol Chem* **273**: 28713-28720.

36. Lyons TJ, Gasch AP, Gaither LA, Botstein D, Brown PO, and Eide DJ. 2000. Genome-wide characterization of the Zap1p zinc-responsive regulon in yeast. *Proc Natl Acad Sci U S A* **97**: 7957-7962.

37. MacDiarmid CW, Gaither LA, and Eide D. 2000. Zinc transporters that regulate vacuolar zinc storage in *Saccharomyces cerevisiae*. *EMBO J.* **19**: 2845-2855.

38. MacDiarmid CW, Milanick MA, and Eide DJ. 2002. Biochemical properties of vacuolar zinc transport systems of *Saccharomyces cerevisiae*. *J Biol Chem* **277**: 39187-39194.

39. MacDiarmid CW, Milanick MA, and Eide DJ. 2003. Induction of the *ZRC1* metal tolerance gene in zinc-limited yeast confers resistance to zinc shock. *J Biol Chem* **278**: 15065-15072.

40. Legatzki A, Franke S, Lucke S, Hoffmann T, Anton A, Neumann D, and Nies DH. 2003. First step towards a quantitative model describing Czc-mediated heavy metal resistance in *Ralstonia metallidurans*. *Biodegradation* **14**: 153-168.

41. Hantke K. 2001. Bacterial zinc transporters and regulators. *Biometals* **14**: 239-249.

42. Higgins CF. 1992. ABC transporters: from microorganisms to man. *Annu Rev Cell Biol* **8**: 67-113.

43. Patzer SI and Hantke K. 1998. The ZnuABC high affinity zinc uptake system and its regulator Zur in *Escherichia coli*. *Mol Microbiol* **28**: 1199-1210.

44. Scarborough GA. 2002. Molecular mechanism of the P-type ATPases. *J Bioenerg Biomembr* **34**: 235-250.

45. Beard SJ, Hashim R, Membrillo-Hernandez J, Hughes MN, and Poole RK. 1997. Zinc(II) tolerance in *Escherichia coli* K-12: evidence that the *zntA* gene (o732) encodes a cation transport ATPase. *Mol Microbiol* **25**: 883-891.

46. Rensing C, B M, and Rosen BP. 1997. The *zntA* gene of *Escherichia coli* encodes a Zn(II)-translocating P-type ATPase. *Proc Natl Acad Sci U S A* **94**: 14326-14331.

47. Hussain D, Haydon MJ, Wang Y, Wong E, Sherson SM, Young J, Camakaris J, Harper JF, and Cobbett CS. 2004. P-type ATPase heavy metal transporters with roles in essential zinc homeostasis in Arabidopsis. *Plant Cell* **16**: 1327-1339.

48. Eide D, Broderius M, Fett J, and Guerinot ML. 1996. A novel iron-regulated metal transporter from plants identified by functional expression in yeast. *Proc Natl Acad Sci U S A* **93**: 5624-5628.

49. Gaither LA and Eide DJ. 2001. Eukaryotic zinc transporters and their regulation. *Biometals* **14**: 251-270.

50. Grass G, Wong MD, Rosen BP, Smith RL, and Rensing C. 2002. ZupT is a Zn(II) uptake system in *Escherichia coli*. *J Bacteriol* **184**: 864-866.

51. Grotz N, Fox T, Connolly E, Park W, Guerinot ML, and Eide D. 1998. Identification of a family of zinc transporter genes from *Arabidopsis* that respond to zinc deficiency. *Proc Natl Acad Sci U S A* **95**: 7220-7224.

52. Lasat MM, Pence NS, Garvin DF, Ebbs SD, and Kochian LV. 2000. Molecular physiology of zinc transport in the Zn hyperaccumulator *Thlaspi caerulescens*. *J Exp Bot* **51**: 71-79.

53. Moreau S, Thomson RM, Kaiser BN, Trevaskis B, Guerinot ML, Udvardi MK, Puppo A, and Day DA. 2002. GmZIP1 encodes a symbiosis-specific zinc transporter in soybean. *J Biol Chem* **277**: 4738-4746.

54. Eide DJ. 2004. The SLC39 family of metal ion transporters. *Pflugers Arch* **447**: 796-800.

55. Eng BH, Guerinot ML, Eide D, and Saier MH. 1998. Sequence analyses and phylogenetic characterization of the ZIP family of metal ion transport proteins. *J Membr Biol* **166**: 1-7.

56. Rogers EE, Eide DJ, and Guerinot ML. 2000. Altered selectivity in an *Arabidopsis* metal transporter. *Proc Natl Acad Sci U S A* **97**: 12356-12360.

57. Liuzzi JP and Cousins RJ. 2004. Mammalian zinc transporters. *Annu Rev Nutr* **24**: 151-172.

58. Nies DH and Silver S. 1995. Ion efflux systems involved in bacterial metal resistances. *J Ind Microbiol* **14**: 186-199.

59. Paulsen IT and Saier MH. 1997. A novel family of ubiquitous heavy metal ion transport proteins. *J Membr Biol* **156**: 99-103.

60. Anton A, Grosse C, Reismann J, Pribyl T, and Nies DH. 1999. CzcD is a heavy metal transporter involved in regulation of heavy metal resistance in *Ralstonia* sp. Strain CH34. *J Bacteriol* **181**: 6876-6881.

61. Kamizono A, Nishizawa M, Teranishi Y, Murata K, and Kimura A. 1989. Identification of a gene conferring resistance to zinc and cadmium ions in the yeast *Saccharomyces cerevisiae*. *Mol Gen Genet* **219**: 161-167.

62. Guffanti AA, Wei Y, Rood SV, and Krulwich TA. 2002. An antiport mechanism for a member of the cation diffusion facilitator family: divalent cations efflux in exchange for K+ and H+. *Mol Microbiol* **45**: 145-153.

63. Persans MW, Nieman K, and Salt DE. 2001. Functional activity and role of cation-efflux family members in Ni hyperaccumulation in *Thlaspi goesingense*. *Proc Natl Acad Sci U S A* **98**: 9995-10000.

64. Chao Y and Fu D. 2004. Kinetic study of the antiport mechanism of an *Escherichia coli* zinc transporter, ZitB. *J Biol Chem* **279**: 12043-12050.

65. Seve M, Chimienti F, Devergnas S, and Favier A. 2004. *In silico* identification and expression of *SLC30* family genes: an expressed sequence tag data mining strategy for the characterization of zinc transporters' tissue expression. *BMC Genomics* **5**: 32.

66. Palmiter RD and Findley SD. 1995. Cloning and functional characterization of a mammalian zinc transporter that confers resistance to zinc. *EMBO J* **14**: 639-649.

67. Palmiter RD. 2004. Protection against zinc toxicity by metallothionein and zinc transporter 1. *Proc Natl Acad Sci U S A* **101**: 4918-4923.

68. Langmade SJ, Ravindra R, Daniels PJ, and Andrews GK. 2000. The transcription factor MTF-1 mediates metal regulation of the mouse ZnT1 gene. *J Biol Chem* **275**: 34803-34809.

69. McMahon RJ, Cousins RJ. 1998. Regulation of the zinc transporter ZnT-1 by dietary zinc. *Proc Natl Acad Sci U S A* **95**: 4841–46.

70. McMahon RJ, Cousins RJ. 1998. Mammalian zinc transporters. *J Nutr* **128**: 667–70.

71. Andrews GK, Wang H, Dey SK, and Palmiter RD. 2004. Mouse zinc transporter 1 gene provides an essential function during early embryonic development. *Genesis* **40**: 74.

72. Palmiter RD, Cole TB, and Findley SD. 1996. ZnT-2, a mammalian protein that confers resistance to zinc by facilitating vesicular sequestration. *EMBO J* **15**: 1784-1791.

73. Palmiter RD, Cole TB, Quaife CJ, and Findley SD. 1996. ZnT-3, a putative transporter of zinc into synaptic vesicles. *Proc Natl Acad Sci U S A* **93**: 14934-14939.

74. Wenzel H, Cole T, Born D, Schwartzkroin P, and Palmiter R. 1997. Ultrastructural localization of zinc transporter-3 (ZnT-3) to synaptic vesicle membranes within mossy fiber boutons in the hippocampus of mouse and monkey. *Proc Natl Acad Sci U S A* **94**: 12676-12681.

75. Huang L and Gitschier J. 1997. A novel gene involved in zinc transport is deficient in the lethal milk mouse. *Nat Genet* **17**: 292-297.

76. Michalczyk AA, Allen J, Blomeley RC, and Ackland ML. 2002. Constitutive expression of hZnT4 zinc transporter in human breast epithelial cells. *Biochem J* **364**: 105-113.

77. Palmiter RD and Huang L. 2004. Efflux and compartmentalization of zinc by members of the SLC30 family of solute carriers. *Pflugers Arch* **447**: 744-751.

78. Kambe T, Narita H, Yamaguchi-Iwai Y, Hirose J, Amano T, Sugiura N, Sasaki R, Mori K, Iwanaga T, and Nagao M. 2002. Cloning and characterization of a novel mammalian zinc transporter, zinc transporter 5, abundantly expressed in pancreatic beta cells. *J Biol Chem* **277**: 19049-19055.

79. Chimienti F, Devergnas S, Favier A, and Seve M. 2004. Identification and cloning of a beta-cell-specific zinc transporter, ZnT-8, localized into insulin secretory granules. *Diabetes* **53**: 2330-2337.

80. Huang L, Kirschke CP, and Gitschier J. 2002. Functional characterization of a novel mammalian zinc transporter, ZnT6. *J Biol Chem* **277**: 26389-26395.

81. Kirschke CP and Huang L. 2003. ZnT7, A novel mammalian zinc transporter, accumulates zinc in the Golgi apparatus. *J Biol Chem* **278**: 4096-4102.

82. Clemens S, Bloss T, Vess C, Neumann D, Nies DH, and Zur Nieden U. 2002. A transporter in the endoplasmic reticulum of *Schizosaccharomyces pombe* cells mediates zinc storage and differentially affects transition metal tolerance. *J Biol Chem* **277**: 18215-18221.

83. Borrelly GP, Harrison MD, Robinson AK, Cox SG, Robinson NJ, and Whitehall SK. 2002. Surplus zinc is handled by Zym1 metallothionein and

Zhf endoplasmic reticulum transporter in *Schizosaccharomyces pombe*. *J Biol Chem* **277**: 30394-30400.

84. Li L and Kaplan J. 1997. Characterization of two homologous yeast genes that encode mitochondrial iron transporters. *J Biol Chem* **272**: 28485-28493.

85. Foury F and Roganti T. 2002. Deletion of the mitochondrial carrier genes *MRS3* and *MRS4* suppresses mitochondrial iron accumulation in a yeast frataxin-deficient strain. *J Biol Chem* **277**: 24475-24483.

86. Conklin DS, McMaster JA, Culbertson MR, and Kung C. 1992. *COT1*, a gene involved in cobalt accumulation in *Saccharomyces cerevisiae*. *Mol Cell Biol* **12**: 3678-3688.

CHAPTER 2

ZINC AND THE MSC2 ZINC TRANSPORTER PROTEIN ARE REQUIRED FOR ENDOPLASMIC RETICULUM FUNCTION

Charissa D. Ellis, Fudi Wang, Colin W. MacDiarmid, Suzanne Clark, Thomas Lyons, and David J. Eide*

Departments of Biochemistry and Nutritional Sciences
University of Missouri, Columbia, MO 65211

*This work is reproduced from *The Journal of Cell Biology* © 2004, Volume 166, Number 3, Issue of August 2, 2004, pp. 325-335 by copyright permission of The Rockefeller University Press.

ABSTRACT

In this report, we show that zinc is required for endoplasmic reticulum (ER) function in *Saccharomyces cerevisiae*. Zinc deficiency in this yeast induces the unfolded protein response (UPR), a system normally activated by unfolded ER proteins. Msc2p, a member of the cation diffusion facilitator (CDF) family of metal ion transporters, was previously implicated in zinc homeostasis. Our results indicate that Msc2p is one route of zinc entry into the ER. Msc2p localizes to the ER when expressed at normal levels. UPR induction in low zinc is exacerbated in an *msc2* mutant. Genetic and biochemical evidence indicate that this UPR induction is due to genuine ER dysfunction. Notably, we found that ER-associated protein degradation (ERAD) is defective in zinc-limited *msc2* mutants. We also show that the vacuolar CDF proteins Zrc1p and Cot1p are other pathways of ER zinc acquisition. Finally, zinc deficiency up-regulates the mammalian ER stress response indicating a conserved requirement for zinc in ER function among eukaryotes.

INTRODUCTION

Zinc is an important cofactor for many proteins that reside in or pass through organelles of the secretory system. For example, packaging of insulin in secretory granules of pancreatic β-cells is dependent on Zn^{2+} (1, 2). Matrix metalloproteases are Zn^{2+}-requiring enzymes that are secreted by cells to modify the extracellular matrix during development and tumor cell metastasis (3). These proteins acquire zinc at an early point in the secretory pathway (4, 5). Addition of phosphoethanolamine groups to glycosylphosphatidylinositol- (GPI-) anchors requires Zn^{2+}-dependent enzymes in the endoplasmic reticulum (ER) (6-8). As a last example, some protein chaperones homologous to *Escherichia coli* DnaJ, like the ER-localized Scj1p of *Saccharomyces cerevisiae*, likely require Zn^{2+} to function in protein folding and in the degradation of misfolded proteins by quality control mechanisms (9-12). These many requirements for Zn^{2+} in the secretory pathway highlight the need for zinc transporters to deliver the metal to those organelles. Despite the importance of these various zinc-dependent processes in normal cell function and disease states such as cancer, the transport proteins responsible for zinc delivery have not yet been identified.

Members of the cation diffusion facilitator (CDF) family of transport proteins are likely candidates to transport Zn^{2+} into the secretory pathway. CDF proteins play conserved roles in transporting Zn^{2+} from the cytosol into organelles or out of the cell in many organisms (13-16). In *E. coli*, for example, the ZitB CDF protein transports excess zinc from the cytosol to the extracellular environment (17). In mammals, ZnT1 similarly transports excess cytosolic zinc

while ZnT2 may detoxify the metal by sequestering it in the late endosome (18-20). Three mammalian CDF proteins implicated in Zn^{2+} transport into the secretory pathway are ZnT5, ZnT6, and ZnT7, each of which having been localized to the Golgi apparatus (21-23). The functional roles of these proteins are not yet clear.

We have learned much about zinc homeostasis from studies of the yeast *S. cerevisiae*. In this yeast, zinc uptake is mediated by the high affinity Zrt1p transporter and the lower affinity Zrt2p and Fet4p proteins (24-26). The genes encoding these transporters are controlled by the Zap1p transcriptional activator protein (27). Zap1p is active in zinc-limited cells, and its activity is repressed in zinc-replete cells. Zap1p binds to one or more zinc-responsive elements (ZREs) in the promoters of its target genes (28).

Zinc storage and detoxification in *S. cerevisiae* is mediated by the vacuole. The Zrc1p and Cot1p proteins, both members of the CDF family, are responsible for zinc transport into the vacuole (29-32). Two other CDF proteins, Mmt1p and Mmt2p, have been implicated in iron transport in the mitochondria (33). The fifth yeast CDF member, and the subject of this report, is Msc2p. Msc2p was first identified in a screen for mutations with altered frequencies of meiotic sister chromatid exchange (34). However, the link between DNA recombination and the *MSC2* gene is unclear; the effects on recombination are allele-specific and not observed in a full *msc2* deletion mutant (35). A more recent study of Msc2p suggested that it played some role in zinc metabolism (36). An *msc2* mutant grew poorly on respired carbon sources at elevated

temperatures and had an abnormally large cell size. Both of these phenotypes were suppressed by addition of excess zinc. In this report, we demonstrate that Msc2p is an ER membrane protein whose role is to maintain proper function of the ER. Our results indicate that key processes in the ER require Zn^{2+} and that Msc2p is involved in supplying Zn^{2+} to this compartment.

EXPERIMENTIAL PROCEDURES

Yeast strains and growth conditions

Media used were YPD, SD, YPGE, and LZM as described previously (37). Strains used are described in **Table 2.1**. Yeast deletion mutants were obtained from Research Genetics. To generate several strains, the *KanMX* cassette with 500 bp flanking the gene to be mutated was amplified by PCR from the appropriate mutant. The PCR fragment was then transformed into the appropriate recipient strain. This method was used to generate strains CEY3-8, CEY27-29, CM158, CM160, CM162, and CM164. CM158 and CM164 were crossed to generate CEY25, and CM160 and CM162 were crossed to generate CEY26. CEY13 and CEY17 are haploid segregants of CEY25 and CEY26, respectively. CEY8 and DY150 were crossed to generate CEY24. CEY19-23 and CEY27-29 are haploid segregants of CEY24.

Yeast Plasmids

pDg2L (ZRE-*lacZ*) (30), pHYC3 (*HIS4-lacZ*) (38), and pMCZ-Y (UPRE-*lacZ*) (39) were described previously. pSN222 (Kex2p-HA) was a gift of Steve Nothwehr (University of Missouri). pRK315 (Pma1p-HA) was a gift of Ralf Kölling (Düsseldorf, Germany). pDN436 (CPY*-HA) was a gift of Davis Ng (Pennsylvania State University). pGEV-TRP1 was co-transformed with pRK315 so that Pma1p-HA expression levels could be controlled by β-estradiol (Sigma) (10^{-7}M) addition (40). pMCZ-YL was constructed by exchanging the *URA3* gene on pMCZ-Y with the *LEU2* gene by marker swapping (41). pDN436U was

Table 2.1. Strains used in this study

Strain	Genotype	Reference
DY150	*MATa ade2 can1 his3 leu2 trp1 ura3*	(36)
DY150 *msc2*	DY150 *msc2::HIS3*	(36)
DY1457	*MATα ade6 can1 his3 leu2 trp1 ura3*	(24)
ZHY1	DY1457 *zrt1::LEU2*	(24)
CM100	*MATα can1 his3 leu2 trp1 ura3*	(30)
CM102	CM100 *zrc1::HIS3*	(30)
CM103	CM100 *cot1::URA3*	(30)
CM104	CM100 *zrc1::HIS3 cot1::URA3*	(30)
CM158	CM100 *scj1::KanMX*	This Work
CM160	CM100 *jem1::KanMX*	"
CM162	DY150 *msc2::HIS3 scj1::KanMX*	"
CM164	DY150 *msc2::HIS3 jem1::KanMX*	"
CEY3	DY150 *ire1::KanMX*	"
CEY4	DY150 *hac1::KanMX*	"
CEY5	DY150 *msc2::HIS3 ire1::KanMX*	"
CEY6	DY150 *msc2::HIS3 hac1::KanMX*	"
CEY7	CM100 *msc2::KanMX*	"
CEY8, 27-29	CM100 *msc2::KanMX zrc1::HIS3 cot1::URA3*	"
CEY13	DY150 *jem1::KanMX*	"
CEY17	DY150 *jem1::KanMX scj1::KanMX*	"
CEY19-21	CM100 *msc2::KanMX zrc1::HIS3*	"
CEY22, 23	CM100 *msc2::KanMX cot1::URA3*	"
CEY24	DY150 X CEY8 diploid *MATa/α can1/can1 ade2/ADE2 his3/his3 leu2/leu2 trp1/trp1 ura3/ura3 msc2::KanMX zrc1::HIS3 cot1::URA3*	"
CEY25	CM158 X CM164 diploid *MATa/α can1/can1 ade2/ADE2 ade6/ADE6 his3/his3 leu2/leu2 trp1/trp1 ura3/ura3 msc2::HIS3 jem1::KanMX scj1::KanMX*	"
CEY26	CM160 X CM162 diploid *MATa/α can1/can1 ade2/ADE2 ade6/ADE6 his3/his3 leu2/leu2 trp1/trp1 ura3/ura3 msc2::HIS3 jem1::KanMX scj1::KanMX*	"

constructed by exchanging the *LEU2* gene on pDN436 with the *URA3* gene (41). To generate pMSC2, the *MSC2* ORF plus ~500 bp of flanking DNA was amplified by PCR from genomic DNA and inserted into *Eco*R1-, *Pst*1-digested pFL38 by homologous recombination (42). Msc2p function was confirmed by complementing the *msc2* mutant. To generate pMSC2HA, the *MSC2* ORF plus ~500 bp promoter and lacking the stop codon was PCR amplified from genomic DNA and inserted into YCpZRC1-HA (32) by homologous recombination. The resulting plasmid has the *MSC2* promoter and ORF followed by three HA tags. The plasmid was confirmed by complementing the *msc2* mutant. To generate pHAC1, the *HAC1* ORF plus ~1300 bp upstream and ~900 bp downstream flanking DNA were amplified from genomic DNA and inserted into *Sac*1-, *Xma*1-digested pRS315 via homologous recombination. To generate pHAC1^{i}, overlap PCR was used to generate the *HAC1* ORF (plus flanking DNA as above) without the intron (43). This fragment was then inserted into pRS315 via homologous recombination. DNA sequencing confirmed the lack of the intron.

Yeast β-galactosidase assays

β-galactosidase assays were performed on protein extracts (44) and specific activity was normalized to protein content.

Subcellular fractionation and immunoblotting

Subcellular fractionation was done largely as described by Roberg et al. (45). Lysates were fractionated on 20-60% sucrose gradients prepared with 10

mM EDTA (-Mg) or with 2 mM $MgSO_4$ (+Mg). Immunoblots were done by standard techniques (46). Blots were visualized with ECL (Amersham Biosciences), and band quantitation was performed using NIH Image 1.61. Antibodies used were mouse anti-HA (12CA5, Roche), rabbit anti-HA (Sigma), mouse anti-Dpm1p (Molecular Probes), mouse anti-Pgk1p (Molecular Probes), goat anti-mouse HRP-conjugated secondary (Pierce), and goat anti-rabbit HRP-conjugated secondary (Pierce).

Assay of ER-associated degradation (ERAD)

Yeast were grown in 200 mL cultures to an OD_{600} = ~ 0.5. Cells were harvested and resuspended in 100 mL fresh medium to a final OD_{600} = ~ 1.0. Cells were grown 30 minutes, then cycloheximide (Sigma) was added to a final concentration of 100 μg/mL. Five mL aliquots of cells were removed at each time point to tubes containing NaN_3 to a final concentration of 10 mM. After the last time point, the cells were collected by centrifugation and washed once with cold buffer containing 10 mM NaN_3, 1 mM EDTA. Cells were resuspended in 1 mL of the same buffer and transferred to microfuge tubes. Cells were pelleted and resuspended in 200 μL cold protein extraction buffer [10 mM Tris-Cl, pH 8, 25 mM ammonium acetate, 1 mM EDTA, 1 mM PMSF, 10% Trichloroacetic acid (Sigma), yeast proteinase inhibitor cocktail (complete mini EDTA-free pellets, Roche)]. An equal volume of glass beads was added and the tubes were vortexed 5 times for 1 min, with 1 min on ice between pulses. Lysates were transferred to fresh tubes. Another 500 μL protein extraction buffer was added to

the glass beads, vortexed 1 min, and then pooled with the previous lysates. Lysates were centrifuged at 14,000 X g at 4°C for 10 min. The supernatant was removed and discarded. The pellets were resuspended in 120 μL buffer I (100 mM Tris base, 3% SDS, 1 mM PMSF), then boiled for 5 min. Insoluble debris was pelleted by centrifuging 5 min at 15,800 x g. The supernatant was transferred to new tubes and protein concentrations were measured using the BIO-RAD D_C protein kit. Ten μg of protein were loaded per lane when analyzed by immunoblotting.

Cell culture, transient transfection, mammalian plasmids and assays

HeLa cells were cultured in DMEM (Invitrogen) plus 0.45% glucose under 5% CO_2. All media contained 100 U/mL penicillin, 100 μg/mL streptomycin, 2 mM L-glutamine and 100 μM MEM non-essential amino acids (Invitrogen) supplemented with 10% fetal bovine serum (Invitrogen). p5xATF6GL3 was a gift of Ron Prywes (Columbia University), and contains five repeats of an ATF6 binding site cloned into a minimal promoter preceding the firefly luciferase gene (47). pSV-β-galactosidase control vector (Promega) was used as a control for transfection efficiency. HeLa cells (~1.2 x 10^6) were seeded in 60 mm plates and transiently transfected using Lipofectamine 2000 (Invitrogen). Both p5xATF6GL3 and pSV-β-galactosidase plasmids were co-transfected in all experiments. Transfection efficiencies were typically 60%. 36-48 hours post-transfection, tunicamycin (Sigma), $ZnCl_2$, or N,N,N´,N´-tetrakis-(2-pyridylmethyl)ethylenediamine (TPEN) (Sigma) was added to the culture medium

at the indicated concentrations. After treatment, the cells were washed 3 times with cold PBS. To generate protein extracts and perform luciferase and β-galactosidase assays, the Luciferase Assay System with Reporter Lysis Buffer (Promega) was used. Luciferase activity was normalized to β-galactosidase activity as an internal control.

RESULTS

Zinc deficiency induces the Unfolded Protein Response

Genome-wide cDNA microarray analysis of gene expression in *S. cerevisiae* indicated that many genes (458) are induced by zinc deficiency (48). This included 46 direct Zap1p targets and 412 genes up-regulated in a Zap1p-independent fashion. Induction of this latter group probably reflects indirect effects of zinc deficiency on cell function. Among the genes indirectly affected by zinc were several involved in the Unfolded Protein Response (UPR). The UPR is a response to the accumulation of unfolded proteins in the ER (49). **Figure 2.1A** summarizes the microarray results for eight genes of the UPR (50) that were up-regulated by two-fold or more in zinc-deficient wild type cells. The up-regulation of these genes is independent of Zap1p; each showed similar induction by zinc deficiency in a *zap1* mutant. The UPR genes induced by zinc deficiency include *ERO1*, *EUG1*, and *PDI1* (encoding proteins involved in protein disulfide isomerization), and *FKB2* (encoding peptidyl-prolyl cis-trans isomerase). In addition, *JEM1*, *KAR2*, *LHS1*, and *SCJ1* were also up-regulated. These genes encode ER chaperones that facilitate the translocation of misfolded ER proteins back to the cytosol for degradation in a process known as ER-associated degradation or ERAD.

These data indicated that zinc deficiency up-regulates the UPR. To confirm this hypothesis, we used a UPR-responsive reporter gene to assess the effect of zinc deficiency on UPR induction. UPR target genes contain UPRE sequences in their promoters that confer this regulation. A UPRE-*lacZ* reporter

Figure 2.1. *Zinc deficiency induces the unfolded protein response (UPR).* A, Microarray analysis of UPR target genes showing ≥ 2-fold induction in low zinc over high zinc in both wild type and *zap1* mutant cells. These data are from experiments previously described (48). B, UPRE-*lacZ* activity in wild type (WT, DY1457) and the *zrt1* mutant (ZHY1) over a range of zinc concentrations in LZM. LZM is zinc limiting because 1 mM EDTA is added to limit metal availability. Shown are representative data from two experiments. C, *HIS4-lacZ* activity in DY1457 and ZHY1 in low (1 μM) and high (1000 μM) zinc in LZM. Shown are representative data from two experiments. The error bars indicate ± 1 S.D.

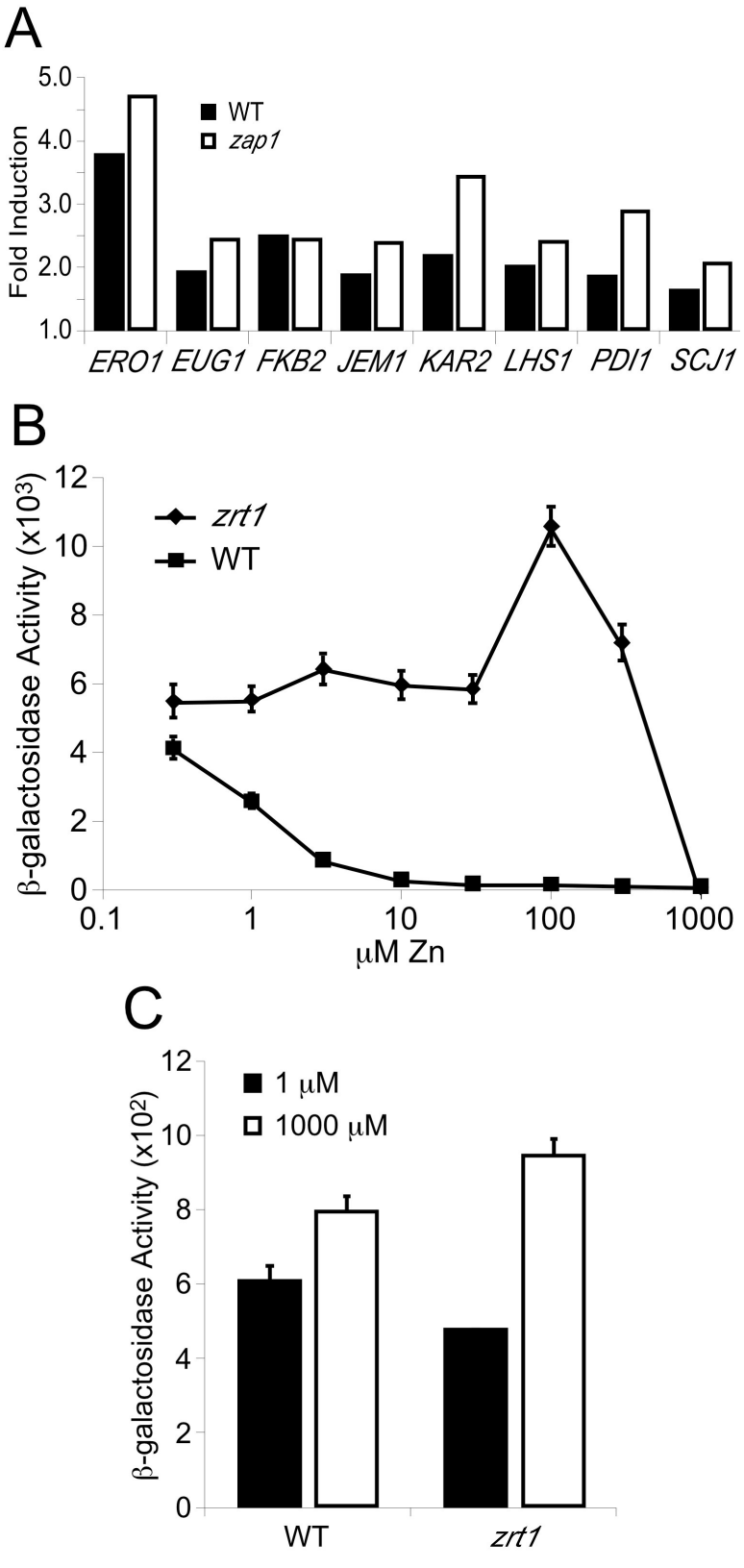
A
5.0
4.0
3.0
2.0
1.0
Fold Induction
WT
zap1
ERO1 EUG1 FKB2 JEM1 KAR2 LHS1 PDI1 SCJ1
B
β-galactosidase Activity (x10³)
12
10
8
6
4
2
0
zrt1
WT
0.1
1
10
100
1000
μM Zn
C
β-galactosidase Activity (x10²)
12
10
8
6
4
2
0
1 μM
1000 μM
WT
zrt1

was highly induced in wild type cells grown in low zinc (e.g. LZM + 0.3 μM Zn) relative to zinc-replete cells (e.g. LZM + 1000 μM Zn) (**Figure 2.1B**). These experiments were performed using LZM medium which is zinc-limiting due to addition of 1 mM EDTA. Adding as little as 10 μM $ZnCl_2$ to LZM was sufficient to repress UPRE-*lacZ* expression. UPRE-*lacZ* induction in low zinc was also observed in *zrt1* mutants defective for zinc uptake. Because Zrt1p is the major zinc uptake transporter in yeast, the *zrt1* mutant is zinc deficient when grown in LZM supplemented with ≤ 300 μM $ZnCl_2$ (24). The UPRE-*lacZ* reporter showed high levels of β-galactosidase activity in the *zrt1* mutant over a wide range of zinc concentrations and was suppressed only by adding 1000 μM zinc to the medium (**Figure 2.1B**). A *HIS4-lacZ* control reporter, which is not responsive to either zinc or unfolded proteins, showed high expression in both the wild type and the *zrt1* mutant strains at all zinc concentrations (**Figure 2.1C**). Therefore, the effects seen with the UPRE-*lacZ* reporter are specific UPR effects and not general effects on β-galactosidase activity. The 2-fold increase in UPRE-*lacZ* expression observed between 30 and 100 μM zinc (**Figure 2.1B**) is similar to that seen with other promoters (e.g. *HIS4-lacZ*, **Figure 2.1C**) and probably reflects a general decrease in expression in severely zinc-deficient cells.

Msc2p localizes to the endoplasmic reticulum

Induction of the UPR in low zinc suggested that zinc transport into the lumen of the ER is required for ER function. A transporter protein possibly

involved in delivering zinc into the ER is encoded by the *MSC2* gene. Previous studies suggested that Msc2p was localized to the endoplasmic reticulum. However, these experiments were done under conditions where Msc2p was overexpressed. Because overexpression can result in protein mislocalization, the true intracellular location of Msc2p was unclear. Therefore, we determined the localization of Msc2p when expressed from its own promoter on a low copy plasmid. To aid detection of Msc2p, we generated an *MSC2* allele with three hemagglutinin (HA) tags fused to its C-terminus. Immunoblots detected only a single band near the predicted molecular mass of Msc2p (data not shown). Moreover, the epitope-tagged protein complemented the temperature-sensitive growth defect phenotype of an *msc2* mutant strain indicating that it is functional.

Attempts to determine the subcellular localization of Msc2p using immunofluorescence microscopy were inconclusive because the level of expression was too low. Therefore, we used sucrose gradient fractionation to assess the distribution of Msc2p. Protein extracts of wild type cells expressing HA-tagged Msc2p were separated on sucrose gradients. After centrifugation, fractions were collected and analyzed by immunoblotting. Previous reports have shown that the presence or absence of Mg^{2+} greatly alters the position of ER vesicles in the gradient (45). Without added Mg^{2+}, the ER co-fractionates with the Golgi apparatus in the middle fractions of the gradient. However, in the presence of Mg^{2+}, the ER localizes to the heavier fractions of the gradient, co-fractionating with the plasma membrane. This shift to heavier fractions is likely due to ribosomes remaining associated with the ER when Mg^{2+} is present. If

Msc2p localizes to the ER, we predicted that the protein would show this Mg^{2+}-dependent shift in these gradients.

Kex2p is a Golgi marker protein and its fractionation, peaking around fraction 6 in the middle of the gradients (**Figure 2.2**), was unaffected by Mg^{2+}. A plasma membrane protein, Pma1p, also was largely unaffected by Mg^{2+} levels with its peak fractionation in the heaviest fractions of both gradients. Dpm1p served as an ER marker. Both Msc2p and Dpm1p showed the diagnostic ER Mg^{2+} shift, being found in the heavier fractions with Mg^{2+} and fractionating in the middle fractions without Mg^{2+}. Because Msc2p co-fractionates with an ER marker protein and shows the characteristic ER Mg^{2+} shift, these studies strongly support the localization of Msc2p to that compartment. In the presence of Mg^{2+}, some Msc2p was also found in lighter fractions that may correspond to the Golgi. Little Dpm1p was found in these lighter fractions.

Mutation of MSC2 alters zinc homeostasis

If Msc2p transports zinc into the ER lumen, we predicted that mutation of the *MSC2* gene would alter homeostasis of cytosolic labile zinc. A useful bioassay of this labile zinc is the Zap1p transcription factor which binds to zinc-responsive elements (ZREs) in it target promoters. Zap1p is active in zinc-limited cells and repressed by high zinc. The zinc response curve of a ZRE-*lacZ* reporter in wild type cells is shown in **Figure 2.3A**. If Msc2p transported zinc into the ER, we predicted that cytosolic zinc levels would increase in an *msc2* mutant strain and repress Zap1p activity. Consistent with this prediction, expression of

Figure 2.2. *Msc2p is localized to the endoplasmic reticulum.* Lysates were prepared from wild type (WT, DY150) cells expressing either pMSC2HA and pSN222 (Kex2p-HA) or pGEV-TRP1 and pRK315 (Pma1p-HA). Extracts were layered onto sucrose gradients for subcellular fractionation. Gradient fractions were subjected to immunoblotting and probed with anti-HA or anti-Dpm1p antibodies. Fractions are numbered from 1 (heaviest) to 11 (lightest). Shown are representative data from three experiments. A, Plot of immunoblot band intensities from fractions prepared +Mg. B, Plot of immunoblot band intensities from fractions processed -Mg. The lines labeled ER, PM, and Golgi denote fractions containing ≥ 50% of the peak values for the corresponding marker protein.

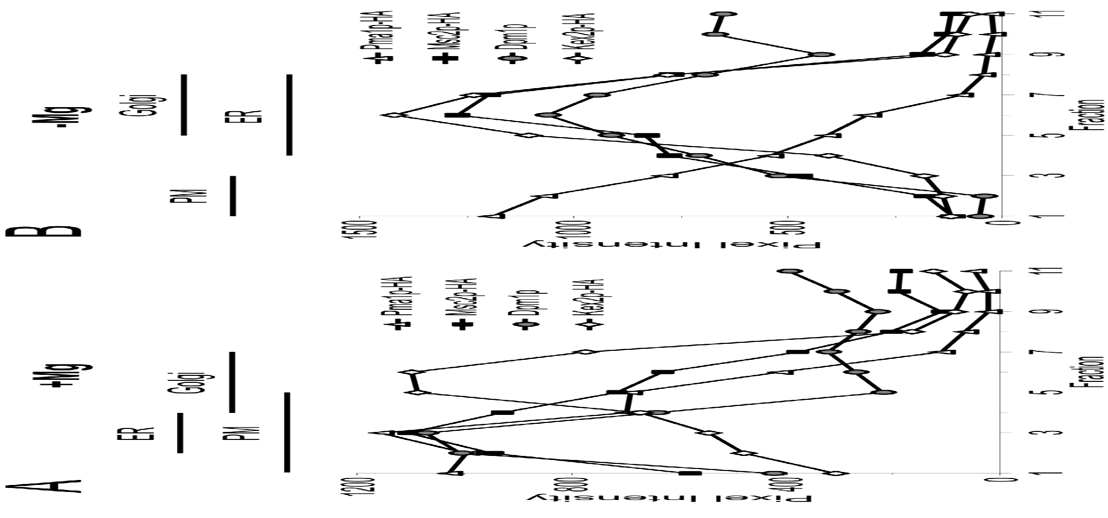
A
+Mg
ER
Golgi
PM
Pixel intensity
1200
800
400
0
1
3
5
7
9
11
Fraction
Pma1p-HA
Dpm1p
Kex2p-HA
B
-Mg
PM
Golgi
ER
1500
1000
500

Figure 2.3. *The msc2 mutant increases labile zinc levels.* A, ZRE-*lacZ* activity in wild type (WT, DY150) and the *msc2* mutant (DY150 *msc2*) grown over a range of zinc concentrations in LZM. Shown are representative data from five experiments. B, *HIS4-lacZ* activity in wild type (WT, DY150) and the *msc2* mutant (DY150 *msc2*) in low (1 μM) and high (1000 μM) zinc in LZM. Shown are representative data from five experiments. The error bars indicate ± 1 S.D.

A
β-galactosidase Activity (x10³)
14
12
10
8
6
4
2
0
WT
msn2
0
10
1
0.1
μM Zn
1000
B
β-galactosidase Activity (x10³)
12
10
8
6
4
2
0
1 μM
1000 μM
WT
msn2

the ZRE-*lacZ* reporter was suppressed in *msc2* cells grown in LZM + 0.3-10 μM $ZnCl_2$ (**Figure 2.3A**). Mutation of *MSC2* did not decrease expression of the *HIS4-lacZ* reporter indicating that the effects of the *msc2* mutation were specific to the ZRE-*lacZ* reporter (**Figure 2.3B**). These results suggest that Msc2p transports zinc from the cytosol into the ER lumen.

Effects of msc2 mutation on UPR induction

If Msc2p transports zinc into the ER, we predicted that an *msc2* mutant would increase induction of the UPR in low zinc relative to wild type cells. This prediction was confirmed using the UPRE-*lacZ* reporter (**Figure 2.4A**). While the wild type strain showed some induction of the UPR in low zinc, this up-regulation was substantially increased in the *msc2* mutant strain. These data suggest that a strain lacking *MSC2* experiences greater ER stress when coupled with zinc deficiency. To determine the metal specificity of this effect, we measured UPRE-*lacZ* expression in an *msc2* mutant under low zinc conditions when higher levels of zinc or other metals were added. While as little as 10 μM zinc suppressed the UPR up-regulation, neither 10 μM nor 100 μM of Fe^{2+}, Cu^{2+}, Cd^{2+}, Mn^{2+}, Ni^{2+}, or Co^{2+} greatly suppressed this up-regulation (**Figure 2.4B**). Therefore, UPR induction in an *msc2* mutant is a zinc-specific effect.

Figure 2.4. *The msc2 mutant increases UPR induction in zinc deficiency.* A, UPRE-*lacZ* activity in wild type (WT, DY150) and the *msc2* mutant (DY150 *msc2*) over a range of zinc concentrations in LZM. Shown are representative data from three experiments. B, UPRE-*lacZ* activity in the *msc2* mutant in LZM + 0.3 μM Zn. The control condition (C) had no added metals. Shown are representative data from two experiments. The error bars indicate ± 1 S.D.

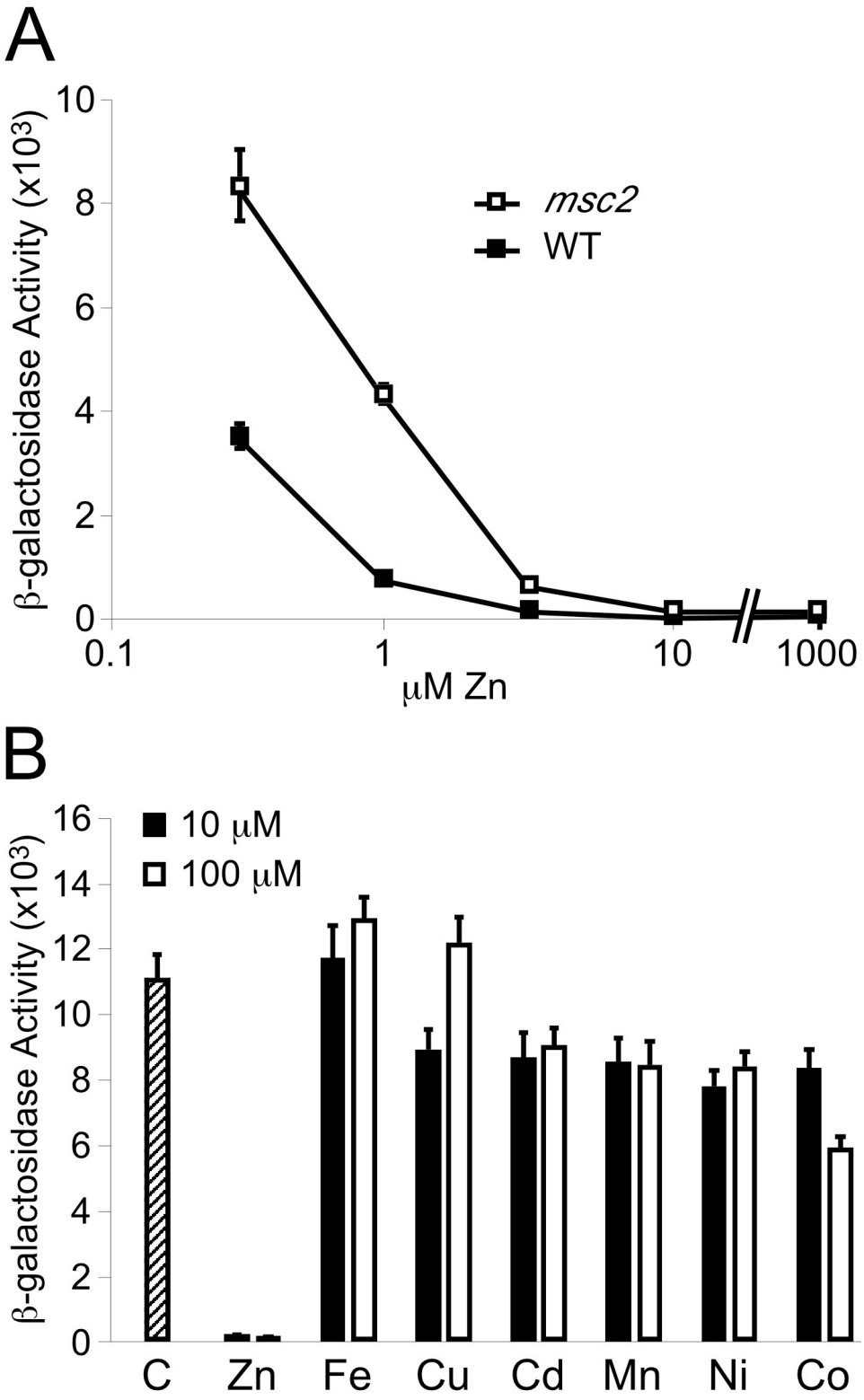
A
β-galactosidase Activity (x10³)
10
8
6
4
2
0
0.1
1
10
1000
μM Zn
msc2
WT
B
β-galactosidase Activity (x10³)
16
14
12
10
8
6
4
2
0
10 μM
100 μM
C
Zn
Fe
Cu
Cd
Mn
Ni
Co

UPRE-lacZ induction by low zinc and msc2 mutation requires a functioning UPR signaling pathway

UPR induction is achieved through a two-protein signaling pathway (for review, see (49)). Ire1p is a transmembrane endoribonuclease protein that senses unfolded proteins in the ER. Hac1p is the transcription factor that responds to that signal to increase expression of UPR target genes. When Ire1p is activated by unfolded ER proteins, it cleaves an intron out of the *HAC1* mRNA. The spliced *HAC1* mRNA is translated into protein (Hac1p^{i}), which then up-regulates UPR target genes. To verify that the induction of the UPR in an *msc2* mutant is dependent upon the Ire1p/Hac1p signaling pathway, we constructed *msc2 ire1* and *msc2 hac1* double mutants and analyzed their UPRE-*lacZ* activity. Dithiothreitol (DTT), a known inducer of the UPR because of its ability to disrupt disulfide bonds in ER proteins, did not cause UPRE-*lacZ* induction in *ire1* and *hac1* mutants in both the wild type and the *msc2* mutant backgrounds (data not shown). These mutants were also impaired for induction of the UPR in low zinc (**Figure 2.5A**). These strains had no such effect on the control *HIS4-lacZ* reporter (data not shown). Therefore, the induction of the UPR in low zinc in an *msc2* mutant requires the full UPR signaling pathway.

One can also envisage that an *msc2* mutant may somehow hyperactivate Hac1p^{i} independently of Ire1p. To test this hypothesis, we introduced an intron-less form of the *HAC1* gene on a low copy plasmid (pHAC1^{i}) into both wild type and *msc2* mutant strains. This plasmid-encoded Hac1p^{i} does not rely upon Ire1p for its activation, and therefore causes constitutive UPR induction. We predicted

Figure 2.5. *The msc2 mutant requires Ire1p and Hac1p for UPR induction.* A, UPRE-*lacZ* activity in wild type (WT, DY150), *msc2* (DY150 *msc2*), *ire1* (CEY3), *hac1* (CEY4), *msc2 ire1* (CEY5), and *msc2 hac1* (CEY6) in low (1 μM) and high (1000 μM) zinc in LZM. Shown are representative data from three experiments. B, UPRE-*lacZ* activity in wild type (WT, DY150) and the *msc2* mutant (DY150 *msc2*) expressing vector (pRS315) or pHAC1^{i} in low (1 μM) zinc in LZM. Shown are representative data from five experiments. The error bars indicate ± 1 S.D.

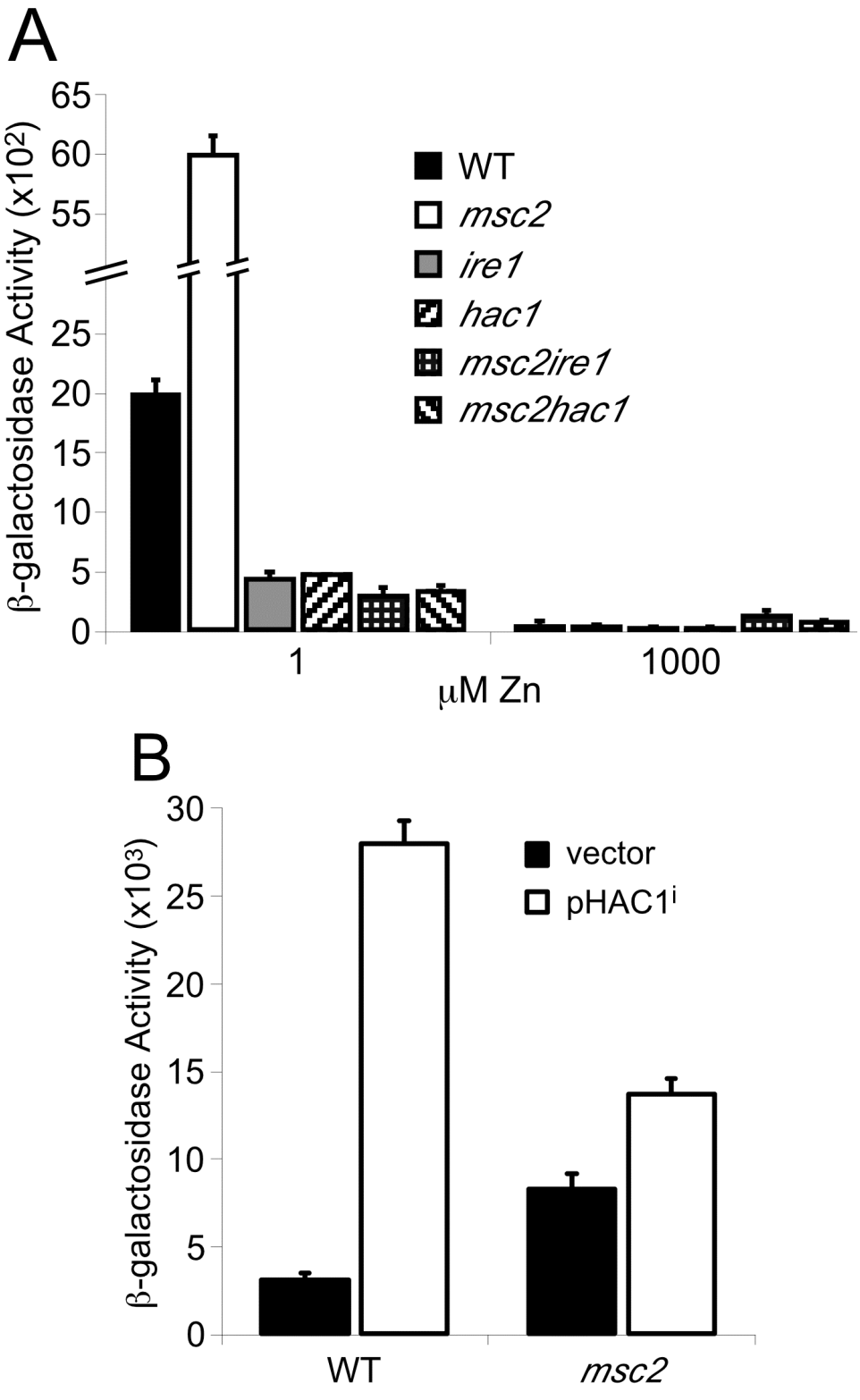
A
β-galactosidase Activity (x10²)
65
60
55
25
20
15
10
5
0
WT
msc2
ire1
hac1
msc2ire1
msc2hac1
1
1000
μM Zn
B
β-galactosidase Activity (x10³)
30
25
20
15
10
5
0
vector
pHAC1ⁱ
WT
msc2

that if the *msc2* mutation made endogenous Hac1p^{i} more active, it would have a similar effect on plasmid-encoded Hac1p^{i}. This was not the case. Introduction of pHAC1^{i} into wild type cells actually caused higher levels of UPRE-*lacZ* activity than was observed in the *msc2* mutant (**Figure 2.5B**). While the reason for the decreased expression in the mutant is not yet known, this result clearly demonstrates that the *msc2* mutation does not increase Hac1p^{i} activity independently of the UPR signaling pathway.

Genetic and biochemical evidence for ER dysfunction in msc2 mutants

The requirement for an intact Ire1p/Hac1p signaling pathway to induce the UPR in response to low zinc and loss of Msc2p function suggested that these factors perturbed ER function. Further evidence supporting this conclusion came from the observation that *msc2 ire1* and *msc2 hac1* mutants exhibit a synthetic lethal growth phenotype. *msc2* single mutants grow poorly at 37°C on YP medium supplemented with glycerol and ethanol, two nonfermentable carbon sources, but show no such defect on medium supplemented with glucose (YPD), a fermentable carbon source (**Figure 2.6**). Similarly, neither *ire1* nor *hac1* mutants exhibit a growth defect on YPD at either 30°C or 37°C. Combining these mutations, i.e. *msc2 ire1* and *msc2 hac1*, resulted in a strong growth defect at 37°C. [The few colonies seen in the *msc2 hac1* mutant at 37°C may be the result of spontaneously arising suppressor mutations. More than 99% of the inoculated *msc2 hac1* cells failed to grow at the elevated temperature.] Introducing the *MSC2* or *HAC1* genes on low copy plasmids (pMSC2, pHAC1)

Figure 2.6. *The msc2 mutant is synthetically lethal with ire1 and hac1 at elevated temperatures.* Yeast cells were grown in YPD or SD liquid medium overnight. Cultures were diluted in fresh medium and 5 μL volumes (10^4 cells) were plated onto YPD plates, incubated at 30°C or 37°C, and photographed after 2 days. Wild type (WT, DY150), *msc2* (DY150 *msc2*), *ire1* (CEY3), *hac1* (CEY4), *msc2 ire1* (CEY5), and *msc2 hac1* (CEY6) were grown and diluted in YPD prior to plating; *msc2 hac1* + pMSC2 and *msc2 hac1* + pHAC1 were grown and diluted in SD prior to plating.

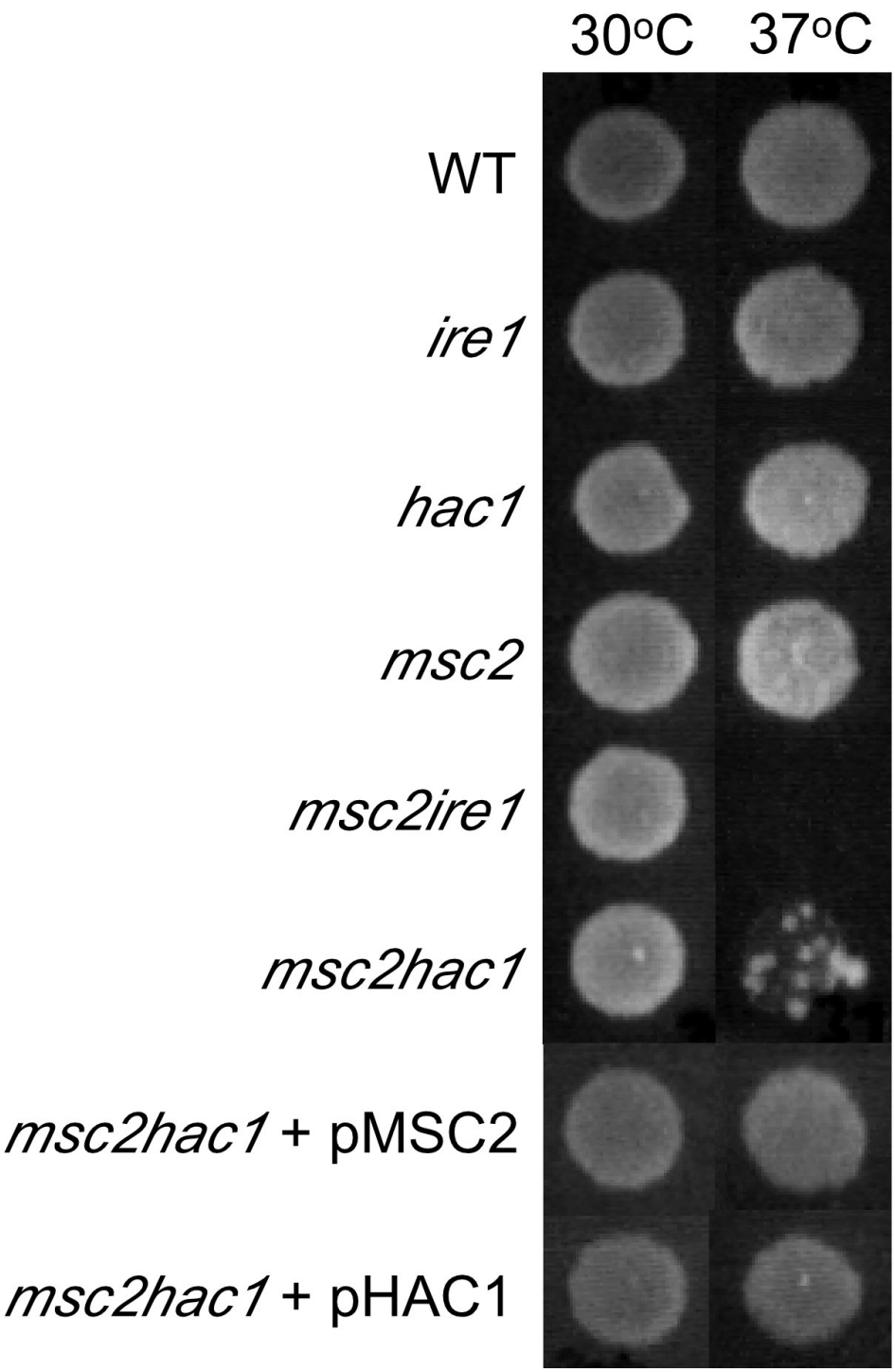
30°C
37°C
WT
ire1
hac1
msc2
msc2ire1
msc2hac1
msc2hac1 + pMSC2
msc2hac1 + pHAC1

back into the *msc2 hac1* mutant restored growth at 37°C. Thus, an *msc2* mutant requires both Ire1p and Hac1p to survive at higher temperatures.

To further test the hypothesis that *msc2* mutation and low zinc causes ER dysfunction, we examined one aspect of ER function, degradation of unfolded proteins through the ERAD pathway. This particular aspect was addressed because Scj1p, an ER lumenal chaperone required for ERAD function, has two predicted zinc binding sites and is likely to require zinc for its activity. The homologous *E. coli* DnaJ protein was shown to be zinc dependent (9, 10). A useful assay of the ERAD system is to monitor the degradation of CPY*, a mutant carboxypeptidase Y protein that fails to fold properly and is degraded by ERAD (51). Wild type and *msc2* mutants were transformed with a plasmid expressing CPY* bearing an HA epitope tag (52). The cells were grown in high or low zinc and then treated with cycloheximide to block further protein synthesis. Aliquots were removed periodically over 60 min for protein extraction and immunoblotting. No difference was observed between wild type and *msc2* mutants in either growth condition (data not shown). The UPR system induces expression of Scj1p and a second, partially redundant chaperone called Jem1p (**Figure 2.1**) (53). While Scj1p is probably zinc-dependent, Jem1p lacks the zinc-binding sites and is therefore likely to be zinc independent. Therefore, increased expression of the Jem1p chaperone may compensate for the loss of zinc-dependent Scj1p activity. To test this hypothesis, we examined CPY* degradation in *jem1* mutant cells lacking the zinc-independent chaperone. CPY* turnover in a *jem1* single mutant was rapid in both zinc-limited and replete cells

(**Figure 2.7**). CPY* degradation in zinc-replete *jem1 msc2* mutants was indistinguishable from the *jem1* single mutant. However, the *jem1 msc2* mutant showed a marked defect in CPY* degradation in low zinc. These studies indicate that zinc deficiency impairs function of components, likely Scj1p, of the ERAD system. Consistent with this hypothesis, CPY* degradation was defective in a *jem1 scj1* double mutant at both zinc levels (**Figure 2.7**).

Zrc1p and Cot1p also contribute to ER zinc

The ability of elevated zinc to suppress UPRE-*lacZ* induction in an *msc2* mutant (**Figure 2.4A**) indicated that other transporters in addition to Msc2p may also provide zinc to the ER. Two possible candidates for this role are Zrc1p and Cot1p, members of the CDF protein family that transport zinc into the vacuole. While the steady state location of these proteins is the vacuole membrane, they must transit through the ER en route to that compartment. Therefore, we tested the contribution of Zrc1p and Cot1p to ER function using the UPRE-*lacZ* reporter. Consistent with Zrc1p and/or Cot1p also contributing to ER zinc, induction of the UPRE-*lacZ* reporter was greatly increased in a zinc-deficient *msc2 zrc1 cot1* triple mutant relative to an *msc2* mutant or wild type cells (**Figure 2.8A**). To determine if either or both Zrc1p and Cot1p were involved, we generated a series of single and double mutants and assayed their effects on UPRE-*lacZ* induction in low zinc and high zinc. In high zinc, all strains tested exhibited no UPRE-*lacZ* induction (**Figure 2.8B**). Under zinc-deficient conditions, *zrc1*, *cot1*, and

Figure 2.7. *The msc2 mutant has defects in ER-associated degradation (ERAD) in low zinc.* LZM cultures of *jem1* (CEY13), *jem1 msc2* (CM164), and *jem1 scj1* (CEY17) expressing the CPY*-HA plasmid (pDN436U) were grown in the presence of cycloheximide for 0-60 minutes before protein extraction. Lysates were analyzed by immunoblotting using mouse anti-HA or mouse anti-Pgk1p antibodies. The intensities of the CPY*-HA bands were normalized to the Pgk1p bands. Each time point was then calculated as the percentage of the zero time point (T_o) for that strain. Shown are the averages of four experiments. A, Plot of percent of T_o for cultures grown in low (1 μM) zinc in LZM. B, Plot of percent of T_o for cultures grown in high (1000 μM) zinc in LZM.

A
1 μM
B
1000 nM
Percent of T0
Time in mycophenolic acid (min)
pgm1
pgm1Δ::pgm1
pgm1Δ::pgm2

Figure 2.8. *Zrc1p and Cot1p may also transport zinc into the ER.* A, UPRE-*lacZ* activity in wild type (WT, CM100), *msc2* (CEY7), and *msc2 zrc1 cot1* (CEY8) over a range of zinc concentrations in LZM. Cells were grown in LZM + 10 μM Zn to deplete internal zinc stores prior to inoculation. Shown are representative data from three experiments. B, UPRE-*lacZ* activity in cells grown in low (1 μM) and high (1000 μM) zinc in LZM: wild type (WT, CM100), *zrc1* (CM102), *cot1* (CM103), *zrc1 cot1* (CM104), *msc2* (CEY7), *msc2 zrc1* (averages of CEY19-21), *msc2 cot1* (averages of CEY22, 23), *msc2 zrc1 cot1* (averages of CEY8, CEY27-29). Shown are data from one representative experiment done in triplicate. Letters refer to values that are significantly different from each other, as determined using the Scheffe's test, with $p < 0.05$. The error bars indicate ± 1 S.D.

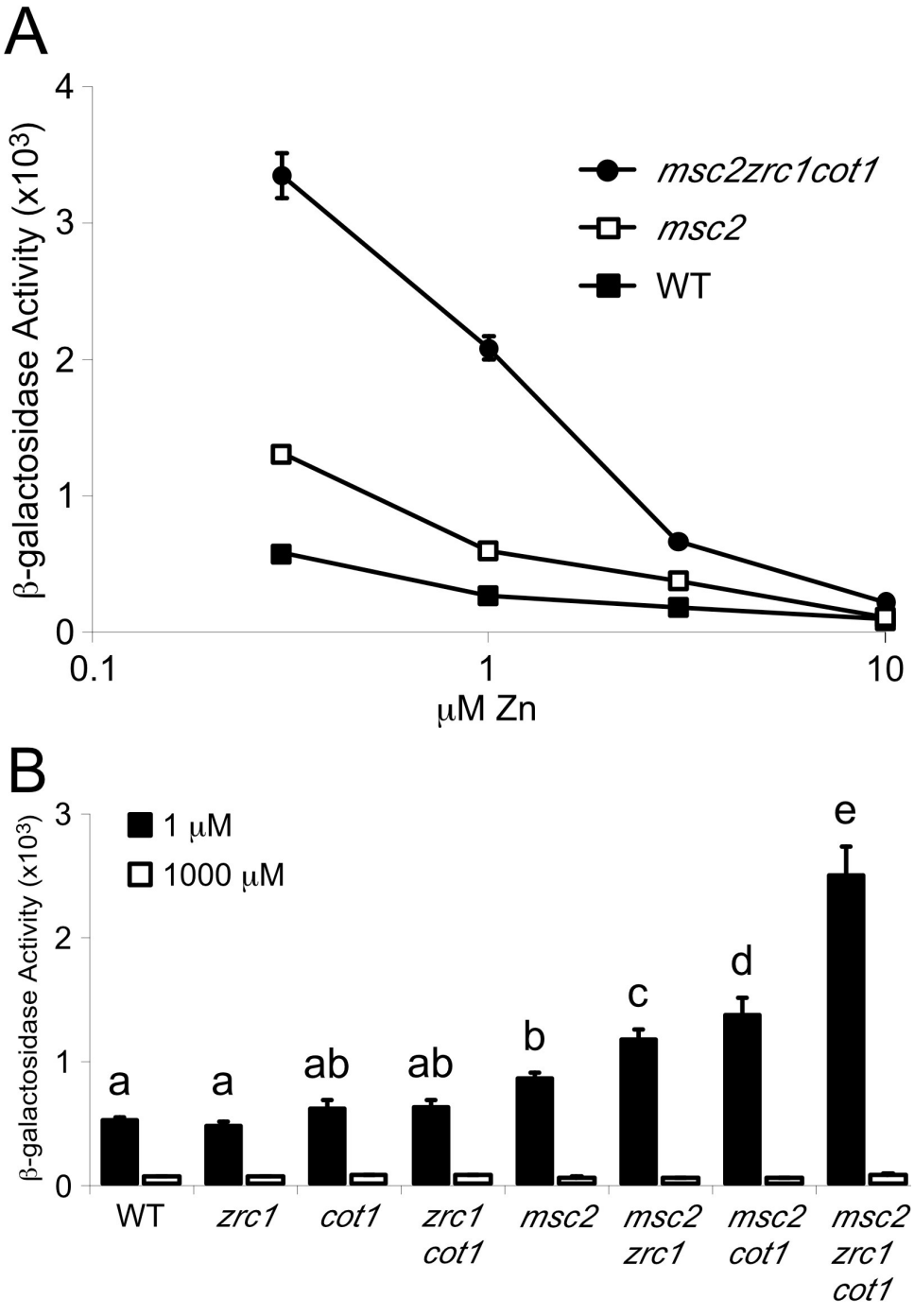
A
β-galactosidase Activity (x10³)
4
3
2
1
0
0.1
1
10
μM Zn
msc2zrc1cot1
msc2
WT
B
β-galactosidase Activity (x10³)
3
2
1
0
1 μM
1000 μM
a
a
ab
ab
b
c
d
e
WT
zrc1
cot1
zrc1 cot1
msc2
msc2 zrc1
msc2 cot1
msc2 zrc1 cot1

zrc1 cot1 cells showed UPR induction indistinguishable from wild type cells. Zinc-deficient *msc2* mutant cells had increased UPRE-*lacZ* expression that was further increased in the *msc2 zrc1* and *msc2 cot1* mutants. Finally, UPRE-*lacZ* induction was highest in the *msc2 zrc1 cot1* mutant. These results suggested that all three transporters contribute to ER function.

Zinc deficiency induces the UPR in mammalian cells

Finally, we addressed if the effects of zinc deficiency on the unfolded protein response was evolutionarily conserved. In mammals, ATF6 is a member of the basic-leucine zipper family of transcription factors that acts analogously to yeast Hac1p to control the UPR (for review, see (54)). ATF6 contains a transmembrane domain and is localized to the ER membrane. Upon ER stress, ATF6 is proteolytically cleaved to release the N-terminal b-Zip-containing domain, which then translocates into the nucleus to activate UPR gene expression. To address if zinc deficiency activates the UPR in mammalian cells, we examined the effects of zinc deficiency on expression of an ATF6-responsive reporter plasmid (p5xATF6GL3) (47) transiently transfected into HeLa cells. p5xATF6GL3 contains five copies of the ATF6 binding site inserted upstream of the firefly luciferase gene. These cells were co-transfected with a *lacZ* gene driven by the SV40 promoter to normalize for differences in transfection efficiency. As shown in **Figure 2.9A**, treating HeLa cells bearing p5xATF6GL3 with tunicamycin, a glycosylation inhibitor and known inducer of ATF6 activity, resulted in a marked induction of luciferase expression. To induce zinc

Figure 2.9. *Zinc deficiency induces the mammalian ER stress response.* HeLa cells were transiently transfected with pSV-β-galactosidase and p5xATF6GL3 plasmids. Cells were then subjected to different treatments, protein was extracted, and β-galactosidase and luciferase assays performed. Luminometer readings were normalized to β-galactosidase activity values to adjust for differences in transfection efficiencies. In all experiments, "un" refers to untransfected cells. A, Luciferase activity in cells treated with (+Tm) and without (-Tm) tunicamycin (12 hours, 2 μM tunicamycin). B, Time course of luciferase activity for cells treated with 5 μM TPEN for 0, 1, 2.5, 5, or 12 hours. C, Concentration response of luciferase activity for cells treated with 0, 1, 2, 3, 4, or 5 μM TPEN for 12 hours. D, Luciferase activity in cells with different 12 hour treatments: no treatment (0), 5 μM TPEN (TPEN), 5 μM TPEN and 5 μM Zn (TPEN+Zn), or 5 μM Zn (Zn). The error bars indicate ± 1 S.D.

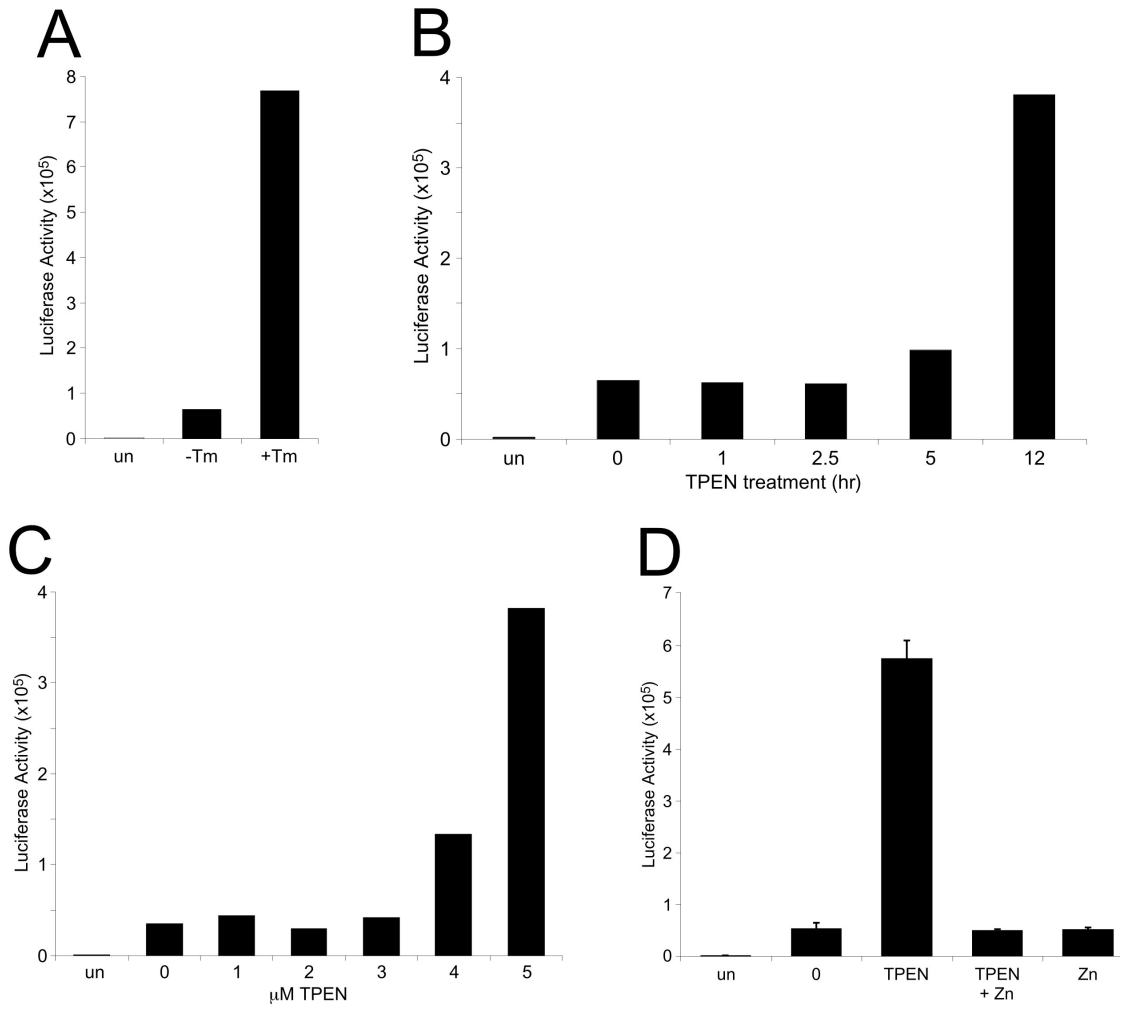
A
Luciferase Activity (x10^5)
0
1
2
3
4
5
6
7
8
un
-Tm
+Tm
B
Luciferase Activity (x10^5)
0
1
2
3
4
un
0
1
2.5
5
12
TPEN treatment (hr)
C
Luciferase Activity (x10^5)
0
1
2
3
4
un
0
1
2
3
4
5
μM TPEN
D
Luciferase Activity (x10^5)
0
1
2
3
4
5
6
7
un
0
TPEN
TPEN + Zn
Zn

deficiency, cells were treated with 5 μM of the zinc chelator N,N,N'N'- tetrakis-(2-pyridylmethyl)ethylenediamine (TPEN). Cells were then harvested over a 12 h period and assayed for luciferase expression. After 5 h of TPEN treatment, a small increase in luciferase activity was observed (**Figure 2.9B**). After 12 h, luciferase activity was induced ~4-fold. No loss of cell viability was detected over this 12 hr period (data not shown) indicating that the induction was not due to necrosis or apoptosis. To determine the concentration of TPEN optimal to triggering UPR induction, we assayed the effects of a range of TPEN concentrations following 12 h treatment. TPEN concentrations of ≤ 3 μM had no effect on ATF6 activity while concentrations of 4 or 5 μM induced expression above basal levels (**Figure 2.9C**). Finally, we addressed if the effects of TPEN on UPR induction were due to zinc deficiency or a pharmacological effect of TPEN. Consistent with zinc deficiency being the cause, simultaneous incubation of cells with 5 μM TPEN and 5 μM $ZnCl_2$ failed to induce ATF6 activity (**Figure 2.9D**). These results suggest that the requirement of the ER for zinc is evolutionarily conserved and that zinc deficiency induces the UPR in a wide range of organisms.

DISCUSSION

In a previous report, Li and Kaplan proposed that Msc2p transports zinc out of the nucleus into the cytosol (36). This hypothesis was based on the tentative localization of overexpressed Msc2p to the nuclear envelope (which is contiguous with the ER membrane) and the observation that the Zap1p transcription factor was completely repressed under their zinc-deficient conditions in an *msc2* mutant. We questioned this hypothesis because the relatively large size of the nuclear pore is unlikely to limit diffusion of Zn^{2+} ions between the cytosol and the nucleus (55). In this report, we propose the alternative model that zinc is required for ER function and Msc2p transports the metal into the ER lumen.

Several lines of evidence support the hypothesis that Msc2p is involved in zinc metabolism. First, Msc2p is a member of the CDF family of metal ion transporters. Studies of CDF proteins in many organisms have established that these proteins transport their metal ion substrate, usually Zn^{2+}, from the cytosol to either outside of the cell or into organelles (13-16). Thus, Msc2p is likely to be a zinc transporter whose topology is consistent with metal transport into the ER lumen. Second, mutations in *msc2* alter zinc homeostasis. While it was shown previously that the Zap1p transcription factor was completely inactive in a zinc-limited *msc2* mutant (36), our experiments further clarified these earlier results by showing that Zap1p can still respond to zinc deficiency in an *msc2* strain. Nonetheless, the suppression of ZRE-*lacZ* expression caused by the *msc2* mutation that we observed (**Figure 2.3**) is consistent with *msc2* mutants having

elevated pools of labile cytosolic zinc. Third, mutations in *MSC2* result in several phenotypes that are zinc suppressible. Li and Kaplan had shown that the growth defect of *msc2* mutants on respired carbon sources at elevated temperatures is suppressed by zinc (36). Here we document that zinc-deficient cells up-regulate their UPR system and this induction is further increased in an *msc2* mutant. Like the temperature-sensitive growth phenotype, induction of the UPR is zinc suppressible. Finally, we present here genetic evidence that known zinc transporters, Zrc1p and Cot1p, play redundant roles with Msc2p. Their involvement in ER function indicates that Msc2p is also a zinc transporter.

Our results indicate that Msc2p delivers zinc to the lumen of the ER to maintain function of that compartment and, perhaps, other organelles of the secretory pathway. While currently available methods do not allow us to assay lumenal ER zinc directly, several observations indirectly support this hypothesis. First, we found that Msc2p localizes to the ER when expressed at physiological levels from its own promoter. The presence of significant amounts of Msc2p protein in vesicles of lighter density (+Mg^{2+}, **Figure 2.2A**) suggests that some protein may also be found in later compartments of the secretory pathway, perhaps the Golgi. Second, mutation of *MSC2* activates the UPR system. Our results indicate that this induction requires the full UPR signaling pathway consistent with actual ER stress being responsible rather than downstream perturbations of, for example, $Hac1p^{i}$ activity. Third, we found that *msc2* mutants show synthetic growth defects when combined with mutations in either *ire1* or *hac1*. This observation is especially intriguing in light of studies by Ng et al. in

which mutations were identified that were synthetically lethal when combined with an *ire1* mutation (52). This screen identified 16 different genes almost all of which were shown to be involved in ER functions such as glycosylation, GPI-anchor synthesis, or ERAD function. Thus, mutations in genes affecting lumenal ER processing events are lethal when combined with *ire1* mutations. While *msc2* mutants were not identified in this synthetic lethal screen, they too are synthetically lethal with an *ire1* mutation when cells are grown at 37°C. Finally, we directly observed zinc-suppressible defects in one aspect of ER function, ER-associated degradation. We chose to examine this process because Scj1p, a chaperone protein of the ER lumen that is required for ERAD, is likely to be zinc dependent. One caveat to this experiment is that the E3 ubiquitin-protein ligases required for proteasome degradation of unfolded proteins following their export from the ER, Hrd1p/Der3p and Doa10p/Ssm4p, may also be zinc-dependent (56, 57). Therefore, the defects in ERAD observed in *msc2* mutants could be due to disruption of ligase function via alterations in cytosolic zinc homeostasis. This appears not to be the case; degradation of a model cytosolic substrate of Doa10p, the Deg1-βgalactosidase protein (57), was unaffected by either zinc limitation or mutation of *msc2* (data not shown). Compromised function of Hrd1p/Der3p is still formally possible but less likely given the lack of effects on Doa10p function.

In addition to ERAD, it is also likely that other processes occurring in the ER are impaired by zinc deficiency. Several observations suggest that synthesis of GPI-anchors may be disrupted by these perturbations. First, GPI-anchor

synthesis has been found to be zinc dependent both *in vitro* and *in vivo* (7, 8). Second, the yeast *MCD4*, *LAS21,* and *GPI13* genes encode related proteins required for GPI-anchor synthesis (58-61). These proteins all contain conserved domains similar to the zinc-binding sites of alkaline phosphatases (6). While the precise role of these proteins is still unclear, their importance in GPI-anchor synthesis is well documented. *MCD4* and *GPI13* are essential genes while *LAS21* is not. Temperature-sensitive *mcd4* alleles and *las21* mutants have a large cell morphology similar to that seen with *msc2* (36, 62, 63). Suppressors of these mutations also link their activity to Msc2p. The large cell phenotype of *las21* is suppressed by overexpression of the *HSP150* gene (59). Hsp150p is a cell wall protein of unknown function. We have found *HSP150* overexpression also suppresses the *msc2* temperature-sensitive growth defect and large cell phenotype (data not shown). Finally, *MCD4* is a direct Zap1p target gene and is induced ≥ 4-fold by zinc deficiency (48). These results suggest that GPI-anchor synthesis is sensitive to zinc deficiency, and *MCD4* is up-regulated to maintain sufficient activity in zinc-limited cells. Golgi function was unimpaired by mutation of the *MSC2* gene; analysis of the kinetics of wild type CPY processing indicated no differences between wild type and mutant cells in high or low zinc (data not shown).

In this study, we have identified three different transporters that likely contribute to ER zinc: Zrc1p, Cot1p, and Msc2p. Of these three, Msc2p appears to play the predominant role because mutation of this gene alone had the strongest effect on UPR induction. While Msc2p is resident in the ER

membrane, Zrc1p and Cot1p are most abundant in the vacuolar membrane (32, 64). We can suggest two possible mechanisms to explain how Zrc1p and Cot1p could supply zinc to the ER. First, these proteins may mediate zinc transport soon after insertion into the ER membrane and prior to their transit to the vacuole. Alternatively, zinc may be transferred from the vacuole lumen to the ER by retrograde vesicular trafficking.

The *ZRC1* gene is a Zap1p target and induced by zinc deficiency (48, 65). This was a surprising finding given the importance of this transporter in zinc storage and detoxification. Our previous results indicated that *ZRC1* up-regulation in low zinc is required to tolerate "zinc shock" (66). Zinc shock occurs when zinc-limited cells, which express high levels of the Zrt1p zinc uptake transporter, are resupplied with zinc. The role of Zrc1p in supplying zinc to the ER is an additional reason why the *ZRC1* gene may be induced in low zinc; i.e. to maintain ER zinc levels. However, given the relatively minor role Zrc1p plays in maintaining ER function (**Figure 2.8**), our results argue that zinc shock tolerance is the major reason for the regulation of *ZRC1* expression by Zap1p.

We also predict that additional pathways contribute to ER zinc. UPR induction in the *msc2 zrc1 cot1* triple mutant is still suppressible by adding 10 μM $ZnCl_2$ to the medium. One possible route to bypass the loss of Msc2p, Zrc1p, and Cot1p activity is via fluid-phase endocytosis of zinc followed by its retrograde vesicular transport to the ER. While formally possible, we do not favor this model based on our results. Specifically, while UPR induction in the *msc2 zrc1 cot1* mutant is suppressed by 10 μM zinc, it requires 100-fold more zinc to suppress

UPRE-*lacZ* activity in a *zrt1* mutant (**Figure 2.1A**). Zrt1p transports zinc across the plasma membrane into the cytoplasm. Therefore, the much higher levels of zinc required to suppress UPRE-*lacZ* expression in a *zrt1* mutant strongly argues that that zinc must pass through the cytosol before entering the ER.

Msc2p is related to the Zhf1 protein of *S. pombe* (67, 68). Like Msc2p, Zhf1 is a member of the CDF family of metal ion transporters. Furthermore, immunoelectron microscopy localized Zhf1 protein to the ER membrane. However, the phenotypic effects of *zhf1* mutations argue that this protein plays a very different role in zinc metabolism. While Msc2p is important for supplying zinc to the ER for organelle function, Zhf1 appears to be required for zinc storage and detoxification. For example, *zhf1* mutations increase the sensitivity of cells to exogenous zinc indicating its role in detoxification. *zhf1* mutants also have decreased zinc accumulation in cells indicating its role in zinc storage. For Msc2p, we found no effect of *msc2* mutations on zinc tolerance either in wild type or *zrc1 cot1* mutant cells that are greatly sensitized to exogenous zinc (data not shown). Li and Kaplan showed that *msc2* mutants actually hyperaccumulate zinc (36). Thus, the effects of *zhf1* mutations in *S. pombe* are much more similar to mutations altering Zrc1p and Cot1p of *S. cerevisiae*. The ER of *S. pombe* may play a role in zinc storage and detoxification similar to that of the vacuole in *S. cerevisiae*.

Another protein related to Msc2p is mammalian ZnT5. While most members of the CDF family have only 6 transmembrane domains, Msc2p and ZnT5 are predicted to have ~15 transmembrane domains. For each, the

conserved CDF region is found at the C-terminus with several transmembrane domains attached to their N-termini. ZnT5 was localized to the Golgi when expressed from the CMV promoter in HeLa cells and is widely expressed in mammalian tissues (21). Expression was especially high in the β cells of the pancreas in which zinc is transported into secretory vesicles for the packaging of insulin. Finally, ZnT5-dependent zinc transport activity could be observed in Golgi-derived vesicles *in vitro*. Given our results indicating that zinc transport into the secretory pathway is important for ER stress and UPR induction, we predict that ZnT5 or related proteins carry out this important role in mammalian cells. Consistent with this hypothesis, we have found that expression of ZnT5 in *msc2* mutant yeast can suppress phenotypic defects of this mutant under certain conditions (Ellis, et al., unpublished results).

Acknowledgments

The authors thank J. Kaplan, A. Cooper, S. Nothwehr, R. Prywes, and D. Ng for providing strains and/or plasmids and W. Folk for use of his luminometer. This work was supported by NIH grants GM56285 and GM69786. C.D.E. was supported by an MU Life Sciences Predoctoral Fellowship.

REFERENCES

1. Dodson G and Steiner D. 1998. The role of assembly in insulin's biosynthesis. *Curr Opin Struct Biol* **8**: 189-194.
2. Huang XF and Arvan P. 1995. Intracellular transport of proinsulin in pancreatic b-cells. *J Biol Chem* **270**: 20417-20423.
3. Chang C and Werb Z. 2001. The many faces of metalloproteases: cell growth, invasion, angiogenesis and metastasis. *Trends Cell Biol* **11**: S37-43.
4. Kang T, Nagase H, and Pei D. 2002. Activation of membrane-type matrix metalloproteinase 3 zymogen by the proprotein convertase furin in the trans-Golgi network. *Cancer Res* **62**: 675-681.
5. Pei D and Weiss SJ. 1995. Furin-dependent intracellular activation of the human stromelysin-3 zymogen. *Nature* **375**: 244-247.
6. Galperin MY and Jedrzejas MJ. 2001. Conserved core structure and active site residues in alkaline phosphatase superfamily enzymes. *Proteins* **45**: 318-324.
7. Sevlever D, Mann KJ, and Medof ME. 2001. Differential effect of 1,10-phenanthroline on mammalian, yeast, and parasite glycosylphosphatidylinositol anchor synthesis. *Biochem Biophys Res Commun* **288**: 1112-1118.
8. Mann KJ and Sevlever D. 2001. 1,10-Phenanthroline inhibits glycosylphosphatidylinositol anchoring by preventing

phosphoethanolamine addition to glycosylphosphatidylinositol anchor precursors. *Biochemistry* **40**: 1205-1213.

9. Linke K, Wolfram T, Bussemer J, and Jakob U. 2003. The roles of the two zinc binding sites in DnaJ. *J Biol Chem* **278**: 44457-44466.

10. Tang W and Wang C. 2001. Zinc fingers and thiol-disulfide oxidoreductase activities of chaperone DnaJ. *Biochemistry* **40**: 14985-14994.

11. Silberstein S, Schlenstedt G, Silver PA, and Gilmore R. 1998. A role for the DnaJ homologue Scj1p in protein folding in the yeast endoplasmic reticulum. *J Cell Biol* **143**: 921-933.

12. Nishikawa SI, Fewell SW, Kato Y, Brodsky JL, and Endo T. 2001. Molecular chaperones in the yeast endoplasmic reticulum maintain the solubility of proteins for retrotranslocation and degradation. *J Cell Biol* **153**: 1061-1070.

13. Nies DH and Silver S. 1995. Ion efflux systems involved in bacterial metal resistances. *J Ind Microbiol* **14**: 186-199.

14. Paulsen IT and Saier MH. 1997. A novel family of ubiquitous heavy metal ion transport proteins. *J Membr Biol* **156**: 99-103.

15. Gaither LA and Eide DJ. 2001. Eukaryotic zinc transporters and their regulation. *Biometals* **14**: 251-270.

16. Palmiter RD and Huang L. 2004. Efflux and compartmentalization of zinc by members of the SLC30 family of solute carriers. *Pflugers Arch* **447**: 744-751.

17. Grass G, Fan B, Rosen BP, Franke S, Nies DH, and Rensing C. 2001. ZitB (YbgR), a member of the cation diffusion facilitator family, is an additional zinc transporter in *Escherichia coli*. *J Bacteriol* **183**: 4664-4667.

18. Palmiter RD and Findley SD. 1995. Cloning and functional characterization of a mammalian zinc transporter that confers resistance to zinc. *EMBO J* **14**: 639-649.

19. Palmiter RD, Cole TB, and Findley SD. 1996. ZnT-2, a mammalian protein that confers resistance to zinc by facilitating vesicular sequestration. *EMBO J* **15**: 1784-1791.

20. Kobayashi T, Beuchat M, Lindsay M, Frias S, Palmiter RD, Sakuraba H, Parton RG, and Gruenberg J. 1999. Late endosomal membranes rich in lysobisphosphatidic acid regulate cholesterol transport. *Nat Cell Biol* **1**: 113-118.

21. Kambe T, Narita H, Yamaguchi-Iwai Y, Hirose J, Amano T, Sugiura N, Sasaki R, Mori K, Iwanaga T, and Nagao M. 2002. Cloning and characterization of a novel mammalian zinc transporter, zinc transporter 5, abundantly expressed in pancreatic beta cells. *J Biol Chem* **277**: 19049-19055.

22. Huang L, Kirschke CP, and Gitschier J. 2002. Functional characterization of a novel mammalian zinc transporter, ZnT6. *J Biol Chem* **277**: 26389-26395.

23. Kirschke CP and Huang L. 2003. ZnT7, A novel mammalian zinc transporter, accumulates zinc in the Golgi apparatus. *J Biol Chem* **278**: 4096-4102.

24. Zhao H and Eide D. 1996. The yeast *ZRT1* gene encodes the zinc transporter of a high affinity uptake system induced by zinc limitation. *Proc Natl Acad Sci U S A* **93**: 2454-2458.

25. Zhao H and Eide D. 1996. The *ZRT2* gene encodes the low affinity zinc transporter in *Saccharomyces cerevisiae*. *J Biol Chem* **271**: 23203-23210.

26. Waters BM and Eide DJ. 2002. Combinatorial control of yeast *FET4* gene expression in response to iron, zinc, and oxygen. *J Biol Chem* **277**: 33749-33757.

27. Zhao H and Eide DJ. 1997. Zap1p, a metalloregulatory protein involved in zinc-responsive transcriptional regulation in *Saccharomyces cerevisiae*. *Mol Cell Biol* **17**: 5044-5052.

28. Zhao H, Butler E, Rodgers J, Spizzo T, and Duesterhoeft S. 1998. Regulation of zinc homeostasis in yeast by binding of the ZAP1 transcriptional activator to zinc-responsive promoter elements. *J Biol Chem* **273**: 28713-28720.

29. Kamizono A, Nishizawa M, Teranishi Y, Murata K, and Kimura A. 1989. Identification of a gene conferring resistance to zinc and cadmium ions in the yeast *Saccharomyces cerevisiae*. *Mol Gen Genet* **219**: 161-167.

30. MacDiarmid CW, Gaither LA, and Eide D. 2000. Zinc transporters that regulate vacuolar zinc storage in *Saccharomyces cerevisiae*. *EMBO J* **19**: 2845-2855.

31. Miyabe S, Izawa S, and Inoue Y. 2001. Zrc1 is involved in zinc transport system between vacuole and cytosol in *Saccharomyces cerevisiae*. *Biochem Biophys Res Commun* **282**: 79-83.

32. MacDiarmid CW, Milanick MA, and Eide DJ. 2002. Biochemical properties of vacuolar zinc transport systems of Saccharomyces cerevisiae. *J Biol Chem* **277**: 39187-39194.

33. Li L and Kaplan J. 1997. Characterization of two homologous yeast genes that encode mitochondrial iron transporters. *J Biol Chem* **272**: 28485-28493.

34. Thompson DA and Stahl FW. 1999. Genetic control of recombination partner preference in yeast meiosis: isolation and characterization of mutants elevated for meiotic unequal sister-chromatid recombination. *Genetics* **153**: 621-641.

35. Thompson DA and Stahl FW. 2003. Genetic Control of Recombination Partner Preference in Yeast Meiosis. Isolation and characterization of mutants elevated for meiotic unequal sister-chromatid recombination. *Genetics* **164**: 1241.

36. Li L and Kaplan J. 2000. The yeast gene *MSC2*, a member of the cation diffusion facilitator family, affects the cellular distribution of zinc. *J Biol Chem* **276**: 5036-5043.

37. Gitan RS, Luo H, Rodgers J, Broderius M, and Eide D. 1998. Zinc-induced inactivation of the yeast ZRT1 zinc transporter occurs through endocytosis and vacuolar degradation. *J Biol Chem* **273**: 28617-28624.

38. Hinnebusch AG, Lucchini G, and Fink GR. 1985. A synthetic *HIS4* regulatory element confers general amino acid control on the cytochrome c gene (*CYC1*) of yeast. *Proc Natl Acad Sci U S A* **82**: 498-502.

39. Kawahara T, Yanagi H, Yura T, and Mori K. 1997. Endoplasmic reticulum stress-induced mRNA splicing permits synthesis of transcription factor Hac1p/Ern4p that activates the unfolded protein response. *Mol Biol Cell* **8**: 1845-1862.

40. Gao CY and Pinkham JL. 2000. Tightly regulated, beta-estradiol dose-dependent expression system for yeast. *Biotechniques* **29**: 1226-1231.

41. Cross FR. 1997. 'Marker swap' plasmids: convenient tools for budding yeast molecular genetics. *Yeast* **13**: 647-653.

42. Ma H, Kunes S, Schatz PJ, and Botstein D. 1987. Plasmid construction by homologous recombination in yeast. *Gene* **58**: 201-216.

43. Ho SN, Hunt HD, Horton RM, Pullen JK, and Pease LR. 1989. Site-directed mutagenesis by overlap extension using the polymerase chain reaction. *Gene* **77**: 51-59.

44. Ausubel FM, Brent R, Kingston RE, Moore DD, Seidman JG, Smith JA, and Struhl K. 1995. *Current Protocols in Molecular Biology.* New York, NY: John Wiley & Sons.

45. Roberg KJ, Rowley N, and Kaiser CA. 1997. Physiological regulation of membrane protein sorting late in the secretory pathway of *Saccharomyces cerevisiae*. *J Cell Biol* **137**: 1469-1482.

46. Harlow E and Lane D. 1988. *Antibodies: a laboratory manual.* Cold Spring Harbor: Cold Spring Harbor Press.

47. Wang Y, Shen J, Arenzana N, Tirasophon W, Kaufman RJ, and Prywes R. 2000. Activation of ATF6 and an ATF6 DNA binding site by the endoplasmic reticulum stress response. *J Biol Chem* **275**: 27013-27020.

48. Lyons TJ, Gasch AP, Gaither LA, Botstein D, Brown PO, and Eide DJ. 2000. Genome-wide characterization of the Zap1p zinc-responsive regulon in yeast. *Proc Natl Acad Sci U S A* **97**: 7957-7962.

49. Patil C and Walter P. 2001. Intracellular signaling from the endoplasmic reticulum to the nucleus: the unfolded protein response in yeast and mammals. *Curr Opin Cell Biol* **13**: 349-355.

50. Travers KJ, Patil CK, Wodicka L, Lockhart DJ, Weissman JS, and Walter P. 2000. Functional and genomic analyses reveal an essential coordination between the unfolded protein response and ER-associated degradation. *Cell* **101**: 249-258.

51. Finger A, Knop M, and Wolf DH. 1993. Analysis of two mutated vacuolar proteins reveals a degradation pathway in the endoplasmic reticulum or a related compartment of yeast. *Eur J Biochem* **218**: 565-574.

52. Ng DT, Spear ED, and Walter P. 2000. The unfolded protein response regulates multiple aspects of secretory and membrane protein biogenesis and endoplasmic reticulum quality control. *J Cell Biol* **150**: 77-88.

53. Nishikawa S and Endo T. 1997. The yeast JEM1p is a DnaJ-like protein of the endoplasmic reticulum membrane required for nuclear fusion. *J Biol Chem* **272**: 12889-12892.

54. Harding HP, Calfon M, Urano F, Novoa I, and Ron D. 2002. Transcriptional and translational control in the mammalian unfolded protein response. *Annu Rev Cell Dev Biol* **18**: 575-599.

55. Shulga N, Mosammaparast N, Wozniak R, and Goldfarb DS. 2000. Yeast nucleoporins involved in passive nuclear envelope permeability. *J Cell Biol* **149**: 1027-1038.

56. Bordallo J and Wolf DH. 1999. A RING-H2 finger motif is essential for the function of Der3/Hrd1 in endoplasmic reticulum associated protein degradation in the yeast Saccharomyces cerevisiae. *FEBS Lett* **448**: 244-248.

57. Swanson R, Locher M, and Hochstrasser M. 2001. A conserved ubiquitin ligase of the nuclear envelope/endoplasmic reticulum that functions in both ER-associated and Matalpha2 repressor degradation. *Genes Dev* **15**: 2660-2674.

58. Gaynor EC, Mondesert G, Grimme SJ, Reed SI, Orlean P, and Emr SD. 1999. *MCD4* encodes a conserved endoplasmic reticulum membrane

protein essential for glycosylphosphatidylinositol anchor synthesis in yeast. *Mol Biol Cell* **10**: 627-648.

59. Tohe A and Oguchi T. 1999. Las21 participates in extracellular/cell surface phenomena in *Saccharomyces cerevisiae*. *Genes Genet Syst* **74**: 241-256.

60. Taron CH, Wiedman JM, Grimme SJ, and Orlean P. 2000. Glycosylphosphatidylinositol biosynthesis defects in Gpi11p- and Gpi13p-deficient yeast suggest a branched pathway and implicate gpi13p in phosphoethanolamine transfer to the third mannose. *Mol Biol Cell* **11**: 1611-1630.

61. Flury I, Benachour A, and Conzelmann A. 2000. YLL031c belongs to a novel family of membrane proteins involved in the transfer of ethanolaminephosphate onto the core structure of glycosylphosphatidylinositol anchors in yeast. *J Biol Chem* **275**: 24458-24465.

62. Ni L and Snyder M. 2001. A genomic study of the bipolar bud site selection pattern in *Saccharomyces cerevisiae*. *Mol Biol Cell* **12**: 2147-2170.

63. Mondesert G, Clarke DJ, and Reed SI. 1997. Identification of genes controlling growth polarity in the budding yeast *Saccharomyces cerevisiae*: a possible role of N-glycosylation and involvement of the exocyst complex. *Genetics* **147**: 421-434.

64. Li L and Kaplan J. 1998. Defects in the yeast high affinity iron transport system result in increased metal sensitivity because of the increased expression of transporters with a broad transition metal specificity. *J Biol Chem* **273**: 22181-22187.

65. Miyabe S, Izawa S, and Inoue Y. 2000. Expression of ZRC1 coding for suppressor of zinc toxicity is induced by zinc-starvation stress in Zap1-dependent fashion in *Saccharomyces cerevisiae*. *Biochem Biophys Res Commun* **276**: 879-884.

66. MacDiarmid CW, Milanick MA, and Eide DJ. 2003. Induction of the *ZRC1* metal tolerance gene in zinc-limited yeast confers resistance to zinc shock. *J Biol Chem* **278**: 15065-15072.

67. Clemens S, Bloss T, Vess C, Neumann D, Nies DH, and Zur Nieden U. 2002. A transporter in the endoplasmic reticulum of *Schizosaccharomyces pombe* cells mediates zinc storage and differentially affects transition metal tolerance. *J Biol Chem* **277**: 18215-18221.

68. Borrelly GP, Harrison MD, Robinson AK, Cox SG, Robinson NJ, and Whitehall SK. 2002. Surplus zinc is handled by Zym1 metallothionein and Zhf endoplasmic reticulum transporter in *Schizosaccharomyces pombe*. *J Biol Chem* **277**: 30394-30400.

CHAPTER 3

EVIDENCE FOR A ZINC TRANSPORT COMPLEX IN THE ENDOPLASMIC RETICULUM OF *SACCHAROMYCES CEREVISIAE*

Charissa D. Ellis, Michelle Mooney, Colin W. MacDiarmid, Amanda J. Bird, and David J. Eide

Departments of Biochemistry and Nutritional Sciences
University of Missouri, Columbia, MO 65211

ABSTRACT

In this report, we demonstrate a novel interaction between two members of the cation diffusion facilitator (CDF) family in *Saccharomyces cerevisiae*. One CDF member in yeast, Msc2p, was shown recently to be involved in zinc transport into the endoplasmic reticulum (ER) and required for ER function. We present evidence here of a newly recognized CDF family member in yeast, Zrg17p. *ZRG17* was previously identified as a zinc-regulated gene controlled by the zinc-responsive Zap1p transcription factor. A *zrg17* mutant exhibits the same zinc-suppressible phenotypes as an *msc2* mutant, including an induction of the unfolded protein response (UPR) in low zinc. Zrg17p localizes to the ER and is regulated by zinc at the protein level. Msc2p and Zrg17p physically interact, as determined by co-immunoprecipitation. Therefore, we propose that Msc2p and Zrg17p form a zinc transport complex in the ER membrane to maintain the function of this compartment. We also demonstrate that ZnT5 and ZnT6, the closest mammalian homologues of Msc2p and Zrg17p, may functionally interact. These results indicate that interactions between CDF members may be a common phenomenon.

INTRODUCTION

Zinc is required by all organisms because of the essential roles zinc plays in cells. In particular, zinc is important for the activity of many proteins that reside in or move through the secretory pathway. In pancreatic beta cells, zinc is needed for the association of proinsulin into homohexamers, which takes place in the endoplasmic reticulum (ER) and/or Golgi (1, 2). The subsequent maturation of secreted insulin granules also requires zinc (1). Killer T cells present antigen peptides on their cell surface bound to major histocompatibility complex (MHC) class I molecules. The processing of some of these peptides takes place in the ER by the ER-associated aminopeptidase (ERAAP), which utilizes zinc in its active site (3, 4). Zinc metalloenzymes responsible for attaching phosphoethanolamine groups to glycosylphosphatidylinositol- (GPI-) anchors are resident ER proteins (5, 6). The Scj1p protein chaperone in the ER of yeast is a DnaJ homologue needed for ER-associated degradation (ERAD) (7, 8). Scj1p requires zinc for its function (9, 10). Lastly, protein folding in the ER and overall proper ER function were recently found to require zinc (10).

Because of these and other needs for zinc, eukaryotic cells must utilize zinc transport proteins in their plasma membranes and intracellular organelles. To maintain zinc levels in times of zinc deficiency and to have an efficient means of transport, cells must also regulate the transporters responsible for the uptake and cellular distribution of zinc. The budding yeast *Saccharomyces cerevisiae* has been an excellent model system for studying zinc transport and regulation. Initial uptake of zinc into the cytoplasm of yeast is accomplished through three

transporters on the plasma membrane: Zrt1p, Zrt2p, and Fet4p (11-13). In times of zinc deficiency, zinc stores in the vacuole are mobilized by the Zrt3p protein to supply zinc to the cytoplasm and other organelles (14). Alternatively, when zinc levels in the cytoplasm become replete or toxic, the Zrc1p protein is involved in transporting zinc into the vacuole to be stored (15).

The genes for all of the above yeast proteins are regulated by the zinc-responsive transcription factor, Zap1p. Zap1p up-regulates genes in zinc-deficient conditions by binding to an eleven base pair consensus sequence, a zinc-responsive element (ZRE), found in one or more copies in the promoters of its target genes (16). Lyons et al. performed microarray analysis on the yeast transcriptome and determined that at least 46 genes are regulated by Zap1p (17). This Zap1p regulon includes genes whose protein products are involved in zinc homeostasis (including zinc transporters and Zap1p itself), ethanol metabolism (such as alcohol dehydrogenase), DNA metabolism (with the biosynthesis of DNA bases), and many of unknown function (17).

While most of the yeast zinc transporters known to date have been shown to be Zap1p targets, the Msc2p protein is not. Msc2p is a member of the cation diffusion facilitator (CDF) family of heavy metal ion transporters (18, 19). Many eukaryotic members of the CDF family have been shown to transport heavy metals, in particular zinc, out of the cytoplasm into intracellular organelles (18, 20). Msc2p has recently been shown to be localized to the ER and is involved with zinc uptake into this compartment (10, 21). An *msc2* mutant exhibits an up-regulation of the unfolded protein response (UPR) and has defects in ERAD,

suggesting that Msc2p and zinc are needed for proper ER function (10). The UPR and ERAD defects as well as other phenotypes of the *msc2* mutant are all suppressible by zinc. This suggested there were other zinc transporters in the ER/secretory pathway. Zrc1p, and its vacuolar homologue Cot1p, were found to potentially contribute to ER zinc levels, for an *msc2 zrc1 cot1* triple mutant caused a further up-regulation of the UPR in low zinc than that seen in an *msc2* mutant alone. However, even this triple mutant was suppressed by elevated zinc (10). These observations led us to look for more potential zinc transporters in the secretory pathway. One such candidate was Zrg17p.

Previous studies on *ZRG17* determined it to be a Zap1p target and regulated by zinc at the mRNA level, i.e., *ZRG17* is up-regulated in low zinc and down-regulated in high zinc (17, 22). A *zrg17* mutant has an abnormal large cell morphology, which is suppressed by the addition of higher amounts of zinc in the medium (22). An *msc2* mutant also exhibits this zinc-suppressible large cell phenotype (21). The Zrg17p protein is predicted to be an integral membrane protein with six or seven transmembrane domains (22). A C-terminal green fluorescent protein (GFP) fusion construct of Zrg17p showed an ER localization, though this localization is tentative since the functionality of the fusion protein was not determined (23). Lastly, a yeast two-hybrid screen looking for potential interactions between proteins across the entire yeast proteome determined a possible interaction between Msc2p and Zrg17p (24).

These data suggest that Msc2p and Zrg17p interact to form a complex that transports zinc into the ER. In support of this hypothesis, we observed that

msc2 and *zrg17* mutants both exhibit the same, but non-additive, phenotypes. We localized Zrg17p to the ER using a functional hemagglutinin- (HA-) tagged fusion construct. We demonstrated via co-immunoprecipitation that Msc2p and Zrg17p physically interact. Lastly, we determined that Zrg17p is a distant member of the CDF family and suggest that other CDF family members may interact to form hetero-complexes for heavy metal transport.

EXPERIMENTAL PROCEDURES

Yeast strains and media

Media used were YPD, SD, YPGE, and LZM as described previously (25). Yeast strains DY150 (*MATa ade2 can1 his3 leu2 trp1 ura3*) and DY150 *msc2* (DY150 *msc2::HIS3*) (21), BY4741 (*MATa his3 leu2 met15 ura3*) (Research Genetics), ZRG17-TAP (BY4741 *ZRG17*::TAP) and MSC2-TAP (BY4741 *MSC2*::TAP) (Open Biosystems) have been described previously. To generate mutant strains CEY9 (DY150 *zrg17::KanMX*) and CEY11 (DY150 *msc2::HIS3 zrg17::KanMX*), the *KanMX* cassette with 500 bp flanking the *ZRG17* ORF was amplified by PCR from the *zrg17* yeast deletion mutant (Research Genetics). The PCR fragment was then transformed into DY150 or DY150 *msc2* to generate CEY9 and CEY11, respectively.

Plasmids

Plasmids used are described in **Table 3.1**. pZnT5 was a gift from Taiho Kambe (Kyoto University, Kyoto, Japan) (26), and pZnT6 was a gift from Liping Huang (University of California, Davis, CA) (27). pRS316GAL1LEU2, pYES2L, and pZnT5L were generated by swapping the *URA3* gene on pRS316GAL1, pYES2, and pZnT5, respectively, for the *LEU2* gene using the marker swap plasmid pUL9 (28). pZRG17 and pZRG17HA were constructed the same way as pMSC2 and pMSC2HA (10). Briefly, PCR products containing the ZRG17 promoter and ORF (and terminator in the case of pZRG17) were put into pFL38 or YCpZRC1-HA by homologous recombination to generate pZRG17 and

Table 3.1. Plasmids used in this study

Plasmid	Relevant Genotype	Reference/ Source
pTF63	High copy expression vector	(29)
YEpMSC2-myc	*MSC2*-myc in pTF63	(21)
pRS316GAL1	Low copy expression vector	(30)
pRS316GAL1LEU2	Low copy expression vector	This Work
pGAL-ZRG17HA	*ZRG17*-3xHA driven by *GAL1* promoter	This Work
YEp24	High copy expression vector	(31)
pHSP150	*HSP150* in YEp24	This Work
pMCZ-Y (UPRE-*lacZ*)	High copy expression of UPRE-*lacZ*	(32)
pDg2L (ZRE-*lacZ*)	High copy expression of ZRE-*lacZ*	(14)
pRK315	*PMA1*-HA driven by *GAL1* promoter	(33)
pGEV-TRP1	GAL4.ER.VP16 expression system	(34)
pZRG17	*ZRG17* in low copy vector	This Work
pZRG17HA	*ZRG17*-3xHA in low copy vector	This Work
pMSC2	*MSC2* in low copy vector	(10)
pMSC2HA	*MSC2*-3xHA in low copy vector	(10)
pYES2	High copy expression vector	Invitrogen
pYES2L	High copy expression vector	This Work
pYES2-ZnT5 (pZnT5)	*ZnT5* driven by *GAL1* promoter	(26)
pZnT5L	*ZnT5* driven by *GAL1* promoter	This Work
pYES2-ZnT6 (pZnT6)	*ZnT6* driven by *GAL1* promoter	(27)

Unless otherwise noted, genes are driven by their own promoters.

pZRG17HA, respectively (35). To generate the pGAL-ZRG17HA construct, the *ZRG17* ORF starting at the fourth in-frame ATG plus 3xHA tags and termination sequence from pZRG17HA was amplified by PCR. This fragment was then inserted into the *Sac*1 site of the vector pRS316GAL1LEU2 by homologous recombination. (We determined the annotation in the *Saccharomyces* Genome Database (SGD) to be incorrect for the ATG translation start site of the *ZRG17* gene.) All of the above plasmids encoding *ZRG17* constructs were confirmed to be functional by complementation of the *zrg17* mutant growth phenotype on YPGE plates at 37°C. pGEV-TRP1 was co-transformed with pRK315 and pGAL-ZRG17HA so that expression levels of Pma1p-HA and Zrg17p-HA could be controlled by the addition of β-estradiol (Sigma) (10^{-7} M or 10^{-6} M, respectively) (34).

Isolation of pHSP150

In a screen to identify suppressors of the *msc2* mutant 37°C growth defect on YPGE medium, the *msc2* mutant was transformed with a yeast genomic library in the overexpression vector YEp24. After initial selection for the plasmids, transformed cells were harvested with water and subsequently plated onto YPGE plates at a concentration of ~ 10,000 cells per plate. YPGE plates were grown at 37°C for three or four days and screened for colonies. Plasmids were harvested from these colonies and sequenced. One of the plasmids isolated was pHSP150, whose insert consists of a genomic fragment from yeast chromosome X and contains the entire *HSP150* gene.

Growth assays

The desired strains were grown overnight in YPD or SD with the appropriate auxotrophies and 10^{-6} M β-estradiol where indicated. These cultures were subsequently diluted into the same medium, and 5 μL of diluted culture, yielding 10^4 or 10^3 cells, were spotted onto YPGE plates. Where indicated, different concentrations of $ZnCl_2$ and/or 10^{-6} M β-estradiol were added to the plates. The plates were grown 3 to 4 days and photographed.

β-galactosidase assays and subcellular fractionation

β-galactosidase assays, with specific activity normalized to protein content, and subcellular fractionation, where protein extracts were fractionated on sucrose gradients +/- Mg^{2+}, were performed as described previously (10).

Zrg17p dendrogram

Related sequences were identified using a PSI-BLAST-generated Position-Specific Scoring Matrix and the resulting dendrogram is a neighbor-joined tree generated using ClustalW (36).

Protein lysates, co-immunoprecipitation, and immunoblotting

Protein lysates for immunoblotting were obtained as follows. Yeast cultures were grown to an OD_{600} = ~ 1.0 in LZM medium containing 1 μM or 1000 μM Zn. The cells were harvested, washed once with water, and resuspended in MIB (0.6 M mannitol, 20 mM HEPES-KOH, pH 7.4). Protein lysates were

obtained using glass beads in the presence of protease inhibitors (1 mM PMSF, 50 μg/mL leupeptin, 10 μg/mL pepstatin A, 1 mM EDTA (all from Sigma), mini EDTA-free protease inhibitor cocktail pellets (Roche)) and vortexing 10 x 30 seconds, with 30 seconds on ice in-between pulses. The cell debris was pelleted by centrifuging 2 minutes at 500 x g at 4°C. The resulting supernatant was the total protein lysate. To separate membrane-bound proteins from cytosol, total protein lysates were centrifuged 30 minutes at ~ 100,000 x g at 4°C in a TLS55 swinging bucket rotor in a Beckman Optima TL tabletop ultracentrifuge. The membrane pellet was resuspended in MIB plus protease inhibitors. Ten μg protein was loaded per lane for SDS-PAGE and immunoblotting.

Protein lysates for co-immunoprecipitation were obtained as described above, with the exception that they were generated in 50 mM NaCl instead of MIB. The lysates were then solubilized with 3% LM (n-dodecyl-β-D-maltoside) (MP Biomedicals) on ice for 2 hours. The insoluble proteins were pelleted by centrifuging 15 minutes at 15,000 x g at 4°C. The detergent-soluble protein lysates were diluted 1:3 into IPP150 buffer (10 mM Tris-Cl, pH 8.0, 150 mM NaCl), then 50 μL IgG-Sepharose beads (Amersham Pharmacia) were added to each lysate. The lysates + beads were rotated at 4°C for 30 minutes, after which the beads were washed 4 times with IPP150 buffer + 0.1% LM. The beads were resuspended in elution buffer (50 mM Tris-Cl, pH 8.0, 10 mM EDTA, 1% SDS) and incubated at 65°C for 30 minutes to elute the proteins off the beads. Equal volumes of eluted protein lysates were loaded onto SDS-PAGE for immunoblotting.

When denatured by boiling, epitope-tagged Zrg17p exhibited high molecular weight aggregates on immunoblots (data not shown). Therefore, lysates containing epitope-tagged Zrg17p were always denatured for 30 minutes at either 37°C or 65°C prior to SDS-PAGE. Immunoblots were done by standard techniques (37). Blots were visualized with POD (Roche). Band quantitation to determine fold difference in protein levels was performed using NIH Image 1.61. Antibodies used were rabbit anti-HA (Sigma), mouse anti-HA (12CA5, Roche), mouse anti-Dpm1p (Molecular Probes), rabbit anti-Kex2p (gift of Steven Nothwehr, University of Missouri, Columbia, MO), goat anti-mouse HRP-conjugated secondary (Pierce), and goat anti-rabbit HRP-conjugated secondary (Pierce).

RESULTS

msc2 and zrg17 mutants exhibit the same phenotypes

An *msc2* mutant was shown previously to exhibit several zinc-suppressible phenotypes, including an abnormal large cell morphology (21). Since a *zrg17* mutant also exhibited this same zinc-suppressible large cell phenotype (22), we wondered if a *zrg17* mutant would exhibit other phenotypes seen in an *msc2* mutant. Therefore, we generated an isogenic strain where the *ZRG17* gene was deleted from the genome (see Experimental Procedures). We also generated an *msc2 zrg17* double deletion strain to determine if the single mutant phenotypes were additive when combined.

An *msc2* mutant was shown to have a growth defect at 37^{o}C when grown on rich medium plates containing glycerol and ethanol, YPGE (21). As seen in **Figure 3.1A**, both the *zrg17* and *msc2 zrg17* mutants also exhibited this same temperature-sensitive growth defect. When ≥ 500 μM zinc was added to the plates, the growth of all three mutants was recovered. To determine if the single mutants were recovered by different amounts of zinc, a range of zinc concentrations was added to the plates. Both *msc2* and *zrg17* single mutants showed slight growth with the addition of 100 μM zinc and were recovered similarly by the addition of 250 μM Zn, though the *msc2* mutant grew slightly better than the *zrg17* mutant at this concentration. The double mutant showed similar growth to the single mutants at all zinc concentrations, demonstrating that this phenotype is not additive.

Figure 3.1. *The msc2 and zrg17 mutants exhibit a zinc-suppressible 37°C growth defect.* Yeast cells were grown in liquid medium overnight. Cultures were diluted into fresh medium and 5 μL volumes were plated onto YPGE plates, incubated at 30°C or 37°C, and photographed after 3 or 4 days. A, Wild type (WT, DY150), *msc2* (DY150 *msc2*), *zrg17* (CEY9), and *msc2 zrg17* (CEY11) cells were grown overnight in YPD, and 10^4 cells were plated onto YPGE plates containing the indicated amounts of $ZnCl_2$. B, Wild type (WT, DY150), *msc2* (DY150 *msc2*), *zrg17* (CEY9), and *msc2 zrg17* (CEY11) cells expressing YEp24 (vector) or pHSP150 were grown overnight in SD, and 10^4 cells were plated onto YPGE plates. C, Wild type (WT, DY150), *msc2* (DY150 *msc2*), and *zrg17* (CEY9) cells were grown overnight in SD + 10^{-6} M β-estradiol. 10^3 cells were plated onto YPGE plates containing 10^{-6} M β-estradiol and the indicated amounts of $ZnCl_2$. All strains expressed pGEV-TRP1, as well as the following plasmid combinations: pTF63 + pRS316GAL1LEU2 (vectors), YEpMSC2-myc + pRS316GAL1LEU2 (YEpMSC2-myc), or pTF63 + pGAL-ZRG17HA (pGAL-ZRG17HA).

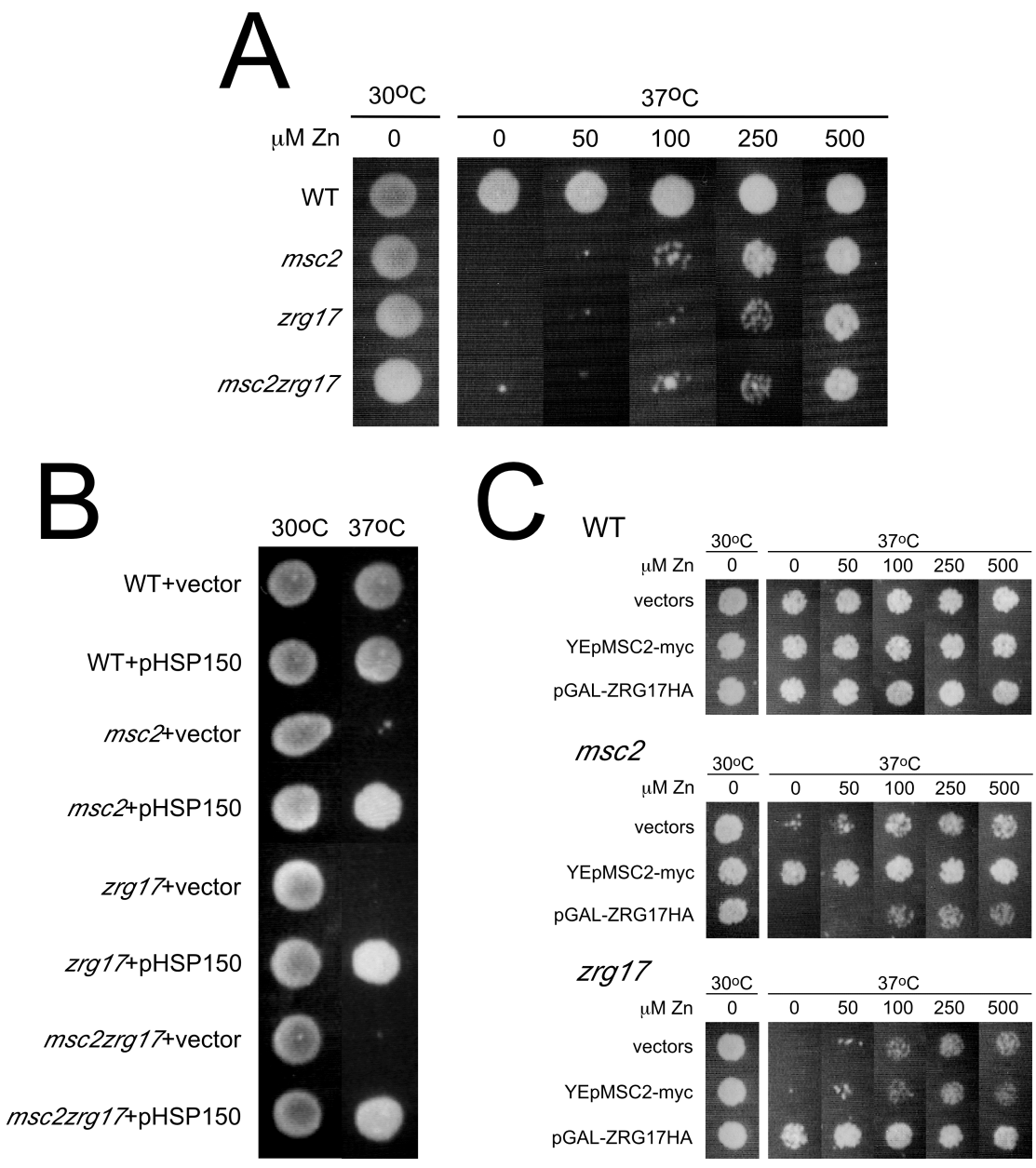
A
30°C
37°C
μM Zn
0
0
50
100
250
500
WT
msc2
zrg17
msc2zrg17
B
30°C
37°C
WT+vector
WT+pHSP150
msc2+vector
msc2+pHSP150
zrg17+vector
zrg17+pHSP150
msc2zrg17+vector
msc2zrg17+pHSP150
C
WT
30°C
37°C
μM Zn
0
0
50
100
250
500
vectors
YEpMSC2-myc
pGAL-ZRG17HA
msc2
30°C
37°C
μM Zn
0
0
50
100
250
500
vectors
YEpMSC2-myc
pGAL-ZRG17HA
zrg17
30°C
37°C
μM Zn
0
0
50
100
250
500
vectors
YEpMSC2-myc
pGAL-ZRG17HA

We performed an overexpressor screen looking for genes that could suppress the *msc2* mutant 37°C growth defect and isolated a genomic fragment that contained the *HSP150* gene (see Experimental Procedures). Hsp150p is a cell wall protein whose exact function is unknown. As seen in **Figure 3.1B**, the genomic fragment containing *HSP150* (pHSP150) suppressed the growth defect of the *zrg17* mutant as well as the *msc2 zrg17* double mutant. This suggests that Msc2p and Zrg17p are involved with the same function or pathway in the cell, since the same gene can suppress both the *msc2* and *zrg17* mutants.

If Msc2p and Zrg17p separately perform the same function in the cell (e.g., ER zinc transport), then overexpression of one gene might be able to compensate for the loss of the other. Therefore, we generated a C-terminal 3xHA-tagged construct of *ZRG17* driven by the *GAL1* promoter, which can generate high expression of *ZRG17* through use of the β-estradiol inducible pGEV system (see Experimental Procedures). We also overexpressed *MSC2* using a C-terminal myc-tagged construct on a high copy plasmid (21). C-terminal HA-tagged constructs of *MSC2* and *ZRG17* on low copy plasmids (pMSC2HA and pZRG17HA) complement the 37°C growth defect of the *msc2* and *zrg17* mutants, respectively (data not shown). This indicates that C-terminal tags do not interfere with the activity of the Msc2p and Zrg17p proteins at normal levels.

To determine if overexpression of one gene compensates for the loss of the other, we introduced the *MSC2* and *ZRG17* overexpression systems into the *msc2* and *zrg17* single mutants and grew them on YPGE plates at 37°C. **Figure 3.1C** shows that, without added zinc in the plates, the *msc2* mutant was only

recovered by the overexpression of *MSC2*, and the *zrg17* mutant was only recovered by the overexpression of *ZRG17*. Even with additional zinc added to the plates, overexpression of *ZRG17* did not encourage growth of the *msc2* mutant above expression of vectors alone, and vice versa for the *zrg17* mutant. Therefore, overexpression of Msc2p and Zrg17p cannot compensate for loss of the other protein. This result suggests one of two things. Either Msc2p and Zrg17p perform separate steps in the same pathway, or they interact together so that both are needed to perform the same function in the same compartment.

Another phenotype of the *msc2* mutant is the up-regulation of the unfolded protein response (UPR) in zinc-limiting conditions (10). The UPR is a response by cells whereby they up-regulate protein chaperones and degradation systems to refold and/or degrade misfolded proteins in the ER. We introduced a UPR reporter construct (UPRE-*lacZ*) into the *zrg17* and *msc2 zrg17* mutants and determined the activity of this reporter over a range of zinc concentrations. Like the *msc2* mutant, the *zrg17* and double mutants also exhibited elevated UPRE-*lacZ* activity in low zinc (LZM + 0.3-10 μM $ZnCl_2$) compared to wild type cells (**Figure 3.2**). The double mutant showed a similar amount of activity as both single mutants, demonstrating that this phenotype is also not additive. (The different expression levels at LZM + 1 μM $ZnCl_2$ between the *msc2* mutant and the *zrg17* and *msc2 zrg17* mutants is not reproducible in other experiments; the three mutants show similar levels of UPRE-lacZ activity at LZM + 1 μM $ZnCl_2$.) We have shown previously that activity of a *HIS4-lacZ* reporter, which is not responsive to either zinc or unfolded proteins, showed high expression in both

Figure 3.2. *The msc2 and zrg17 mutants increase UPR induction in zinc deficiency.* UPRE-*lacZ* activity in wild type (WT, DY150), *msc2* (DY150 *msc2*), *zrg17* (CEY9), and *msc2 zrg17* (CEY11) strains over a range of zinc concentrations in LZM. Shown is one representative experiment from a total of three independent experiments. The error bars indicate ± 1 S.D.

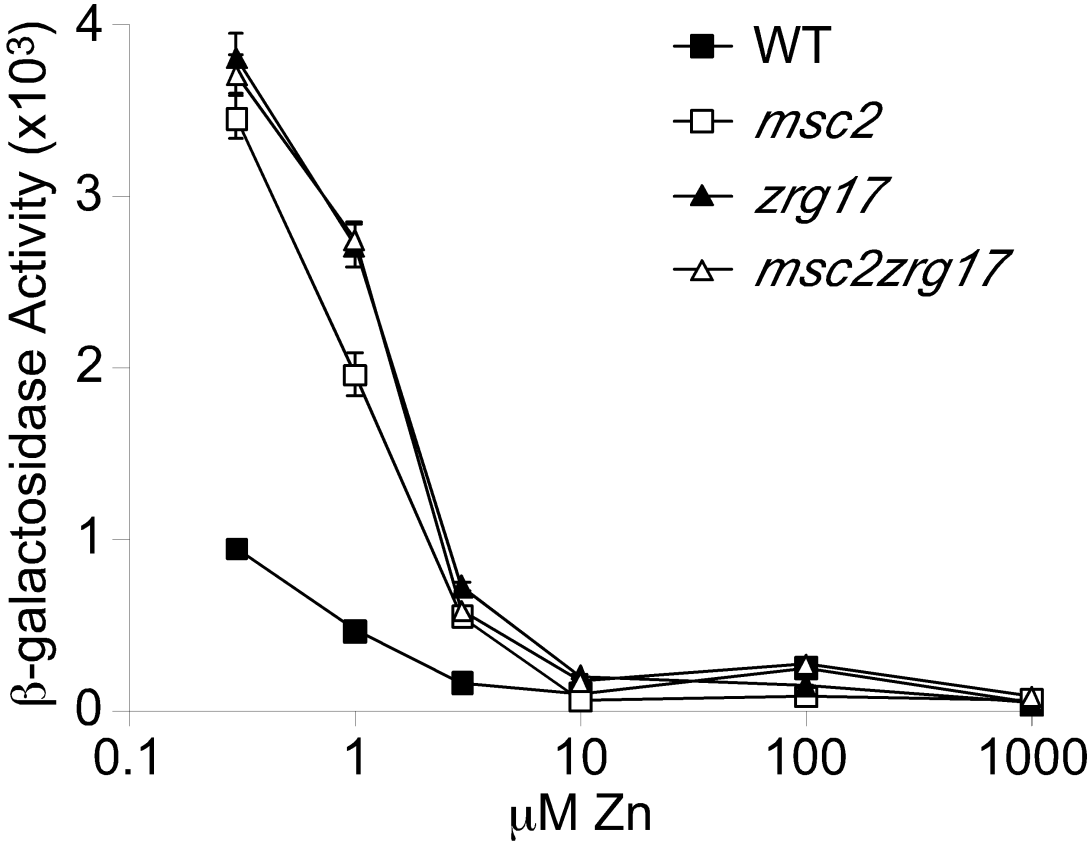
β-galactosidase Activity (x10³)
4
3
2
1
0
0.1
1
10
100
1000
μM Zn
WT
msc2
zrg17
msc2zrg17

wild type and mutant strains at all zinc concentrations (10). This indicates that the results presented here are specific to the UPRE-*lacZ* reporter and not a general effect on all *lacZ* reporters. Therefore, the UPRE-*lacZ* results suggest that Zrg17p is needed to maintain protein folding in the ER and perhaps ER function.

Msc2p has been postulated to be involved with zinc transport, due in part to the result that an *msc2* mutant may have elevated cytoplasmic zinc levels in zinc-deficient medium, as determined using a ZRE-*lacZ* reporter (10). If Msc2p and Zrg17p are involved in the same process, then perhaps a *zrg17* mutant also affects the cytosolic zinc pool. Therefore, we introduced the ZRE-*lacZ* reporter into the *zrg17* and *msc2 zrg17* mutants to determine if these strains also have higher levels of cytoplasmic zinc. In wild type cells, Zap1p is more active in low zinc, resulting in high activity of the ZRE-*lacZ* reporter (**Figure 3.3**). Then, with increasing zinc concentrations, Zap1p becomes less active, resulting in decreased expression of the reporter. The reporter expression profile in the *msc2*, *zrg17*, and *msc2 zrg17* mutants was quite different from the wild type profile. All three mutants had lower reporter activity in LZM + 1-30 μM $ZnCl_2$ than that seen in wild type cells. Once more, this phenotype was not additive in the double mutant. These results suggest that Zap1p is sensing higher amounts of zinc in the cytoplasm of these mutants, and is consistent with Zrg17p, like Msc2p, being needed to sequester this zinc into an intracellular compartment.

Figure 3.3. *The msc2 and zrg17 mutants increase labile zinc levels.* ZRE-*lacZ* activity in wild type (WT, DY150), *msc2* (DY150 *msc2*), *zrg17* (CEY9), and *msc2 zrg17* (CEY11) strains grown over a range of zinc concentrations in LZM. Shown is one representative experiment from a total of three independent experiments. The error bars indicate ± 1 S.D.

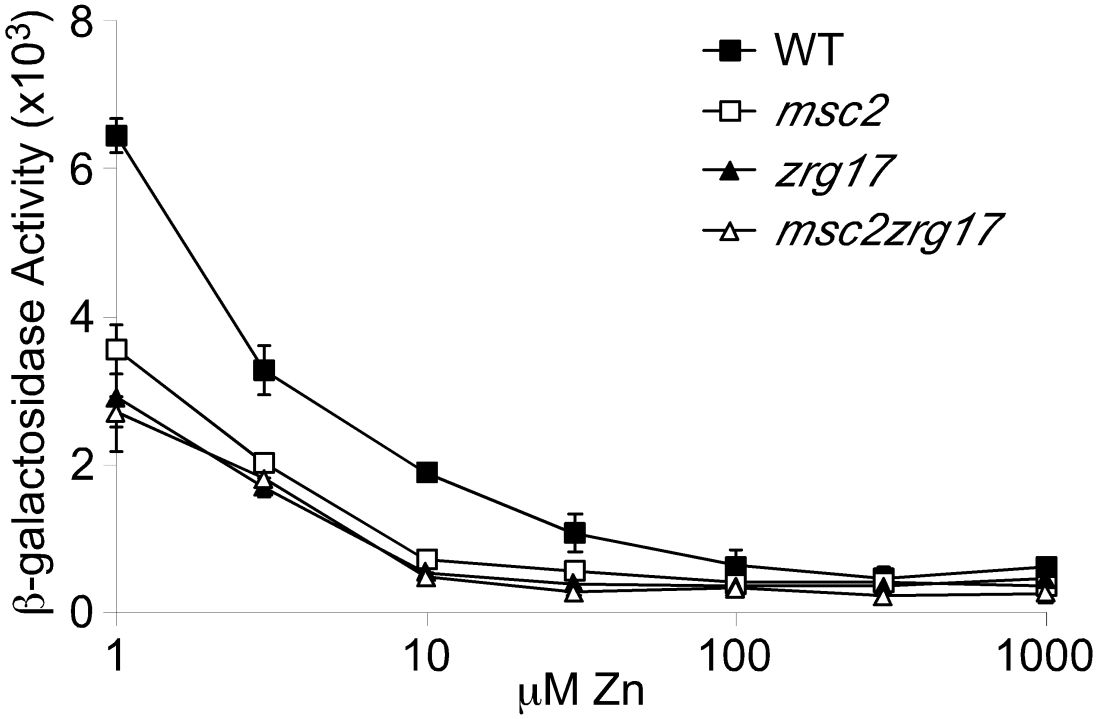
β-galactosidase Activity (x10³)
8
6
4
2
0
1
10
100
1000
μM Zn
WT
msc2
zrg17
msc2zrg17

Zrg17p is localized to the endoplasmic reticulum (ER)

With the *zrg17* mutant exhibiting the same phenotypes as an *msc2* mutant, this suggested that Zrg17p might be working in the same compartment as Msc2p, which was previously established to be the ER (10, 21). Previous localization studies of Zrg17p using fluorescence microscopy of a C-terminal GFP-tagged construct of Zrg17p suggested it to be localized to the ER (23). However, this tagged construct was not shown to be functional, leaving this localization tentative. Therefore, we set out to determine if Zrg17p was indeed localized to the ER.

We generated a construct of *ZRG17* on a low copy plasmid, where *ZRG17* was driven by its own promoter and had three HA tags fused to its C-terminus (see Experimental Procedures). This construct of Zrg17p was shown to be functional by its complementation of the *zrg17* mutant 37^{o}C growth defect (data not shown). This HA-tagged Zrg17p, when detected on immunoblots, gave two bands when the protein was denatured at 37^{o}C (see **Figures 3.4** and **3.6A**). The upper band of this doublet is the appropriate size for a 3xHA-tagged Zrg17p. However, in recent experiments, we have observed that the lower band of this doublet disappeared when denatured at higher temperatures (65^{o}C) (see **Figure 3.5B**), suggesting that the doublet is due to differences in the folded state of the protein and not due to glycosylation or other protein modifications.

We determined the localization of Zrg17p using subcellular fractionation. Briefly, protein lysates were generated from wild type cells grown in low zinc (LZM + 1 μM $ZnCl_2$) and expressing the HA-tagged Zrg17p construct. These

lysates were layered onto 20%-60% sucrose gradients and centrifuged overnight at 4^{o}C. Gradient fractions were collected and proteins were visualized by immunoblotting, using antibodies against HA or organellar marker proteins. The presence of magnesium has been shown to alter the position of ER vesicles in sucrose gradients (38). In the absence of magnesium (and in the presence of EDTA), the ER co-fractionates with the Golgi apparatus in the middle fractions of the gradient. However, in the presence of magnesium, the ER shifts to heavier fractions, co-fractionating with the plasma membrane. This shift to heavier fractions is likely due to ribosomes remaining associated with the ER when magnesium is present. If Zrg17p is localized to the ER, it should exhibit this diagnostic magnesium shift.

Figure 3.4 shows the immunoblot results of fractions from gradients prepared with or without magnesium. Significantly more Zrg17p was found in the heavier fractions of the gradient prepared with magnesium than the gradient without magnesium, co-fractionating with the plasma membrane marker, HA-tagged Pma1p. Zrg17p was found strictly in the middle fractions of the gradient prepared without magnesium, co-fractionating with the Golgi marker, Kex2p. In both gradients, Zrg17p co-localized with the ER marker, Dpm1p, which also showed the magnesium shift. Since Zrg17p shows the diagnostic magnesium shift for the ER and co-localizes with an ER marker, these data support the localization of Zrg17p to the ER. In the gradient containing magnesium, some Zrg17p was also found in the middle fractions, suggesting not all Zrg17p is found

Figure 3.4. *Zrg17p is localized to the endoplasmic reticulum.* Lysates were prepared from wild type (DY150) cells expressing either pZRG17HA (grown in LZM + 1 μM $ZnCl_2$) or pGEV-TRP1 + pRK315 (Pma1p-HA) (grown in SD + 10^{-7} M β-estradiol). Extracts were layered onto sucrose gradients for subcellular fractionation. Gradient fractions were subjected to immunoblotting and probed with anti-HA, anti-Kex2p, or anti-Dpm1p antibodies. Fractions are numbered from 1 (heaviest) to 11 (lightest). Shown are immunoblots of +Mg and -Mg gradient fractions, which are representative of four independent experiments. Note that Zrg17p-HA appears as two bands due to the incomplete denaturation of the protein at 37°C.

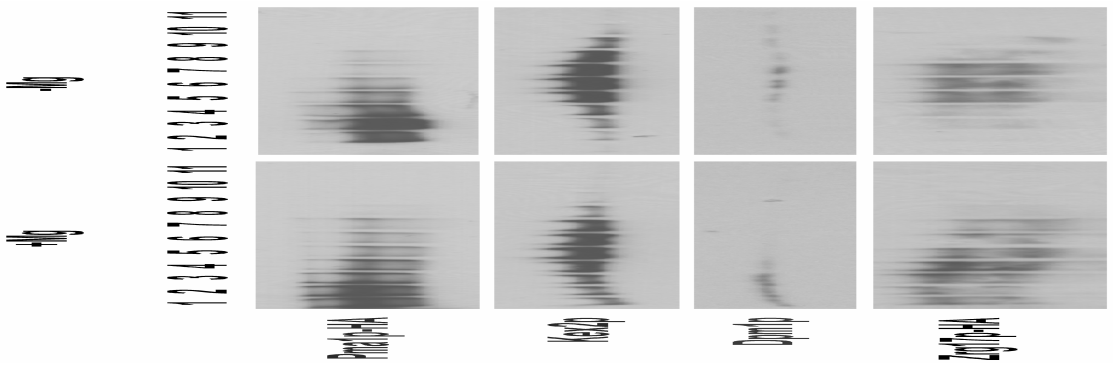

in the ER. There might be some Golgi localization of Zrg17p. This was also the case for the localization of Msc2p (10).

Msc2p and Zrg17p physically interact

With Msc2p and Zrg17p both localizing to the ER, coupled with the previous study suggesting that these two proteins interacted (24), we wanted to determine if Msc2p and Zrg17p work together as a complex. To do this, we performed co-immunoprecipitation of HA-tagged Msc2p and tandem affinity purification- (TAP-) tagged Zrg17p. The TAP tag consists of a calmodulin binding protein followed by a tobacco etch virus (TEV) protease cut site and ends with protein A, which can bind to IgG proteins (39). We obtained a strain where a TAP tag was fused to the C-terminus of *ZRG17* in the genome, and we verified functionality of this strain by its wild type levels of UPR induction in low zinc (data not shown).

Protein lysates for co-immunoprecipitation (co-IP) were generated from cells grown in low zinc (LZM + 1 μM $ZnCl_2$). The lysates were solubilized with detergent then added to IgG-Sepharose beads. The proteins were allowed to bind to the beads, then the beads were washed and proteins eluted. The eluted proteins were analyzed by immunoblotting by probing with a rabbit anti-HA antibody, which can recognize both the HA and TAP tags. If Msc2p and Zrg17p specifically interact with each other, Msc2p-HA should be precipitated only when Zrg17p-TAP is present to bind to IgG-Sepharose beads.

The immunoblotting results are shown in **Figure 3.5**. Wild type cells expressing untagged Msc2p (**Figure 3.5A**, lane 5) showed a non-specific band seen in a beads-only mock co-IP control (data not shown). Wild type cells expressing HA-tagged Msc2p showed a weak Msc2p band (lane 6), indicating some non-specific binding of Msc2p-HA to the IgG-Sepharose beads. ZRG17-TAP cells expressing untagged Msc2p showed the Zrg17p band (lane 7). Lastly, ZRG17-TAP cells expressing HA-tagged Msc2p showed both Msc2p and Zrg17p bands (lane 8). Despite some non-specific binding of Msc2p-HA to the IgG-Sepharose beads in the absence of Zrg17p-TAP, approximately five to ten times more Msc2p-HA was recovered when Zrg17p-TAP was present. This result indicates that Msc2p and Zrg17p physically interact in low zinc. This interaction was also observed using cells grown in high zinc (data not shown).

To confirm the interaction between Msc2p and Zrg17p, we also performed the reciprocal experiment using TAP-tagged Msc2p and HA-tagged Zrg17p (**Figure 3.5B**). Here, we obtained similar results, where five to ten times more Zrg17p-HA was precipitated in the presence of Msc2p-TAP. To verify that this interaction between Msc2p and Zrg17p was specific and not a general interaction between two ER proteins, we also checked for the presence of Dpm1p in our co-IP samples. No detectable Dpm1p was seen in any of these samples (data not shown), indicating that the interaction between Msc2p and Zrg17p was specific and not due to incomplete solubilization of ER membranes.

Figure 3.5. *Msc2p and Zrg17p physically interact.* Lysates were prepared from cells grown in LZM + 1 μM $ZnCl_2$ for co-immunoprecipitation. Lysates were solubilized with detergent, diluted with buffer, and added to IgG-Sepharose beads. Bound proteins were eluted off the beads and subjected to immunoblotting, probing with anti-HA antibody, which recognizes both HA and TAP tags. The asterisk denotes a background band observed in all co-IP samples regardless of the presence or absence of tagged proteins. Shown are representative immunoblots from three independent experiments. A, Co-immunoprecipitation of wild type (BY4741) and ZRG17-TAP cells expressing pMSC2 or pMSC2HA. B, Co-immunoprecipitation of wild type (BY4741) and MSC2-TAP cells expressing pZRG17 or pZRG17HA.

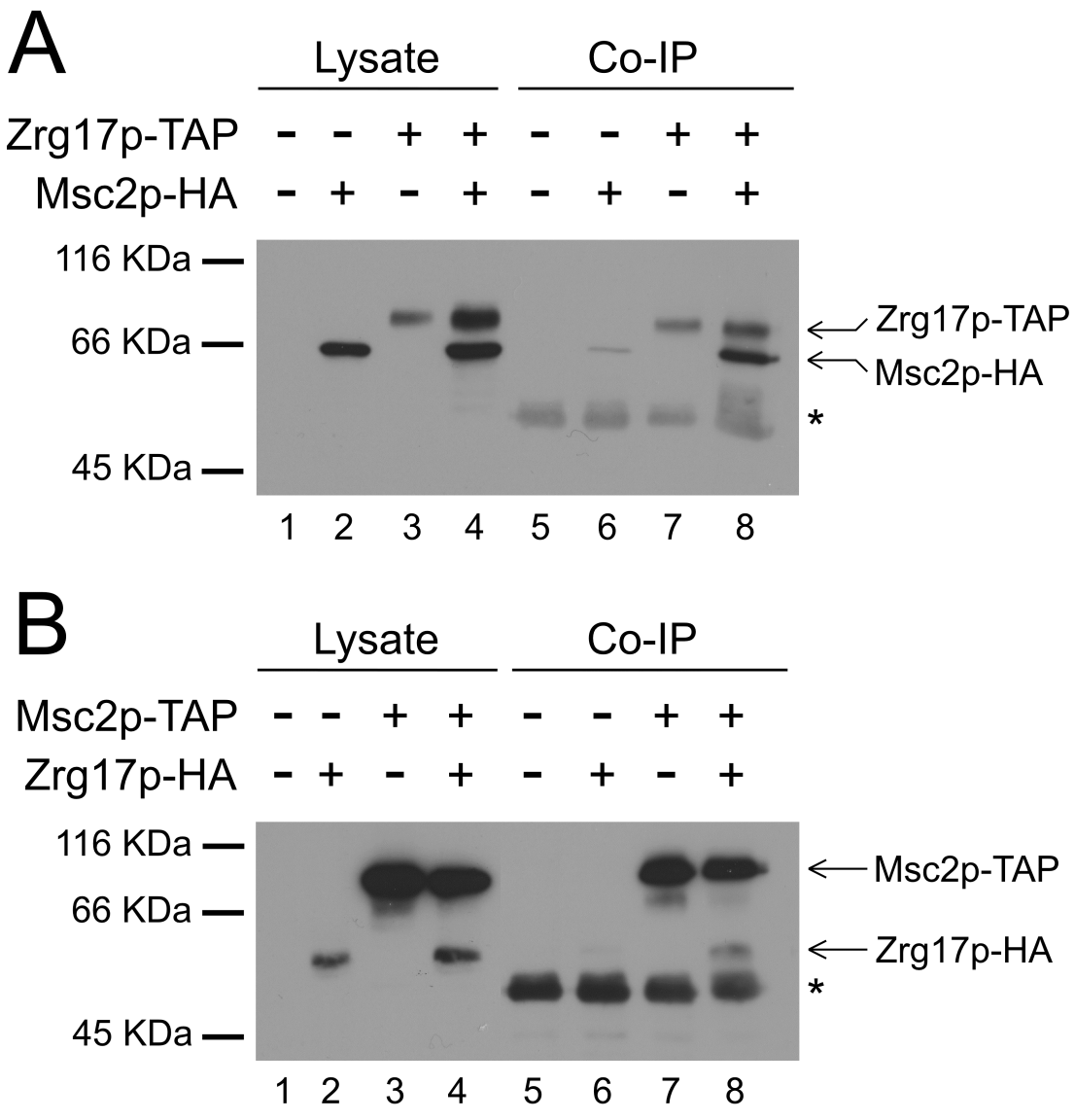
A
Lysate
Co-IP
Zrg17p-TAP - - + + - - + +
Msc2p-HA - + - + - + - +
116 KDa
66 KDa
45 KDa
Zrg17p-TAP
Msc2p-HA
*
1 2 3 4 5 6 7 8
B
Lysate
Co-IP
Msc2p-TAP - - + + - - + +
Zrg17p-HA - + - + - + - +
116 KDa
66 KDa
45 KDa
Msc2p-TAP
Zrg17p-HA
*
1 2 3 4 5 6 7 8

Msc2p and Zrg17p protein levels are regulated by zinc

ZRG17 is a Zap1p target and is regulated by zinc at the mRNA level (17, 22). *MSC2*, on the other hand, is not a Zap1p target nor regulated by zinc (17). These data suggest that Zrg17p may regulate the activity of the Msc2p-Zrg17p complex, such that the levels of Zrg17p in the ER membrane determine the zinc transport activity of the complex. Therefore, we determined if Msc2p and/or Zrg17p protein levels were regulated by zinc. We generated protein lysates of cells grown in low zinc (LZM + 1 μM $ZnCl_2$) or high zinc (LZM + 1000 μM $ZnCl_2$) and expressing the HA-tagged constructs of Msc2p or Zrg17p driven by their own promoters on low copy plasmids. To look for an enrichment of these proteins in membranes, the membrane-bound fractions were separated from the cytosolic fractions in the lysates. The lysates and membranes were then subjected to immunoblotting.

Zrg17p had approximately three-fold higher protein levels in low zinc than in high zinc, both in total protein lysates and in the fractions enriched for membranes (**Figure 3.6A**). Interestingly, Msc2p also showed three to four times higher protein levels in low zinc than in high zinc (**Figure 3.6B**). Since this regulation of Msc2p protein levels cannot be due to different levels of transcript, this indicates a post-transcriptional regulation of Msc2p protein. An attractive hypothesis would be that the interaction with Zrg17p prevents Msc2p degradation. In low zinc, when more Zrg17p is present, Msc2p is not effectively degraded. However, in high zinc, with lower levels of Zrg17p, less Msc2p is found complexed to Zrg17p, and the uncomplexed Msc2p proteins would be

Figure 3.6. *Msc2p and Zrg17p protein levels are regulated by zinc.* Lysates were prepared from wild type cells grown in low zinc (LZM + 1 μM $ZnCl_2$) or high zinc (LZM + 1000 μM $ZnCl_2$). Membrane-bound proteins were separated from cytosol by high-speed ultracentrifugation. Total protein lysates (L) and membrane fractions (M) from two or three independent samples were subjected to immmunoblotting, probing with anti-HA antibody. Shown are representative immunoblots from two independent experiments. A, Wild type (DY150) cells expressing pZRG17 (WT) or pZRG17HA. Blot was probed with mouse anti-HA antibody, which also recognizes a non-specific cytosolic protein. Note that Zrg17p-HA appears as two bands due to the incomplete denaturation of the protein at 37^{o}C. B, Wild type (DY150) cells expressing pMSC2 (WT) or pMSC2HA. Blot was probed with rabbit anti-HA antibody.

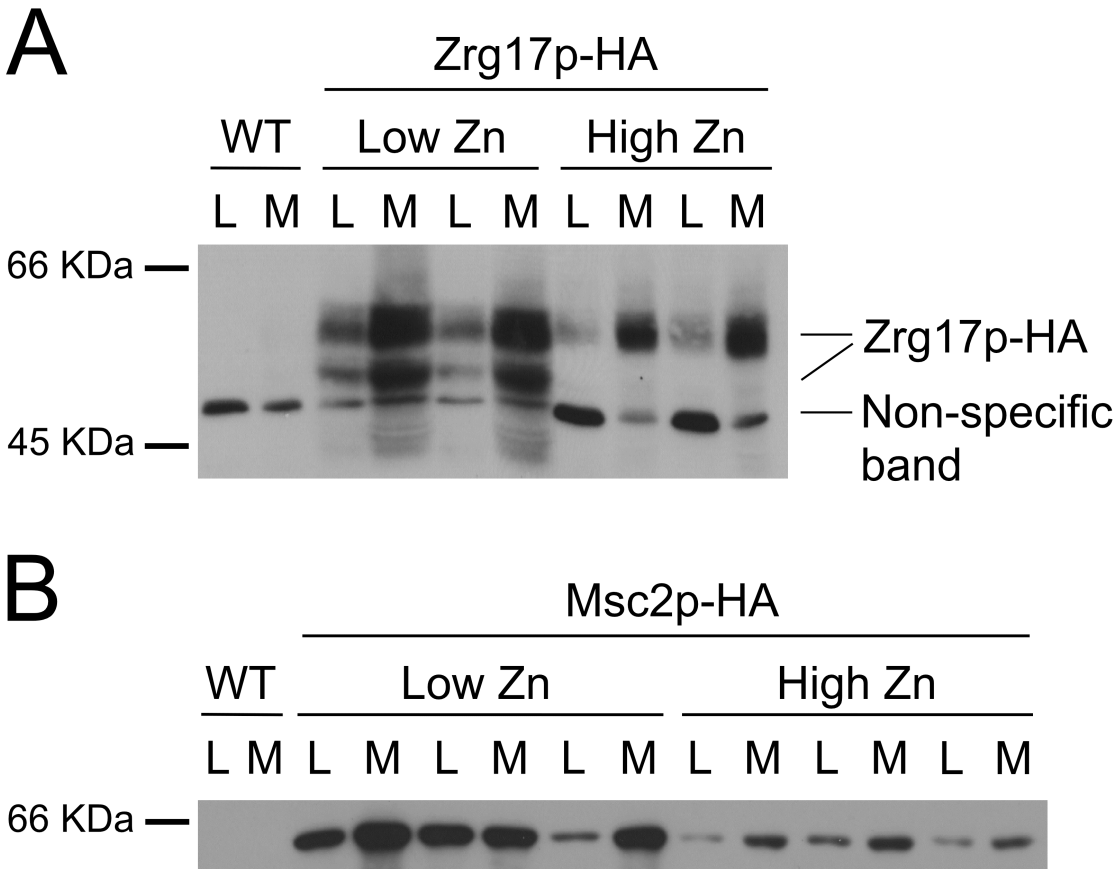
A
Zrg17p-HA
WT
Low Zn
High Zn
L M L M L M L M L M
66 KDa
45 KDa
Zrg17p-HA
Non-specific band
B
Msc2p-HA
WT
Low Zn
High Zn
L M L M L M L M L M L M
66 KDa

targeted for degradation. Therefore, despite the fact that Msc2p protein levels are affected by zinc concentration, Zrg17p may still perform a regulatory role in the complex. More experiments are needed to determine if this is the case.

Zrg17p is a distant relative of the CDF family

Since Msc2p and Zrg17p interact and Msc2p is a CDF protein, we postulated that Zrg17p might be a member of the CDF family, as well. Most CDF family members have been identified by their homology to other known members of the family. Zrg17p has not been previously identified in any of these searches as a CDF member. Using PSI-BLAST, we found that Zrg17p was homologous to several proteins in other fungi and was a distant homologue to the mammalian ZnT6 protein (**Figure 3.7**). ZnT6 is a member of the CDF family, suggesting that Zrg17p is also a member of this family. The co-immunoprecipitation data then suggest that two different CDF members interact.

Mammalian CDF homologues complement the msc2 and zrg17 mutant growth phenotype

The closest mammalian homologue to Msc2p is ZnT5 (18), and we found the closest mammalian homologue to Zrg17p is ZnT6. Given the interaction between Msc2p and Zrg17p, we postulated that their mammalian homologues might also interact. To test this, we introduced plasmids overexpressing *ZnT5* and/or *ZnT6* into the *msc2, zrg17*, and *msc2 zrg17* mutants and determined the ability of the mammalian genes to functionally complement the 37^{o}C mutant

Figure 3.7. *Zrg17p is a distant member of the CDF family.* PSI-BLAST was used to identify homologues to the Zrg17p protein, and a dendrogram of selected homologues was created using ClustalW. Where a common name is not given, the proteins are noted by Genbank accession numbers.

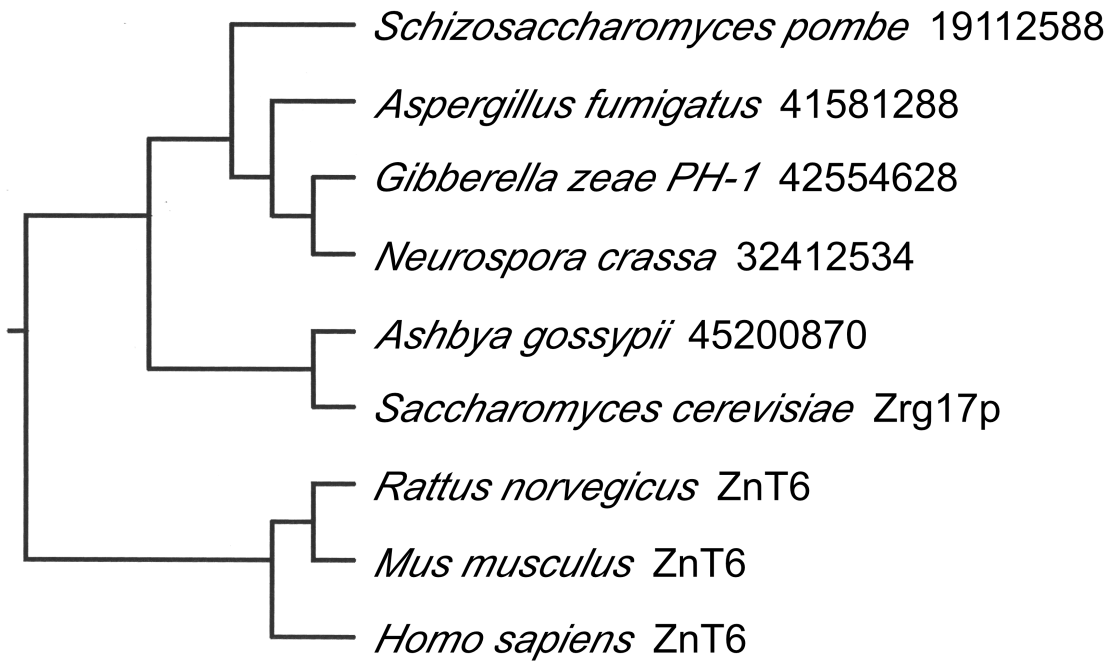
Schizosaccharomyces pombe 19112588
Aspergillus fumigatus 41581288
Gibberella zeae PH-1 42554628
Neurospora crassa 32412534
Ashbya gossypii 45200870
Saccharomyces cerevisiae Zrg17p
Rattus norvegicus ZnT6
Mus musculus ZnT6
Homo sapiens ZnT6

growth defect. As seen in **Figure 3.8**, *ZnT5* or *ZnT6* alone could not suppress the growth phenotype of any of the three mutants. Even when excess zinc was added to the plates, cells expressing just *ZnT5* or *ZnT6* did not grow any better than cells expressing vectors alone. However, when both *ZnT5* and *ZnT6* were present, the growth defect of the mutants was markedly suppressed, with or without additional zinc. These results suggest that ZnT5 and ZnT6 interact in yeast to form a functional complex to transport zinc into the secretory pathway.

Figure 3.8. *Mammalian ZnT5 and ZnT6 functionally complement the 37°C growth defect of the msc2 and zrg17 mutants.* A, Wild type (WT, DY150), B, *msc2* (DY150 *msc2*), C, *zrg17* (CEY9), and D, *msc2 zrg17* (CEY11) cells were grown in SD liquid medium + 10^{-6} M β-estradiol overnight. Cultures were diluted in fresh medium, and 5 μL volumes (10^4 cells) were plated onto YPGE plates containing 10^{-6} M β-estradiol and the indicated amounts of $ZnCl_2$. The plates were incubated at 30°C or 37°C, and photographed after 4 days. All strains expressed pGEV-TRP1, as well as the following plasmid combinations: pYES2 + pYES2L (vectors), pYES2 + pZnT5L (pZnT5), pYES2L + pZnT6 (pZnT6), pZnT5L + pZnT6 (pZnT5 and pZnT6).

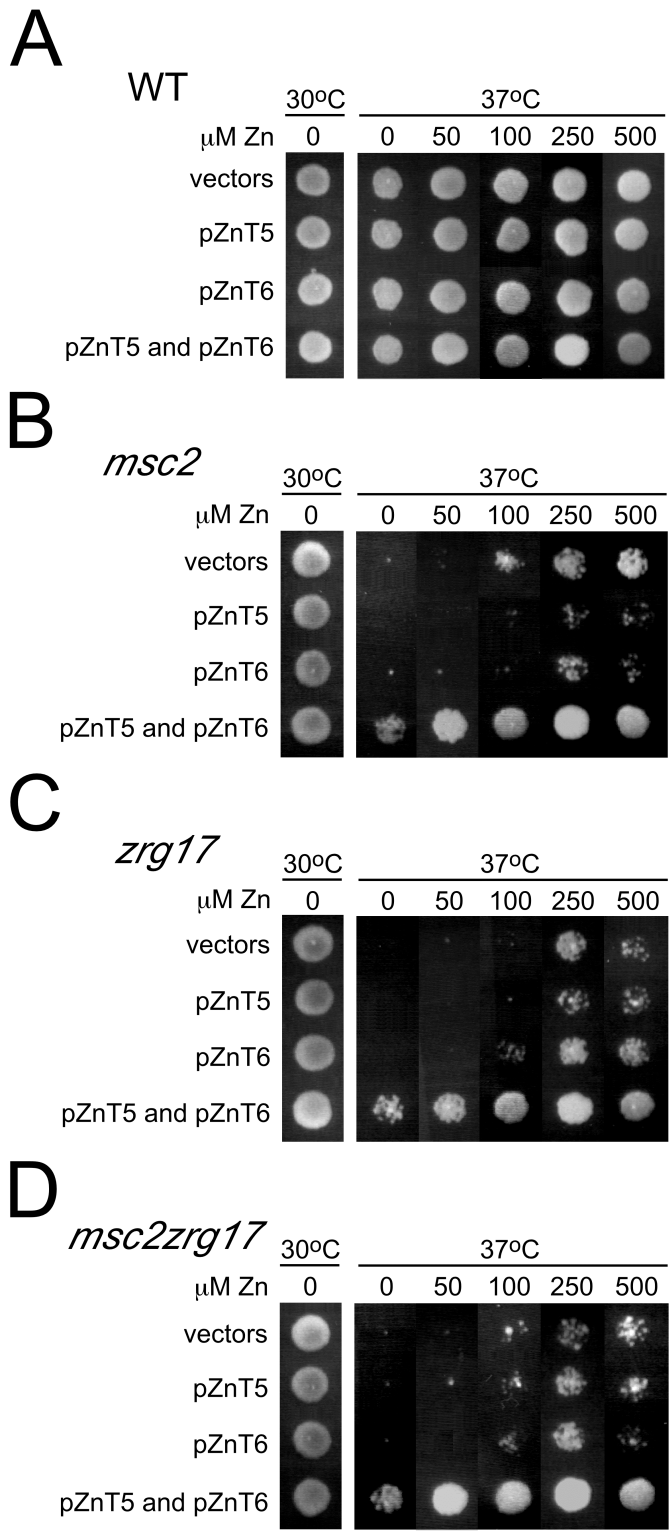
A
WT
30°C
37°C
μM Zn
0
0
50
100
250
500
vectors
pZnT5
pZnT6
pZnT5 and pZnT6
B
msc2
30°C
37°C
μM Zn
0
0
50
100
250
500
vectors
pZnT5
pZnT6
pZnT5 and pZnT6
C
zrg17
30°C
37°C
μM Zn
0
0
50
100
250
500
vectors
pZnT5
pZnT6
pZnT5 and pZnT6
D
msc2zrg17
30°C
37°C
μM Zn
0
0
50
100
250
500
vectors
pZnT5
pZnT6
pZnT5 and pZnT6

Acknowledgments

The authors thank T. Kambe and L. Huang for providing plasmids, R. Sunde for the use of his tabletop ultracentrifuge, and M. Petris and E. Rogers for helpful discussions. This work was supported by NIH grants GM56285 and GM69786. C.D.E. was supported by an NIH Training Grant.

REFERENCES

1. Huang XF and Arvan P. 1995. Intracellular transport of proinsulin in pancreatic β-cells. *J Biol Chem* **270**: 20417-20423.
2. Dodson G and Steiner D. 1998. The role of assembly in insulin's biosynthesis. *Curr Opin Struct Biol* **8**: 189-194.
3. Rock KL, York IA, and Goldberg AL. 2004. Post-proteasomal antigen processing for major histocompatibility complex class I presentation. *Nat Immunol* **5**: 670-677.
4. Serwold T, Gonzalez F, Kim J, Jacob R, and Shastri N. 2002. ERAAP customizes peptides for MHC class I molecules in the endoplasmic reticulum. *Nature* **419**: 480-483.
5. Galperin MY and Jedrzejas MJ. 2001. Conserved core structure and active site residues in alkaline phosphatase superfamily enzymes. *Proteins* **45**: 318-324.
6. Mann KJ and Sevlever D. 2001. 1,10-Phenanthroline inhibits glycosylphosphatidylinositol anchoring by preventing phosphoethanolamine addition to glycosylphosphatidylinositol anchor precursors. *Biochemistry* **40**: 1205-1213.
7. Shen Y, Meunier L, and Hendershot LM. 2002. Identification and characterization of a novel endoplasmic reticulum (ER) DnaJ homologue, which stimulates ATPase activity of BiP in vitro and is induced by ER stress. *J Biol Chem* **277**: 15947-15956.

8. Silberstein S, Schlenstedt G, Silver PA, and Gilmore R. 1998. A role for the DnaJ homologue Scj1p in protein folding in the yeast endoplasmic reticulum. *J Cell Biol* **143**: 921-933.

9. Linke K, Wolfram T, Bussemer J, and Jakob U. 2003. The roles of the two zinc binding sites in DnaJ. *J Biol Chem* **278**: 44457-44466.

10. Ellis CD, Wang F, MacDiarmid CW, Clark S, Lyons T, and Eide DJ. 2004. Zinc and the Msc2 zinc transporter protein are required for endoplasmic reticulum function. *J Cell Biol* **166**: 325-335.

11. Zhao H and Eide D. 1996. The yeast *ZRT1* gene encodes the zinc transporter of a high affinity uptake system induced by zinc limitation. *Proc Natl Acad Sci U S A* **93**: 2454-2458.

12. Zhao H and Eide D. 1996. The *ZRT2* gene encodes the low affinity zinc transporter in *Saccharomyces cerevisiae*. *J Biol Chem* **271**: 23203-23210.

13. Waters BM and Eide DJ. 2002. Combinatorial control of yeast *FET4* gene expression in response to iron, zinc, and oxygen. *J Biol Chem* **277**: 33749-33757.

14. MacDiarmid CW, Gaither LA, and Eide D. 2000. Zinc transporters that regulate vacuolar zinc storage in *Saccharomyces cerevisiae*. *EMBO J* **19**: 2845-2855.

15. MacDiarmid CW, Milanick MA, and Eide DJ. 2002. Biochemical properties of vacuolar zinc transport systems of *Saccharomyces cerevisiae*. *J Biol Chem* **277**: 39187-39194.

16. Zhao H and Eide DJ. 1997. Zap1p, a metalloregulatory protein involved in zinc-responsive transcriptional regulation in *Saccharomyces cerevisiae*. *Mol Cell Biol* **17**: 5044-5052.

17. Lyons TJ, Gasch AP, Gaither LA, Botstein D, Brown PO, and Eide DJ. 2000. Genome-wide characterization of the Zap1p zinc-responsive regulon in yeast. *Proc Natl Acad Sci U S A* **97**: 7957-7962.

18. Gaither LA and Eide DJ. 2001. Eukaryotic zinc transporters and their regulation. *Biometals* **14**: 251-270.

19. Paulsen IT and Saier MH. 1997. A novel family of ubiquitous heavy metal ion transport proteins. *J Membr Biol* **156**: 99-103.

20. Liuzzi JP and Cousins RJ. 2004. Mammalian zinc transporters. *Annu Rev Nutr* **24**: 151-172.

21. Li L and Kaplan J. 2000. The yeast gene *MSC2*, a member of the cation diffusion facilitator family, affects the cellular distribution of zinc. *J Biol Chem* **276**: 5036-5043.

22. Yuan DS. 2000. Zinc-regulated genes in *Saccharomyces cerevisiae* revealed by transposon tagging. *Genetics* **156**: 45-58.

23. Huh WK, Falvo JV, Gerke LC, Carroll AS, Howson RW, Weissman JS, and O'Shea EK. 2003. Global analysis of protein localization in budding yeast. *Nature* **425**: 686-691.

24. Ito T, Chiba T, Ozawa R, Yoshida M, Hattori M, and Sakaki Y. 2001. A comprehensive two-hybrid analysis to explore the yeast protein interactome. *Proc Natl Acad Sci U S A* **98**: 4569-4574.

25. Gitan RS, Luo H, Rodgers J, Broderius M, and Eide D. 1998. Zinc-induced inactivation of the yeast ZRT1 zinc transporter occurs through endocytosis and vacuolar degradation. *J Biol Chem* **273**: 28617-28624.

26. Kambe T, Narita H, Yamaguchi-Iwai Y, Hirose J, Amano T, Sugiura N, Sasaki R, Mori K, Iwanaga T, and Nagao M. 2002. Cloning and characterization of a novel mammalian zinc transporter, zinc transporter 5, abundantly expressed in pancreatic beta cells. *J Biol Chem* **277**: 19049-19055.

27. Huang L, Kirschke CP, and Gitschier J. 2002. Functional characterization of a novel mammalian zinc transporter, ZnT6. *J Biol Chem* **277**: 26389-26395.

28. Cross FR. 1997. 'Marker swap' plasmids: convenient tools for budding yeast molecular genetics. *Yeast* **13**: 647-653.

29. Li L and Kaplan J. 1997. Characterization of two homologous yeast genes that encode mitochondrial iron transporters. *J Biol Chem* **272**: 28485-28493.

30. Liu H, Krizek J, and Bretscher A. 1992. Construction of a *GAL1*-regulated yeast cDNA expression library and its application to the identification of genes whose overexpression causes lethality in yeast. *Genetics* **132**: 665-673.

31. Botstein D, Falco SC, Stewart SE, Brennan M, Scherer S, Stinchcomb DT, Struhl K, and Davis RW. 1979. Sterile host yeasts (SHY): a eukaryotic

system of biological containment for recombinant DNA experiments. *Gene* **8**: 17-24.

32. Kawahara T, Yanagi H, Yura T, and Mori K. 1997. Endoplasmic reticulum stress-induced mRNA splicing permits synthesis of transcription factor Hac1p/Ern4p that activates the unfolded protein response. *Mol Biol Cell* **8**: 1845-1862.

33. Kölling R and Losko S. 1997. The linker region of the ABC-transporter Ste6 mediates ubiquitination and fast turnover of the protein. *EMBO J* **16**: 2251-2261.

34. Gao CY and Pinkham JL. 2000. Tightly regulated, beta-estradiol dose-dependent expression system for yeast. *Biotechniques* **29**: 1226-1231.

35. Ma H, Kunes S, Schatz PJ, and Botstein D. 1987. Plasmid construction by homologous recombination in yeast. *Gene* **58**: 201-216.

36. Thompson JD, Higgins DG, and Gibson TJ. 1994. CLUSTAL W: improving the sensitivity of progressive multiple sequence alignment through sequence weighting, position specific gap penalties and weight matrix choice. *Nucleic Acids Res* **22**: 4673-4680.

37. Harlow E and Lane D. 1988. *Antibodies: a laboratory manual.* Cold Spring Harbor: Cold Spring Harbor Press.

38. Roberg KJ, Rowley N, and Kaiser CA. 1997. Physiological regulation of membrane protein sorting late in the secretory pathway of *Saccharomyces cerevisiae*. *J Cell Biol* **137**: 1469-1482.

39. Bauer A and Kuster B. 2003. Affinity purification-mass spectrometry. Powerful tools for the characterization of protein complexes. *Eur J Biochem* **270**: 570-578.

CHAPTER 4

DISCUSSION

Charissa D. Ellis

A novel interaction

Previous work on Zrg17p suggested it might have a role in zinc homeostasis in yeast. The potential ER localization of Zrg17p (1), coupled with the zinc suppressible large cell phenotype of the *zrg17* mutant (2), and the potential interaction with Msc2p (3) compelled us to further study and characterize this protein. We present evidence here that Zrg17p is a member of the cation diffusion facilitator (CDF) family and interacts with Msc2p to make a functional complex in the membrane of the ER to transport zinc into this compartment. Several CDF members have been postulated or shown to form homodimers or other higher order homo-oligomeric species (4-7). However, no CDF family members to date have been shown to interact with another CDF family member. This is the first definitive evidence of a physical interaction between two different CDF proteins.

Zrg17p is involved with zinc transport into the ER

Several lines of evidence suggest that Zrg17p is involved with zinc transport in yeast. First, *ZRG17* is a Zap1p target and is regulated by zinc at the mRNA (2, 8) and protein levels (**Figure 3.6**). Second, all of the *zrg17* mutant phenotypes are suppressible by zinc. These include the large cell phenotype (2), the 37^{o}C growth defect (**Figure 3.1**), and the up-regulation of the unfolded protein response (UPR) (**Figure 3.2**). Third, a *zrg17* mutant may have increased cytosolic zinc levels in zinc-deficient medium, as determined by ZRE-*lacZ* activity (**Figure 3.3**), suggesting Zrg17p is needed to put that zinc into an intracellular

compartment. Fourth, Zrg17p is a transmembrane domain protein and a distant member of the CDF family (**Figure 3.7**), whose eukaryotic members have often been shown to transport heavy metals, particularly zinc, out of the cytoplasm and into intracellular organelles (9-11). Zrg17p has been localized to the ER and possibly the Golgi ((1), **Figure 3.4**); therefore, Zrg17p could potentially be transporting zinc into these compartments. Lastly, the *zrg17* mutant growth defect at 37^{o}C is suppressed by the expression of both *ZnT5* and *ZnT6* (**Figure 3.8**). ZnT5-dependent transport activity was observed in Golgi-enriched vesicles from HeLa cells (12). Therefore, the ZnT5-ZnT6 complex could be compensating for the lack of zinc transport activity in a *zrg17* mutant. All of the above evidence suggests that Zrg17p is an ER zinc transporter or aids in the transport of zinc into the ER.

Msc2p and Zrg17p form a zinc transport complex

Given the evidence that the *msc2* and *zrg17* mutants exhibit the same zinc-suppressible phenotypes (**Figures 3.1** and **3.2**), and that Zrg17p may be a zinc transporter, this suggests that Msc2p and Zrg17p are involved in the same pathway (i.e., zinc transport) in the cell. Therefore, several models were initially proposed to define the relationship between Msc2p and Zrg17p. (1) Msc2p and Zrg17p work as independent transporters. However, this model is negated by the evidence that overexpression of one protein cannot compensate for the loss of the other (**Figure 3.1**), and the *msc2* and *zrg17* mutant phenotypes are not additive in the double mutant (**Figures 3.1-3.3**). (2) Msc2p and Zrg17p work

together as a complex in the same compartment. This model is supported by the co-immunoprecipitation data that suggest Msc2p and Zrg1p interact (**Figure 3.5**), and by the localization patterns of Msc2p and Zrg17p showing they are both in the ER and possibly the Golgi ((13), **Figure 3.4**). (3) Msc2p and Zrg17p interact, but one may function only as a regulator for the other. The possibilities of Zrg17p serving as the regulator of the complex are discussed in a later section. (4) One protein transports a substrate that is needed for the transport activity of the other protein. For example, Zrg17p may transport protons into the ER so that Msc2p could use an antiport mechanism to exchange protons for zinc. Experiments to determine the transport ability of the complex (discussed in the next section) could address this model. Even if one of these last two models is correct, they could still support the model that Msc2p and Zrg17p interact to form a complex.

Another possibility that could explain the evidence presented in chapter three is that the absence of one protein affects the subcellular localization of the other. In other words, Msc2p may require interaction with Zrg17p to be localized to the ER, and the *zrg17* mutant phenotypes could be explained by the mis-localization of Msc2p. Alternatively, this could be true for Zrg17p in an *msc2* mutant. We have determined by subcellular fractionation and immunofluorescence microscopy that under zinc-replete conditions, Msc2p is localized to the ER in a *zrg17* mutant (data not shown). However, we still need to verify that this occurs in low zinc conditions, as well as determine if Zrg17p is localized normally in an *msc2* mutant.

Further studies on the Msc2p-Zrg17p complex

We can infer zinc transport ability of an Msc2p-Zrg17p complex based on ZRE-*lacZ* activity assays and suppression of the mutant growth phenotypes by ZnT5 and ZnT6. However, the best means of showing transport function of the complex would be a direct assay. This assay would need to be specific to zinc, as well as sensitive enough to detect minute changes in zinc status. Demonstrating an increase in zinc uptake into liposomes containing purified Msc2p and Zrg17p is perhaps the best method. However, alternative methods would determine the zinc transport activity of isolated ER microsomes. One such method would use radioactive zinc and demonstrate an increased uptake of this zinc into microsomes only when both Msc2p and Zrg17p are present. A second method would use a zinc-binding dye or fluorophore, such as zinquin or FuraZin-1, which is more sensitive and safer than using radioactive zinc. This dye would be loaded into microsomes before the addition of zinc, and then the fluorescence given off by the zinc-bound dye would be monitored over time. The rate and maximum amount of fluorescence should depend on the presence of Msc2p and Zrg17p in the microsomal membranes.

Several aspects of the nature of the Msc2p-Zrg17p complex are still to be determined. First and foremost is determining the domains of interaction in both Msc2p and Zrg17p. The interaction is most likely between hydrophobic transmembrane domains (TMs) in the lipid bilayer; however, there may be other parts of the proteins which associate. Strategic mutagenesis of suspected regions of interaction or random mutagenesis of the genes encoding both

proteins could be employed to determine the regions and/or amino acids necessary for interaction. The Msc2p protein has approximately 15 TMs, but the last six are the most homologous to other members of the CDF family. It is entirely possible that the extra nine or so N-terminal TMs of Msc2p are not needed for transport activity but rather for interaction with Zrg17p. Also, we cannot assume that the stoichiometry of the complex is 1:1. Msc2p may also interact with itself, forming more than a 1:1 complex with Zrg17p. An easy way to test if Msc2p interacted with itself would be co-immunoprecipitation with two different tagged versions of Msc2p. This method could also be used to determine if Zrg17p homo-oligomerized. Alternatively, native PAGE could be employed to determine the sizes of Msc2p-Zrg17p oligomers and the possible stoichiometries of the complex.

If the Msc2p-Zrg17p complex is 1:1, this would still amount to about 22 TMs in the complex. If all 22 TMs are needed for transport, it may be that the complex does not transport ionic zinc, but rather a larger molecule such as a zinc-chelate, or a zinc-bound protein. Alternatively, not all 22 TMs may be needed for the transport of zinc into the ER. As discussed below, Zrg17p may merely play a regulatory role to govern the activity of Msc2p and not be needed for the actual transport of zinc. Accordingly, the first nine TMs of Msc2p may not be necessary for transport, either, indicating that the last six TMs of Msc2p encompass the actual transport pore in the membrane. To test this, we could generate a truncated form of Msc2p containing only the last six TMs. If this C-terminal part of the protein is independently functional for zinc transport, we

should be able to see zinc uptake activity of this construct using one of the methods previously described. This assay could be performed in the presence or absence of Zrg17p to determine the effect of Zrg17p on this truncated Msc2p. The truncated protein could also be tested for functionality by its ability to suppress the *msc2* mutant phenotypes, such as the 37^{o}C growth defect and the UPR induction in low zinc.

Lastly, many CDF members transport more than one type of heavy metal (14-17). While the characterization of Msc2p and Zrg17p thus far has been in the context of zinc transport, the complex may have a wider substrate specificity. Assays used to determine the zinc transport ability of the complex can also be used to determine which other metals may be transported by the complex.

Zrg17p may regulate the activity of the complex

We determined that Zrg17p protein levels are regulated by zinc (**Figure 3.6**), which fits nicely with the zinc regulation of *ZRG17* mRNA. This data supports the model that Zrg17p may regulate the activity of the Msc2p-Zrg17p complex. The predication of this would be that more Zrg17p protein is expressed in low zinc so that more complex is formed in the ER membrane, leading to higher zinc transport ability to maintain constant zinc transport in low zinc. To test this regulatory role of Zrg17p, an indirect assay would be to determine the effects of *ZRG17* overexpression on ZRE-*lacZ* activity. Presumably only overexpression of *ZRG17* and not *MSC2* would cause a decrease in cytosolic zinc, resulting in more Zap1p activity and higher ZRE-*lacZ* activity in wild type

cells. A more direct assay would be to examine the amount of fluorescence given off by the zinc-dependent dye in microsomes when different amounts of Zrg17p are expressed, but with a constant level of Msc2p.

Interestingly, while *MSC2* shows no zinc regulation at the mRNA level, Msc2p protein is regulated by zinc. Despite lower levels of Msc2p protein in high zinc, there is still plenty of Msc2p protein present for complex formation, for similar amounts of Msc2p were precipitated in the co-immunoprecipitation experiments in both low and high zinc (data not shown). Two possible reasons for the zinc-dependent protein levels of Msc2p are (1) high zinc slows the translation of Msc2p or (2) Msc2p is being degraded in high zinc. To test if Msc2p translation is affected by zinc concentration, cells could be grown in high or low zinc in the presence of cycloheximide for a period of time to inhibit translation. Then, the cells can be transferred to fresh medium lacking cycloheximide and allowed to re-initiate translation for different lengths of time, after which cells can be harvested to generate protein lysates. If Msc2p translation is slower in high zinc, we should see a difference in the amount of new Msc2p being made in high zinc versus low zinc after the cells are released from cycloheximide inhibition.

For the possibility that the Msc2p protein is being degraded in high zinc, we can propose two models: Zrg17p-dependent and Zrg17p-independent. The Zrg17p-dependent model predicts that when Msc2p is complexed to Zrg17p, it is protected from degradation. However, when less Zrg17p protein is present in high zinc, less complex can be formed, and more Msc2p would be available for

degradation. This model could be tested by examining Msc2p protein levels in a *zrg17* mutant. The prediction here would be that Msc2p protein levels would be lower in low zinc and would be similar to protein levels in high zinc since Zrg17p is not present. The Zrg17p-independent model implies that some other change occurs between low zinc and high zinc that makes Msc2p more susceptible to degradation, such as the activation of a protease in high zinc. If this second model were true, Msc2p protein levels would still be regulated by zinc in a *zrg17* mutant.

A different reason for the zinc regulation of Msc2p could be due to the HA tags present on the C-terminus of the protein, i.e., the HA tags somehow make the protein more likely to be degraded in high zinc. To address this possibility, we could determine the protein levels of a different tagged construct of Msc2p, such as a myc-tagged version, in low and high zinc and see if we get the same results as with the HA-tagged version. We could also try an N-terminal tagged construct in case the position of the tag on the protein affects its zinc regulation. The best test would be to generate an antibody against the Msc2p protein itself, and then look at protein levels in low and high zinc, so as to not have to deal with a tagged protein at all.

Reasons for the YPGE 37^{o}C growth defect of *msc2* and *zrg17* mutants

Perhaps the most interesting phenotype of the *msc2* and *zrg17* mutants is their 37^{o}C growth defect on glycerol-ethanol medium. These mutants grow normally on glucose plates at 37^{o}C, as well as on glycerol-ethanol plates at 30^{o}C.

These results suggest that under normal growth conditions, the mitochondria in these mutants can respire normally. Since Msc2p and Zrg17p localize to the ER instead of to the inner mitochondrial membrane, the reason for a possible respiratory defect of these mutants at 37°C is unclear.

It may be possible that the *msc2* and *zrg17* mutants have a temperature sensitive phenotype that disrupts mitochondrial respiration. To test this, we could isolate mitochondria from wild type, *msc2*, *zrg17*, and/or *msc2 zrg17* mutant cells grown in glycerol-ethanol medium at 30°C, where respiration is still normal. These mitochondria could then be tested for their respiratory capability using an oxygen electrode, which can measure oxygen consumption by the mitochondria. The chamber housing the mitochondria in the electrode can be controlled for temperature, so we could determine the effect of raising the temperature to 37°C on mitochondrial respiration. A similar experiment would be to look at the oxygen consumption of mitochondria isolated from *msc2* and *zrg17* mutants that have been growing in glycerol-ethanol medium at 30°C and then shifted to 37°C for different lengths of time. If the mitochondria from the mutants have a temperature sensitive respiratory defect, the oxygen consumption at 37°C should be greatly diminished relative to wild type mitochondria. However, if the mitochondria from *msc2* and *zrg17* mutants can respire normally, regardless of temperature, then we should not see differences in oxygen consumption between these mitochondria and mitochondria from wild type cells. If no differences are seen in mitochondrial respiration between the mutants and wild type cells, this suggests that the reason for the mutant 37°C growth defect may merely be due

to the combined stresses of heat and respiration (i.e., sub-optimal carbon sources), despite the medium being replete for zinc.

Alternatively, there could be an interesting correlation between the large cell phenotype and the 37°C growth defect. The *msc2* mutant was found to have a greater population of large cells in YPGE medium grown at 37°C than at 30°C (18). We have postulated previously that an *msc2* mutant may be defective in processes involving the attachment or secretion of proteins to the cell wall, including glycosylphosphatidylinositol- (GPI-) anchor synthesis (13). Therefore, on YPGE at 37°C, with the additional stresses of heat and slower growth due to respiration, an *msc2* mutant may not be able to maintain the integrity of its cell wall and limit its cell size, resulting in the large cell phenotype. We have found that when we isolated large cells and placed them on YPD plates, no colonies formed, indicating these large cells are actually dead (D. Eide, unpublished observation). This suggests that perhaps the formation of the large cell phenotype leads to cell death, and hence the 37°C growth defect. Consistent with this hypothesis is our observation that the Hsp150p protein, which is found on the cell wall, suppresses the *msc2* and *zrg17* growth defect (**Figure 3.1**) and the *msc2* mutant large cell phenotype (data not shown) when overexpressed. This suggests that overexpression of Hsp150p helps stabilize the cell wall so that the mutants can retain their normal cell size at 37°C and therefore survive at this higher temperature. Similarly, with enough added zinc in the plates, the defects in the ER/secretory pathway caused by the absence of Msc2p/Zrg17p can be bypassed, and therefore the cells do not become large and die.

To determine if there are cell wall defects in *msc2* and *zrg17* mutants, the integrity of their cell walls can be tested by their sensitivity to the drug calcofluor white. Calcofluor white binds chitin in the cell wall and disrupts cell wall biogenesis (19, 20). If cell wall integrity is compromised, the mutants should be more sensitive to calcofluor white than wild type cells. The strains could be grown on different carbon sources, at different temperatures, and on plates containing different concentrations of zinc to determine the specific stress conditions that may result in compromised cell wall integrity and sensitivity to calcofluor white. These results may tell us if the large cell phenotype and/or the 37^{o}C growth defect are related to weaknesses in the cell walls of the mutants.

Other zinc transporters in the secretory pathway

Since an *msc2 zrg17* mutant is viable and its phenotypes are suppressible by zinc, there must be other zinc transporters in the ER and/or the secretory pathway that supply zinc to these compartments. We have found that Zrc1p and Cot1p aid in zinc transport into the ER, as determined by the elevated UPR induction of a *msc2 zrc1 cot1* triple mutant in low zinc (13). However, even this triple mutant was suppressed by zinc.

There are several approaches we could use to identify other zinc transporters in the secretory pathway. Of particular interest would be to identify a zinc transporter in the Golgi apparatus, as none have yet been discovered in yeast. One method is to identify candidate genes from the yeast genome sequence. Some examples include the following proteins, all of which are P-type

ATPases that have been implicated with metal ion transport, but whose functions are not well-defined. Cod1p/Spf1p has been localized to the ER, and a *cod1* mutant up-regulates the UPR. Cod1p has been implicated with calcium homeostasis, but the actual ionic substrate of Cod1p is unknown (21). Pca1p, whose localization is unknown, was suggested to be a copper transporter, whereas a mutant allele of Pca1p, called Cad2p, was implicated with cadmium tolerance (22, 23). A final example is Pmr1p, which may be involved in transporting manganese and calcium into the Golgi (24, 25).

A second method would be to use a transposon genetic screen in an *msc2 zrg17 zrc1 cot1* mutant to identify other zinc transporters in the secretory pathway. (Presumably this quadruple mutant would be viable since an *msc2 zrc1 cot1* mutant and an *msc2 zrg17* mutant are both viable.) If a transposon disrupts a gene encoding another zinc transporter essential for the function of the secretory pathway, we could screen for it in several ways. One screen would be to look for transposon-insertion mutations that caused a synthetic lethal phenotype in the quadruple mutant on YPD at 37^{o}C. A second screen would look for mutations that exhibit the 37^{o}C growth defect on YPGE and cannot be suppressed by zinc.

However, if the transposon-insertions do not yield any informative mutations (possibly indicating the strains we would be interested in are not viable under normal growth conditions), we could do a suppressor screen. While we have previously done a suppressor screen where we identified *HSP150* as a suppressor of the *msc2* mutant 37^{o}C growth defect, this screen was not

exhaustive, and would be worth doing again in terms of an *msc2 zrg17 zrc1 cot1* mutant. A different suppressor screen could look for genes that when overexpressed suppressed the zinc-deficient phenotype(s) of an *msc2 zrg17 zrc1 cot1* mutant, such as the UPR induction in low zinc.

A mammalian zinc transport complex

While we present novel evidence here of the interaction between two different CDF family members in yeast, this may actually be a common phenomenon with CDF members. The closest mammalian homologue to Msc2p is ZnT5, and the closest mammalian homologue to Zrg17p is ZnT6. Previous studies looked at the effects of overexpression of *ZnT5* or *ZnT6* on yeast growth; however, the results from these experiments were unclear as to the function of these genes in yeast (12, 26). We found that the overexpression of both *ZnT5* and *ZnT6* can suppress the 37^{o}C growth phenotype of the *msc2*, *zrg17*, and *msc2 zrg17* mutants (**Figure 3.8**). This suppression only took place when both *ZnT5* and *ZnT6* were expressed in the same cell, regardless of zinc availability in the medium. (The mammalian proteins must not be able to interact with the yeast proteins or function independently in yeast.) This suggests that ZnT5 and ZnT6 interact in yeast to form a complex that can transport zinc into the secretory pathway.

These results also suggest that ZnT5 and ZnT6 have the potential to form a complex in mammalian cells. Supporting this hypothesis, in mammalian cells *ZnT5* and *ZnT6* are both expressed in the Golgi apparatus (12, 26) and in many

of the same tissues, as determined by EST database mining (27). This mammalian complex also has the potential to be regulated by zinc. *ZnT5* mRNA was shown to be up-regulated by TPEN treatment (or zinc deficiency) in mammalian cells (28), similar to the zinc regulation of *ZRG17* in yeast.

However, *ZnT5* and *ZnT6* are also expressed in tissues where the other is not (27). This might mean several things. First, ZnT5 and ZnT6 might interact with other ZnTs. For example, both *ZnT5* and *ZnT8* are highly expressed in pancreas (12, 27, 29), suggesting that perhaps the proteins of these two genes interact in beta cells to supply zinc for insulin granule formation. Also, ZnT6 might interact with ZnT7, which is the closest mammalian homologue to ZnT5 (27), and is also up-regulated by zinc deficiency (28). Alternatively, it is possible that *ZnT5* and *ZnT6* are indeed expressed in all the same tissues, but the methods used to determine expression levels so far (Northerns, EST database mining) have not been sensitive enough to determine this. Second, ZnT5 and ZnT6 might be able to have some individual transport activity. If so, this might suggest that there would be some advantage to having them interact as a complex, or that the individual activity of the transporters would be greatly enhanced when both ZnT5 and ZnT6 are present. ZnT5 was shown to have transport ability in Golgi vesicles isolated from HeLa cells (12). ZnT6 might also have been expressed endogenously in these cells, so that the transport activity seen was actually that of the complex and not of ZnT5 alone.

The exact function of ZnT5 and ZnT6 in transporting zinc into the Golgi in mammalian cells is unknown. However, a recent report has suggested ZnT5 is

needed to supply zinc to GPI-anchored alkaline phosphatases, which transit through the secretory pathway to the plasma membrane (30). Since ZnT5 and ZnT6 can complement the 37^{o}C growth defect of the *msc2* and *zrg17* mutants (**Figure 3.8**), this suggests that perhaps ZnT5 and ZnT6 perform the same function as Msc2p and Zrg17p: supplying zinc to the secretory pathway to maintain protein folding in the ER and other processes. To test this, we could introduce our UPRE-*lacZ* reporter in the *msc2* and *zrg17* mutant strains expressing *ZnT5* and *ZnT6* and determine if the mammalian proteins can suppress the induction of the UPR in low zinc. Another test would be to knock down *ZnT5* and/or *ZnT6* transcript levels in mammalian cells (through antisense oligonucleotide- or RNAi-mediated mRNA degradation) and look for an induction in the activity of our mammalian ER stress response luciferase reporter. Both of these assays would look at the functional significance of ZnT5 and ZnT6 in the secretory pathway.

Summary

We present here novel evidence that two CDF family members, Msc2p and Zrg17p, interact to form a complex in the ER membrane. The purpose of this complex is to transport zinc into the ER to maintain proper ER function. This includes maintaining protein folding and protein degradation systems in the ER. While Zrc1p and Cot1p aid in supplying zinc to the ER, other zinc transporters in the secretory pathway are yet to be found. The results found in yeast are reflected in mammalian cells. Mammalian cells also require zinc for protein

folding in the ER. Analogous to Msc2p and Zrg17p, the ZnT5 and ZnT6 proteins may potentially interact to form a zinc transport complex in the secretory pathway in mammalian cells. These results suggest that there is a universal requirement for zinc in the function of the ER, and that the interaction between different CDF family members may be a widely seen phenomenon.

REFERENCES

1. Huh WK, Falvo JV, Gerke LC, Carroll AS, Howson RW, Weissman JS, and O'Shea EK. 2003. Global analysis of protein localization in budding yeast. *Nature* **425**: 686-691.
2. Yuan DS. 2000. Zinc-regulated genes in *Saccharomyces cerevisiae* revealed by transposon tagging. *Genetics* **156**: 45-58.
3. Ito T, Chiba T, Ozawa R, Yoshida M, Hattori M, and Sakaki Y. 2001. A comprehensive two-hybrid analysis to explore the yeast protein interactome. *Proc Natl Acad Sci U S A* **98**: 4569-4574.
4. Blaudez D, Kohler A, Martin F, Sanders D, and Chalot M. 2003. Poplar metal tolerance protein 1 confers zinc tolerance and is an oligomeric vacuolar zinc transporter with an essential leucine zipper motif. *Plant Cell* **15**: 2911-2928.
5. Palmiter RD and Findley SD. 1995. Cloning and functional characterization of a mammalian zinc transporter that confers resistance to zinc. *EMBO J* **14**: 639-649.
6. vanderZaal BJ, Neuteboom LW, Pinas JE, Chardonnens AN, Schat H, Verkleij JAC, and Hooykaas PJJ. 1999. Overexpression of a novel *Arabidopsis* gene related to putative zinc-transporter genes from animals can lead to enhanced zinc resistance and accumulation. *Plant Physiol* **119**: 1047-1055.
7. Wei Y, Li H, and Fu D. 2004. Oligomeric state of the *Escherichia coli* metal transporter YiiP. *J Biol Chem* **279**: 39251-39259.

8. Lyons TJ, Gasch AP, Gaither LA, Botstein D, Brown PO, and Eide DJ. 2000. Genome-wide characterization of the Zap1p zinc-responsive regulon in yeast. *Proc Natl Acad Sci U S A* **97**: 7957-7962.

9. Gaither LA and Eide DJ. 2001. Eukaryotic zinc transporters and their regulation. *Biometals* **14**: 251-270.

10. Liuzzi JP and Cousins RJ. 2004. Mammalian zinc transporters. *Annu Rev Nutr* **24**: 151-172.

11. Paulsen IT and Saier MH. 1997. A novel family of ubiquitous heavy metal ion transport proteins. *J Membr Biol* **156**: 99-103.

12. Kambe T, Narita H, Yamaguchi-Iwai Y, Hirose J, Amano T, Sugiura N, Sasaki R, Mori K, Iwanaga T, and Nagao M. 2002. Cloning and characterization of a novel mammalian zinc transporter, zinc transporter 5, abundantly expressed in pancreatic beta cells. *J Biol Chem* **277**: 19049-19055.

13. Ellis CD, Wang F, MacDiarmid CW, Clark S, Lyons T, and Eide DJ. 2004. Zinc and the Msc2 zinc transporter protein are required for endoplasmic reticulum function. *J Cell Biol* **166**: 325-335.

14. Anton A, Grosse C, Reismann J, Pribyl T, and Nies DH. 1999. CzcD is a heavy metal transporter involved in regulation of heavy metal resistance in *Ralstonia* sp. Strain CH34. *J Bacteriol* **181**: 6876-6881.

15. Guffanti AA, Wei Y, Rood SV, and Krulwich TA. 2002. An antiport mechanism for a member of the cation diffusion facilitator family: divalent cations efflux in exchange for K+ and H+. *Mol Microbiol* **45**: 145-153.

16. Kamizono A, Nishizawa M, Teranishi Y, Murata K, and Kimura A. 1989. Identification of a gene conferring resistance to zinc and cadmium ions in the yeast *Saccharomyces cerevisiae*. *Mol Gen Genet* **219**: 161-167.

17. Kim D, Gustin JL, Lahner B, Persans MW, Baek D, Yun DJ, and Salt DE. 2004. The plant CDF family member TgMTP1 from the Ni/Zn hyperaccumulator *Thlaspi goesingense* acts to enhance efflux of Zn at the plasma membrane when expressed in *Saccharomyces cerevisiae*. *Plant J* **39**: 237-251.

18. Li L and Kaplan J. 2000. The yeast gene *MSC2*, a member of the cation diffusion facilitator family, affects the cellular distribution of zinc. *J Biol Chem* **276**: 5036-5043.

19. Elorza MV, Rico H, and Sentandreu R. 1983. Calcofluor white alters the assembly of chitin fibrils in *Saccharomyces cerevisiae* and *Candida albicans* cells. *J Gen Microbiol* **129 (Pt 5)**: 1577-1582.

20. Vossen JH, Muller WH, Lipke PN, and Klis FM. 1997. Restrictive glycosylphosphatidylinositol anchor synthesis in cwh6/gpi3 yeast cells causes aberrant biogenesis of cell wall proteins. *J Bacteriol* **179**: 2202-2209.

21. Cronin SR, Rao R, and Hampton RY. 2002. Cod1p/Spf1p is a P-type ATPase involved in ER function and Ca^{2+} homeostasis. *J Cell Biol* **157**: 1017-1028.

22. Rad MR, Kirchrath L, and Hollenberg CP. 1994. A putative P-type Cu(2+)-transporting ATPase gene on chromosome II of *Saccharomyces cerevisiae*. *Yeast* **10**: 1217-1225.

23. Shiraishi E, Inouhe M, Joho M, and Tohoyama H. 2000. The cadmium-resistant gene, *CAD2*, which is a mutated putative copper-transporter gene (*PCA1*), controls the intracellular cadmium-level in the yeast *S. cerevisiae*. *Curr Genet* **37**: 79-86.

24. Lapinskas PJ, Cunningham KW, Liu XF, Fink GR, and Culotta VC. 1995. Mutations in *PMR1* suppress oxidative damage in yeast cells lacking superoxide dismutase. *Mol Cell Biol* **15**: 1382-1388.

25. Durr G, Strayle J, Plemper R, Elbs S, Klee SK, Catty P, Wolf DH, and Rudolph HK. 1998. The medial-Golgi ion pump Pmr1 supplies the yeast secretory pathway with Ca^{2+} and Mn^{2+} required for glycosylation, sorting, and endoplasmic reticulum-associated protein degradation. *Mol Biol Cell* **9**: 1149-1162.

26. Huang L, Kirschke CP, and Gitschier J. 2002. Functional characterization of a novel mammalian zinc transporter, ZnT6. *J Biol Chem* **277**: 26389-26395.

27. Seve M, Chimienti F, Devergnas S, and Favier A. 2004. *In silico* identification and expression of *SLC30* family genes: an expressed sequence tag data mining strategy for the characterization of zinc transporters' tissue expression. *BMC Genomics* **5**: 32.

28. Devergnas S, Chimienti F, Naud N, Pennequin A, Coquerel Y, Chantegrel J, Favier A, and Seve M. 2004. Differential regulation of zinc efflux transporters ZnT-1, ZnT-5 and ZnT-7 gene expression by zinc levels: a real-time RT-PCR study. *Biochem Pharmacol* **68**: 699-709.

29. Chimienti F, Devergnas S, Favier A, and Seve M. 2004. Identification and cloning of a beta-cell-specific zinc transporter, ZnT-8, localized into insulin secretory granules. *Diabetes* **53**: 2330-2337.

30. Suzuki T, Ishihara K, Migaki H, Matsuura W, Kohda A, Okumura K, Nagao M, Yamaguchi-Iwai Y, and Kambe T. 2004. Zinc transporters, ZnT5 and ZnT7, are required for the activation of alkaline phosphatases, zinc-requiring enzymes that are GPI-anchored to cytoplasmic membrane. *J Biol Chem* **in press**.

VITA

Charissa (Nonhof) Ellis was born on August 25, 1977, in Hutchinson, Kansas. Because her mother entered the military, she attended public school in Kansas, Colorado, Germany, and Nebraska. She received a B.A. in Biology and Mathematics with a minor in Chemistry in 1999 from Hastings College in Hastings, Nebraska. She obtained a Ph.D. in Biochemistry in 2004 from the Department of Biochemistry at the University of Missouri in Columbia, MO. While in graduate school, in July 2000, she married William (Bill) Ellis and has been married to him for four and one-half years. She is currently working as a postdoc in the lab of Dr. David Eide at the University of Wisconsin-Madison while pursuing a teaching position in a small liberal arts college in the Midwest.